รายงานการวิจัยฉบับสมบูรณ์

สมการอย่างง่ายสำหรับการทำนายและการออกแบบการทนไฟของคานคอนกรีตเสริม

ผู้วิจัย ดร. ปฐเมศ ผาณิตพจมาน
ที่ปรึกษา ผศ.ดร.ภาสกร ชัยวิริยะวงศ์

งานวิจัยนี้ได้รับทุนอุดหนุนการวิจัย จากเงินรายได้
คณะวิศวกรรมศาสตร์ ประจำปีงบประมาณ 2554

บทคัดย่อ

การออกแบบการทนไฟของโครงสร้างคอนกรีตเสริมเหล็กนอกจากวิธีการกำหนดขนาดหน้าตัด (Prescriptive method) แล้ว การออกแบบการทนไฟของโครงสร้างคอนกรีตเสริมเหล็กภายใต้อุณหภูมิไฟที่หลากหลายจำเป็นต้องมีการประเมินโดยการวิเคราะห์การถ่ายเทความร้อนและการวิเคราะห์เชิงโครงสร้าง โดยภายใต้อุณหภูมิสูงการเปลี่ยนแปลงคุณสมบัติเชิงกลตามอุณหภูมิส่งผลต่อกำลังของโครงสร้าง การวิเคราะห์เชิงตัวเลขที่มีใช้งานโดยทั่วไปจึงเป็นเทคนิคที่มีความซับซ้อนและต้องการผู้ที่มีความชำนาญเฉพาะ ดังนั้นวิธีการออกแบบหรือคำนวนอย่างง่ายและใช้งานได้จริง จึงมีความจำเป็นอย่างยิ่งในการสนับสนุนวิศวกรในการออกแบบ

เพื่อให้การทำนายอุณหภูมิภายในหน้าตัดคอนกรีตสี่เหลี่ยมซึ่งสัมผัสความร้อนในสองมิติมีความสะดวกขึ้น การศึกษานี้ได้เสนอวิธีการวิเคราะห์เชิงพลังงาน (Energy based method) โดยวิธีนี้อยู่บนพื้นฐานการกำหนดการกระจายอุณหภูมิด้วยฟังค์ชั่นยกกำลังซึ่งมีการกำหนดลักษณะฟังค์ชั่นไว้ล่วงหน้า และการอนุรักษ์พลังงาน ซึ่งสามารถนำมาใช้งานร่วมกับโปรแกรมสเปรตชีต ฟังค์ชั่นยกกำลังที่เสนอนั้นมีความเหมาะสมกับอุณหภูมิไฟที่มีลักษณะเพิ่มขึ้นทางเดียว ดังเช่น อุณหภูมิไฟมาตรฐาน การวิเคราะห์การถ่ายเทความร้อนในสองมิติประมาณโดยการรวมผลเฉลยแบบหนึ่งมิติในสองทิศทาง วิธีที่นำเสนอยืนยันความแม่นยำโดยการเทียบผลการทำนายอุณหภูมิกับผลการทดสอบในอดีตและผลการวิเคราะห์โดยวิธีไฟไนเอลิเมนต์ อย่างไรก็ตามความแม่นยำของวิธีนี้มีข้อจำกัดเฉพาะในกรณีที่อุณหภูมิต่ำสุดในหน้าตัดต้องน้อยว่า 0.2 เท่าของอุณหภูมิสูงสุด

การศึกษานี้ยังได้พัฒนาวิธีการวิเคราะห์เชิงหน้าตัด (Cross sectional analysis) ในการทำนายความสามารถในการต้านทานโมเมนต์ของคานคอนกรีตเสริมเหล็ก ทั้งนี้การกระจายอุณหภูมิในหน้าตัดสองมิติเป็นข้อมูลนำเข้าที่ใช้ในการวิเคราะห์ ความสามารถในการต้านทานโมเมนต์อยู่บนพื้นฐานการสมดุลของแรงซึ่งสอดคล้องกับความเครียดของเอลิเมนต์ในหน้าตัดและอุณหภูมิซึ่งมีการวิเคราะห์ไว้ก่อน การคำนวนนี้คำนึงถึงการเปลี่ยนแปลงความสัมพันธ์ของความเค้นและความเครียดแบบไม่เชิงเส้น วิธีการที่ได้รับการพัฒนาใช้ได้กับคานที่ออกแบบการเสริมเหล็กแบบสมดุลและต่ำกว่าสมดุล ความสามารถในการต้านทานโมเมนต์ยืนยันความแม่นยำกับการวิเคราะห์โดยวิธีไฟไนเอลิเมนต์ ซึ่งพบว่าวิธีดังกล่าวถือเป็นวิธีที่มีศักยภาพในการทำนายความต้านทานโมเมนต์ภายใต้สภาวะการเกิดเพลิงไหม้ อย่างไรก็ตามความต้านทานโมเมนต์สูงสุดของวิธีไฟไนเอลิเมนต์โดยทั่วไปมีค่ามากกว่าความต้านทานโดยวิธีการวิเคราะห์เชิงหน้าตัด อาจกล่าวได้ว่าวิธีการวิเคราะห์เชิงหน้าตัดที่นำเสนอมีความปลอดภัย

วิศวกรด้านความปลอดภัยจากอัคคีภัยสามารถประยุกต์ใช้วิธีการที่นำเสนอในการประมาณความสามารถในการต้านทานโมเมนต์ของคานคอนกรีตเสริมเหล็ก แนวคิดการออกแบบที่นำเสนอเป็นประโยชน์ต่อการออกแบบด้านความปลอดภัยจากอัคคีภัย

ABSTRACT

In addition to the prescriptive method used in design, the fire resistance of reinforced concrete structures under various fire scenarios needs to be assessed by combined heat transfer and structural analysis. Under elevated temperatures, reinforced concrete (RC) structures are affected by variation of the mechanical properties with temperature. The available numerical simulations are complicated techniques and require an expert user. Simplified and practical approaches which enable engineers to design RC structures accounting for the mechanical variation are required.

To simply predict temperature within rectangular concrete sections subjected to various fire loads in two directions, the energy based method is proposed for practical use. The method is based on a pre-determined power function as the temperature profile, and conservation of energy: it can be implemented in a spreadsheet. The power function is suitable for monotonically increasing fire curves such as the nominal temperature-time curves. The analysis of two dimensional heat transfer is approximated by superposition of one-dimensional solutions. By comparing the temperature prediction with the previous experimental and FEM results, the method is validated. However, the method has its limitations; in particular the lowest temperature needs to remain less than 0.2 times the highest, or the energy estimated becomes inaccurate.

The study develops a cross sectional analysis to predict the moment capacity of RC beams. The two-dimensional temperature distribution is used as the input data in the analysis. The capacity is computed based on the force equilibrium corresponding to the assumed element strain and the pre-determined element temperature. The variation of nonlinear stress-strain relationship with temperature is adopted in the analysis. The developed method is limited to under or normal-reinforced beams. The predicted moment capacity is validated with the finite element analysis. The cross sectional approach is found to be a potential method to predict the moment capacity under fire. However, the ultimate capacities of the FE model are normally higher than the capacity of the sectional analysis. It implicitly describes the safety of the sectional analysis.

Fire safety engineers may apply the proposed method to evaluate the moment capacity. Knowledge of these is necessary for fire safety design.

กิตติกรรมประกาศ

โครงการวิจัยนี้สำเร็จลุล่วงได้ด้วยการสนับสนุนของทุนอุดหนุนวิจัยจากเงินรายได้คณะวิศวกรรมศาสตร์ มหาวิทยาลัยสงขลานครินทร์ ประเภทโครงการวิจัยแบบมุ่งเป้า ประจำปีงบประมาณ 2554 และขอขอบคุณ ผศ. ดร. ภาสกร ชัยวิริยะวงศ์ ที่ปรึกษาโครงการฯ ซึ่งให้ข้อแนะนำอันเป็นประโยชน์ต่องานวิจัย สุดท้ายขอขอบคุณภาควิชาวิศวกรรมโยธา ฯ ซึ่งอำนวยความสะดวกในการดำเนินงานวิจัยจนสมบูรณ์

คำนำ

การออกแบบการทนไฟเป็นข้อกำหนดตามกฎหมายในประเทศไทย รวมถึงเป็นข้อกำหนดการออกแบบด้านความปลอดภัยจากอัคคีภัยที่ต้องคำนึงถึง ปัจจุบันการออกแบบโครงสร้างคอนกรีตเสริมเหล็กภายใต้สภาวะการเกิดเพลิงไหม้ตามมาตรฐานทั่วไป เป็นลักษณะการออกแบบโดยใช้ตารางระยะหุ้มของคอนกรีต ซึ่งยังมีข้อจำกัดการใช้งานอยู่มาก ทั้งในด้านขนาดหน้าตัดและอุณหภูมิไฟที่ระบุไว้ในมาตรฐาน ดังนั้นการออกแบบโครงสร้างคอนกรีตเสริมเหล็กที่มีลักษณะต่างออกไป จำเป็นต้องประยุกต์ใช้โปรแกรมวิเคราะห์ต่างๆ เช่น ไฟไนเอลิมเมนต์ซึ่งยังมีความยุ่งยากในการใช้งานและปัญหาในการเข้าถึงโปรแกรมที่จะใช้งานอยู่มาก จากเหตุดังกล่าวจึงเป็นปัญหาแก่วิศวกรในการระบุอัตราการทนไฟ รวมถึงการออกแบบการทนไฟให้แก่โครงสร้าง

ผู้วิจัยได้เล็งเห็นว่าการพัฒนาวิธีการออกแบบอย่างง่ายซึ่งสามารถประยุกต์ใช้งานได้กับโปรแกรมการคำนวณทั่วไป เช่น Spreadsheet program มีความจำเป็นในการสนับสนุนความปลอดภัยด้านอัคคีภัย ผู้วิจัยจึงได้เริ่มการพัฒนาการออกแบบอย่างง่ายที่ใช้ได้กับขนาดหน้าตัดโครงสร้างและอุณหภูมิไฟแบบต่างๆ โดยในโครงการวิจัยเริ่มพัฒนาการออกแบบอย่างง่ายในส่วนของความสามารถในการต้านทานโมเมนต์ของคานคอนกรีตเสริมเหล็กภายใต้สภาวะการเกิดเพลิงไหม้

ผู้วิจัยหวังเป็นอย่างยิ่งว่าวิธีการออกแบบที่นำเสนอจะเป็นประโยชน์ในการใช้งานจริงต่อไป

สารบัญ

บทนำของโครงการวิจัย

โครงสร้างคอนกรีตเสริมเหล็กมีการใช้งานอย่างแพร่หลายในปัจจุบัน แม้ว่าโครงสร้างคอนกรีตเสริมเหล็กมีความสามารถในการทนไฟได้สูง จากคุณสมบัติของการหน่วงความร้อนของคอนกรีต อย่างไรก็ตามเมื่ออุณหภูมิสูงขึ้นโครงสร้างคอนกรีตเสริมเหล็กมีการเสียกำลัง และอาจนำไปสู่การพังทลายได้ ดังนั้นองค์อาคารคอนกรีตเสริมเหล็กจำเป็นต้องมีการออกแบบหรือประเมินความสามารถในการทนไฟของโครงสร้าง โดยปัจจุบันการออกแบบตามมาตรฐานเป็นลักษณะการออกแบบโดยใช้ตารางระยะหุ้มของคอนกรีต ซึ่งสามารถใช้งานได้เฉพาะหน้าตัดและอุณหภูมิไฟที่กำหนดเท่านั้น ดังนั้นวิธีการออกแบบตามมาตรฐานยังมีข้อจำกัดอยู่มากในการออกแบบโครงสร้างคอนกรีตเสริมเหล็กที่มีลักษณะต่างออกไป อาจใช้แบบจำลองไฟไนเอลิเมนต์ในการวิเคราะห์ อย่างไรก็ตามการสร้างแบบจำลองและการวิเคราะห์โดยวิธีดังกล่าวยังมีความซับซ้อนและไม่สามารถใช้งานได้โดยสะดวก

ดังนั้นในโครงการศึกษานี้จึงได้พัฒนาแนวทางการออกแบบโครงสร้างคอนกรีตเสริมเหล็กอย่างง่าย โดยเริ่มต้นพัฒนาในส่วนของความสามารถในการต้านทานโมเมนต์ของคานคอนกรีตเสริมเหล็ก โดยพิจารณาในสองส่วนคือ การวิเคราะห์การถ่ายเทความร้อนซึ่งทำให้ได้ค่าการกระจายอุณหภูมิภายในหน้าตัด และการทำนายความสามารถในการต้านทานโมเมนต์ของคานคสล.ที่อุณหภูมิสูง

การพัฒนาแบบจำลองอย่างง่ายในการทำนายการกระจายตัวของอุณหภูมิของคานคสล. ที่อุณหภูมิสูงได้ ผู้วิจัยได้ประยุกต์ใช้การวิเคราะห์อุณหภูมิโดยวิธี Finite different ซึ่งหาผลเฉลยโดยวิธีเชิงตัวเลข (Numerical Method) บนพื้นฐานกฎอนุรักษ์พลังงาน ซึ่งครอบคลุมการถ่ายเทความร้อนโดยการนำความร้อน การพาความร้อน และการแผ่รังสีความร้อนของหน้าตัดคานเพื่อให้อยู่ในรูปสมการอย่างง่าย ส่วนการพัฒนาแบบจำลองในการทำนายความสามารถในการต้านทานโมเมนต์ของคานคสล.ที่อุณหภูมิสูง ได้ปรับปรุงวิธี Sectional analysis เพื่อใช้ในการทำนายความสามารถในการต้านทานโมเมนต์ของคานคสล.ที่อุณหภูมิสูง โดยการแบ่งหน้าตัดคานเป็นส่วนย่อยในลักษณะสองมิติ ซึ่งหน้าตัดคานแต่ละส่วนจะมีอุณหภูมิที่แตกต่างกันไปขึ้นอยู่กับผลของการถ่ายเทความร้อน

วัตถุประสงค์ของโครงการวิจัย

1.1. วิเคราะห์ผลกระทบของความร้อน และลักษณะหน้าตัดต่อความต้านทานการทนไฟของคานคอนกรีตเสริมเหล็ก

1.2. พัฒนาแบบจำลองและสมการในการวิเคราะห์อย่างง่าย เพื่อใช้ในการทำนายหรือออกแบบความสามารถในการทนไฟของคานคอนกรีตเสริมเหล็ก

ระเบียบวิธีการวิจัยของโครงการวิจัย

การสร้างสมการการออกแบบอย่างง่ายสำหรับการวิเคราะห์การทนไฟของคาน คสล. จำเป็นต้องพิจารณาในสองส่วนคือ การวิเคราะห์การถ่ายเทความร้อนซึ่งทำให้ได้ค่าการกระจายอุณหภูมิภายในหน้าตัด และการทำนายความสามารถในการต้านทานโมเมนต์ของคานคสล.ที่อุณหภูมิสูง ทั้งนี้ผู้วิจัยได้ดำเนินการวิจัยในส่วนที่เกี่ยวข้องดังนี้

การพัฒนาแบบจำลองอย่างง่ายในการทำนายการกระจายตัวของอุณหภูมิของคานคสล. ที่อุณหภูมิสูงได้ ผู้วิจัยได้เขียนโปรแกรมสำหรับการวิเคราะห์อุณหภูมิโดยวิธี Finite different ซึ่งหาผลเฉลยโดยวิธีเชิงตัวเลข (Numerical Method) โดยอาศัยพื้นฐานของการอนุรักษ์พลังงาน ซึ่งครอบคลุมการถ่ายเทความร้อนโดยการนำความร้อน การพาและการแผ่รังสีความร้อนของหน้าตัดคานเพื่อให้อยู่ในรูปอย่างง่าย

การพัฒนาแบบจำลองอย่างง่ายในการทำนายความสามารถในการต้านทานโมเมนต์ของคานคสล.ที่อุณหภูมิสูง ได้ปรับปรุงวิธี Sectional analysis เพื่อใช้ในการทำนายความสามารถในการต้านทานโมเมนต์ของคาน คสล.ที่อุณหภูมิสูง โดยการแบ่งหน้าตัดคานเป็นส่วนย่อยในลักษณะสองมิติ ซึ่งหน้าตัดคานแต่ละส่วนจะมีอุณหภูมิที่แตกต่างกันไปขึ้นอยู่กับผลของการถ่ายเทความร้อน แบบจำลองดังกล่าวสมมุติการกระจายความเครียดในหน้าตัดคานตลอดความลึกในลักษณะเชิงเส้นซึ่งสอดคล้องกับการสมมุติตำแหน่งแกนสะเทินของของหน้าตัด (Neutral Axial) โดยความเครียดแต่ละส่วนย่อยสามารถคำนวณเป็นความเค้นได้ตามความสัมพันธ์ระหว่างความเค้นและความเครียดที่แตกต่างกันตามระดับอุณหภูมิของแต่ละส่วนย่อย โดยผลของการสมมุติตำแหน่งแกนสะเทิน และความสมดุลระหว่างแรงอัดและแรงดึงในหน้าตัด สามารถใช้ในการทำทายความต้านทานโมเมนต์ได้

สมการต่างๆที่นำเสนอจะนำมาเปรียบเทียบกับผลการทดสอบจากการทบทวนวรรณกรรม และผลการวิเคราะห์โดยวิธีไฟไนเอลิเม้นต์ เพื่อยืนยันประสิทธิภาพของวิธีที่นำเสนอ นอกจากนี้เพื่อให้เกิดประโยชน์ต่อการใช้งานจริงระเบียบวิธีการคำนวณที่นำเสนอมีการประยุกต์ใช้งานรวมกับโปรแกรมการคำนวณประเภท Spreadsheet program เพื่อง่ายต่อการใช้งานในการออกแบบ

ผลการวิจัยและวิเคราะห์ผลการวิจัย

ทั้งนี้โครงการวิจัยได้แบ่งการศึกษาเป็น 5 ส่วน คือ

บทความที่ 1 แนวคิดการพัฒนาสมการการทำนายอุณหภูมิคอนกรีต 1 มิติ

นำเสนอผ่านบทความวิชาการในวารสารนานาชาติ

P. Panedpojaman, 2012, "Energy Based Temperature Profile for Heat Transfer Analysis of Concrete Section Exposed to Fire on One Side", World Academy of Science, Engineering and Technology, Issue 65, pp. 897-902.

บทตวามที่ 2 การพัฒนาสมการการทำนายอุณหภูมิคอนกรีต 1 มิติ

นำเสนอผ่านบทความวิชาการในวารสารนานาชาติ

P. Panedpojaman, 2012, "Spreadsheet Calculation of Energy Based Method to Predict Temperature in Concrete Slabs", International Review of Civil Engineering, Vol. 3, N. 5, pp. 403-411. (ปรากฏในฐานข้อมูล EBSCO)

บทความที่ 3 การพัฒนาสมการการทำนายอุณหภูมิคอนกรีต 2 มิติ

นำเสนอผ่าน**ร่างบทความวิชาการ (Under Review)** ในวารสารนานาชาติ

P. Panedpojaman, P. Chaiviriyawong, (Under review), “Energy Based Method to Predict Temperature within Rectangular Concrete Sections”, Fire Safety Journal (อยู่ในฐานข้อมูล ISI)

บทความที่ 4 การทำนายความสามารถในการต้านทานโมเมนต์ของคานคสล.ที่อุณหภูมิสูง โดยวิธี Sectional analysis

นำเสนอผ่านบทความวิชาการการประชุมวิชาการระดับนานาชาติ

P. Panedpojaman, 2012, “Predicting Moment Capacity of RC Beams under Fire by Using Two-dimensional Sectional Analysis”, 4th KKU International Engineering Conference, Khonkaen, Thailand, 10-12 May 2012, pp. 93-99. (ผู้ขอมีส่วนร่วมร้อยละ 100)

บทความที่ 5 ข้อจำกัดและความแม่นยำในการทำนายการต้านทานโมเมนต์ของคานคสล.ที่อุณหภูมิสูง โดยวิธี Sectional analysis

นำเสนอผ่านบทความวิชาการการประชุมวิชาการระดับนานาชาติ

P. Panedpojaman, P. Chaiviriyawong, 2013, “Simplified Computation and Finite Element Investigation of Fire Exposed Concrete Beams”, International Conference on Advances in Mechanical Engineering and Civil Engineering , *Pattaya, Thailand, 19-20 January 2013, pp 190-195.*

Energy Based Temperature Profile for Heat Transfer Analysis of Concrete Section Exposed to Fire on One Side

Pattamad Panedpojaman

***Abstract*—**For fire safety purposes, the fire resistance and the structural behavior of reinforced concrete members are assessed to satisfy specific fire performance criteria. The available prescribed provisions are based on standard fire load. Under various fire scenarios, engineers are in need of both heat transfer analysis and structural analysis. For heat transfer analysis, the study proposed a modified finite difference method to evaluate the temperature profile within a cross section. The research conducted is limited to concrete sections exposed to a fire on their one side. The method is based on the energy conservation principle and a pre-determined power function of the temperature profile. The power value of 2.7 is found to be a suitable value for concrete sections. The temperature profiles of the proposed method are only slightly deviate from those of the experiment, the FEM and the FDM for various fire loads such as ASTM E 119, ASTM 1529, BS EN 1991-1-2 and 550 ^{o}C. The proposed method is useful to avoid inconvenience of the large matrix system of the typical finite difference method to solve the temperature profile. Furthermore, design engineers can simply apply the proposed method in regular spreadsheet software.

***Keywords*—**temperature profile, finite difference method, concrete section, one-side fire exposed, energy conservation

I. Introduction

REINFORCED concrete (RC) members are impacted under fire due to raising temperatures in their cross sections. The high temperature significantly reduces the mechanical properties of concrete and steel [1]. Fire resistance of RC members are generally specified in codes and standards such as AS 3600 [2], Eurocode 2 [3] and ACI 216.1 [4]. The provisions specify minimum cross-section dimensions and minimum clear cover to the reinforcing bars based on experimental tests or pre-determined analysis under specific fire curves such as ASTM E 119 [5], ISO 834[6] etc. As a result, they are prescriptive and cannot evaluate the fire resistance under different fire scenarios and conditions. For different fire scenarios, engineers are in need of alternative design tools.

To investigate the structural behavior of concrete structures, both heat transfer analysis and structural analysis are required. For heat transfer analysis, the finite element method (FEM) has proven to be a powerful method to predict the temperatures in reinforced concrete sections during fire exposure [7, 8]. Difficulty of using the FEM or cost of finite element software makes it impractical for design engineers.

P. Panedpojaman, Dr., is with Civil Engineering Department, Prince of Songkla University, Hat-Yai, Songkhla, Thailand, 90110 (phone: 006674-287140; fax: 006674-459396; e-mail: ppattamad@eng.psu.ac.th).

The authors would like to acknowledge Faculty of Engineering, Prince of Songkla University, Thailand for providing the financial support for this research project (contract no. ENG-55-2-7-02-0139-S).

The finite difference method (FDM) is considered as a simpler method for evaluating temperature profile within a cross section exposed to fire. The FDM is widely developed and adopted for RC sections during fire exposure [9-12]. Note that the effect of the reinforcing steel of RC sections on the heat transfer analysis is neglected due to its small area relative to concrete area [9].

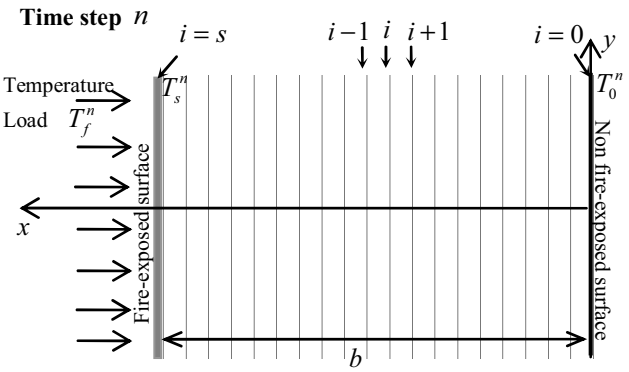

Fig. 1 Nodal network of a section exposed to a fire on its one side

The previous researches [9-12] were conducted based on the typical FDM. In the FDM, the physical system of a cross-section exposed to a fire on its one side is represented by a nodal network as shown in Fig. 1. The FDM replaces the governing equations and corresponding boundary conditions of heat transfer analysis by a set of algebraic equations. When the temperatures of all nodal points are known at any particular time t, the temperatures after a time increment Δt can be computed [13]. Size of the grid spacing Δx and the time increment Δt depends on geometry of cross sections, accuracy of the solution and the stable condition of the method. To compute the temperature profile, the method establishes a matrix of the temperatures of all nodal points at each time step. For a case of the large matrix generated, the method may not be convenient to find its solution corresponding to the stable condition.

To avoid the inconvenient of the large matrix to solve the temperature profile, this study modified the FDM based on the pre-determined shape function of the temperature profile and the energy conservation. The research conducted in this paper is limited to concrete sections exposed to a fire on their one side.

II. Energy Based Heat Transfer Analysis

Consider sections exposed to a fire on their one side which is infinite in the direction of the y-coordinate, with the thickness b in direction of the x-coordinate as shown in Fig.

1. For isotropic and homogeneous media, the conductive heat flux q in the x direction is given by Fourier's heat conduction law as

$$-k\frac{\partial T}{\partial x}=q \tag{1}$$

where k is the thermal conductivity and T is the temperature.

The governing differential equation of the heat conduction is considered based on the energy conservation for conduction through an elemental volume. The energy conservation consists of net rate of heat entering by conduction, rate of energy generated internally and rate of increase of internal energy. In one-dimensional Cartesian coordinates, the full conduction equation is derived as

$$k\frac{\partial^2 T}{\partial x^2}+g=\rho c\frac{\partial T}{\partial t} \tag{2}$$

where g is the heat generation and c is the specific heat.

For a system of the one dimensional with the constant thermal properties and without the heat generation (i.e., $g=0$), unsteady-state conduction problem is governed by

$$\frac{\partial^2 T}{\partial x^2}=\frac{\rho c}{k}\frac{\partial T}{\partial t} \tag{3}$$

This equation is employed to compute temperatures of the internal section as a function of time. Once a convection and radiation boundary condition exists such as in case of fire, the boundary has to be considered separately. For the one dimensional system, the boundary condition at $x=b$ is

$$-k\frac{\partial T}{\partial x}=q=-h\left(T_f-T_s\right)-\varepsilon\sigma\left(T_f^4-T_s^4\right) \tag{4}$$

T_f is the fire temperature which is a function of time. Based on (3) and (4), the temperature profile in the section with a convection and radiation boundary condition can complicatedly be solved. The FEM can be used to evaluate the solution.

A. Finite Difference Method

The finite difference method is a numerical technique which can be applied to the partial differential equations. The finite difference of derivatives involves the approximation of a differential equation by algebraic equations. The equations are pointwise continuous which is applicable throughout the region and space considered.

To apply the FDM, a network of grid points by dividing x and t domains into small intervals of Δx, as shown in Fig. 1, and Δt. According to the network, T_i^n represents the temperature at location $x=i\Delta x$ at $t=n\Delta t$. i is the number of a grid point whereas n is the number of a time step. If the forward-difference approximation is used in (3), the finite-difference equation is represented as

$$\frac{T_{i+1}^n+T_{i-1}^n-2T_i^n}{\left(\Delta x\right)^2}=\frac{k}{\rho c}\frac{T_i^{n+1}-T_i^n}{\Delta t} \tag{5}$$

The finite difference equation in (5) is employed to compute temperatures of the internal grid points as a function of time.

Note that from the forward-difference approximation of time derivative, the solutions are not stable for all situations. To avoid the violation of the second law of thermodynamics, the stable condition of $\left(k/\rho c\right)\left(\Delta t\Delta x^2\right)\le 0.5$ has to be satisfied [13].

The finite difference form of the boundary condition at $i=s$, (4) may be expressed as

$$-k\frac{T_s^n-T_{s-1}^n}{\Delta x}=q^n \tag{6}$$

where

$$q^n=-h\left(T_f^n-T_s^n\right)-\varepsilon\sigma\left(\left(T_f^n\right)^4-\left(T_s^n\right)^4\right) \tag{7}$$

Due to the intervals of Δx in the FDM, the effect of the heat capacity of the system next to the boundary must be included in (6) [13] as

$$-k\frac{T_s^n-T_{s-1}^n}{\Delta x}-q^n=\rho c\frac{\Delta x}{2}\frac{T_s^{n+1}-T_s^n}{\Delta t} \tag{8}$$

This equation can be rearranged as

$$T_s^{n+1}=\frac{2\Delta t}{\rho c\Delta x}\left[-k\frac{T_s^n-T_{s-1}^n}{\Delta x}-q^n\right]+T_s^n \tag{9}$$

Therefore, T_s^{n+1} can be solved based on temperature of the previous step.

If T_f is an increasing functions, the value of T_s^{n+1} must be larger than the value of T_s^n. As a result, another stable condition has to be satisfied:

$$-k\frac{T_s^n-T_{s-1}^n}{\Delta x}-q^n>0 \tag{10}$$

To compute the temperature profile, the method employs a matrix of the temperatures of all nodal points at each time step. For a case of the large matrix, the method may be difficult to find its solution corresponding to the stable condition.

B. Modified Finite Difference Method

To simplify the FDM, this study adopts the energy conservation principle and a pre-determined shape function of the temperature profile. Based on the energy conservation principle, the provided heat energy from fire load Q_p balances the received heat energy Q_r, which is the internal energy in the fire-exposed section. The internal energy is to take into consideration the heat capacity of the system and the temperature profile as shown in Fig. 2. The energy equations are describes as follows:

$$Q_p{}^n=Q_r{}^n \tag{11}$$

$$Q_p{}^n=\sum_{m=1}^{n}A\left(-q^m\right)\Delta t \tag{12}$$

$$Q_r{}^n=\int_0^b\rho cA\left(T^n(x)-T_r\right)dx \tag{13}$$

A is the surface area. Due to a uniform temperature load through out the fire-exposed surface is assumed, the surface

area can be considered as unit area (i.e., $A=1$). $T^n(x)$ is the energy based temperature profile within the cross section.

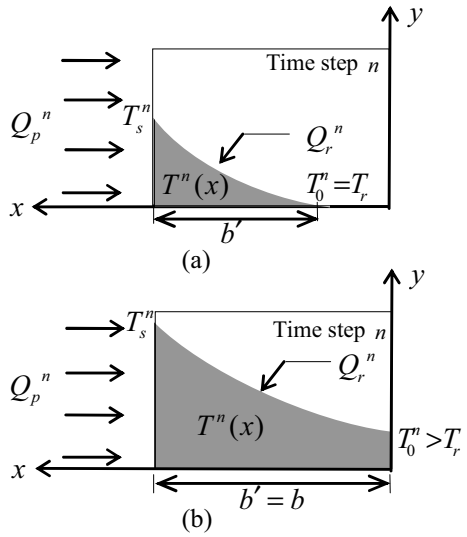

Fig. 2 Energy conservation of the fire-exposed section: (a) Low energy case; (b) High energy case

Through the energy conservation principle, T_s^{n+1} in (9) and the temperature profile can simply be solved when the shape function of $T^n(x)$ is known. In the study, the shape function is assumed to be a power function as

$$T^n(x) = Cx^{\alpha} + T_0^n \tag{14}$$

where

$$C = \frac{T_s^n - T_0^n}{b'^{\alpha}} \tag{15}$$

α is the power of the function; and

b' is described in Fig.2.

Equation (9) can be modified by substituting the term of $\left(T_{s-1}^n - T_s^n\right)/\Delta x$ with the derivative function of (14) as described in (16). The equation of T_s^{n+1} in (9) and the stable condition in (10) can be rewritten in (17) and (18), respectively.

$$\frac{T_{s-1}^n - T_s^n}{\Delta x} \approx \left.\frac{dT^n(x)}{dx}\right|_{x=b} = \alpha\frac{T_s^n - T_0^n}{b'} \tag{16}$$

$$T_s^{n+1} = \frac{2\Delta t}{\rho c \Delta x}\left[-k\alpha\frac{T_s^n - T_0^n}{b'} - q^n\right] + T_s^n \tag{17}$$

$$-k\alpha\frac{T_s^n - T_0^n}{b'} - q^n > 0 \tag{18}$$

For each Δt, the difference between T_f^n and T_s^n varies. When the difference is narrow, the value of $-q^n$ in (7) may not enough to satisfy (18). The dissatisfaction can exist in any time step in both typical FDM and proposed method. Once the dissatisfaction is found, Δt should be increase otherwise such step should be neglected and postponed to the next step. Note that due to the pre-determined shape function cannot violate of the second law of thermodynamics within the sections, the stable condition of $(k/\rho c)\left(\Delta t \Delta x^2\right) \le 0.5$ is omitted in the proposed method. When the value of α is pre-determined, only T_s^n and T_0^n are unknown variables to solve T_s^{n+1} in (17). Therefore, the large matrix system of the FDM can be avoided.

To specify $T^n(x)$ in (14), T_s^n can be obtained from (17) of the previous step whereas T_0^n can be compute through the energy conservation equation (11) and (13). Two cases of the energy based temperature profile as shown in Fig. 2 are considered as follows:

1) Low energy case: $T_0^n = T_r$ and

$$b' = \frac{Q_p^n(\alpha+1)}{\rho c\left(T_s^n - T_r\right)} \tag{19}$$

2) High energy case: $T_0^n > T_r$, $b' = b$ and

$$T_0^n = \frac{1}{\alpha}\left[(\alpha+1)\left(\frac{Q_p^n}{\rho c b} + T_r\right) - T_s^n\right] \ge T_r \tag{20}$$

where T_r is the room temperature.

The procedure to predict the temperature profile in the fire exposed section under a fire load can be summarized as illustrated in Fig. 3.

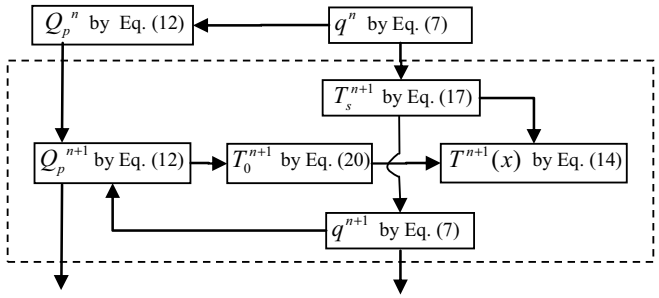

Fig. 3 Procedure to predict the temperature profile in a section at time step $n+1$

III. Investigation of The Pre-determined Shape Function

The research conducted is limited to concrete sections. To investigate the suitable value of the power α for concrete sections, the temperature profile of concrete sections analyzed by the FEM, ANSYS software, is compared with the proposed method with different values of the power. The concrete sections exposed to the standard fire of ASTM E 119 [5] on their one side as shown in Fig. 4 are specified in the comparison. The sections have a thickness of 100 mm and 300 mm. To analyze temperature profile in the section by the ANSYS model [14], the sections are modeled with three-dimensional solid elements, Solid70, having eight nodes with a single degree of freedom (i.e., temperature) at each node. The surface element, Surf152, is used to account for heat convection and radiation of the fire temperature.

The thermal properties of concrete as shown in Fig. 5 are specified in accordance with BS EN 1992-1-2 (2004) [15]. To simplify the computation and due to the value of c less varies with temperature, the value of c is assumed to be a constant value of $1x10^3$ J/kg°K for the proposed method. The concrete density of 2400 kg/m^3 is specified to be constant for both FEM and proposed method. The coefficient of heat transfer-convection h of 25 W/m^2°K, Stefan Boltzmann constant of 5.67 x 10^{-8} W/m^2°K^4 and the resultant emissivity of 0.56 are used according to BS EN 1991-1-2 (2002) [3].

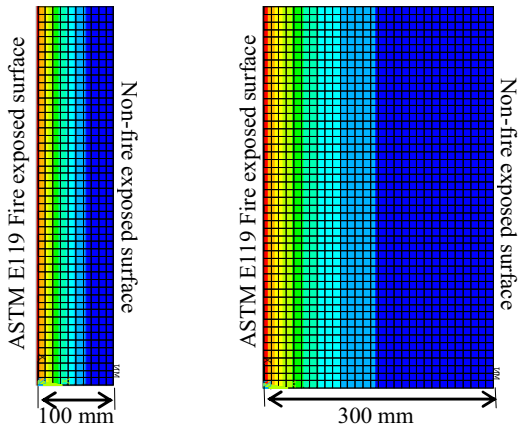

Fig. 4 Concrete sections exposed to the standard fire of ASTM E 119 and temperature profile by the FEM

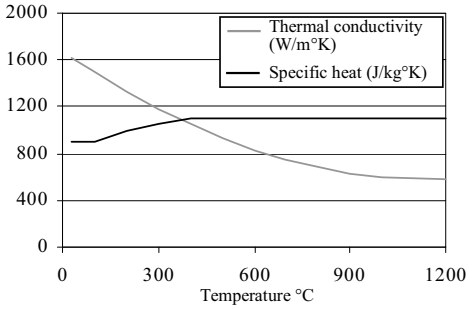

Fig. 5 Thermal properties of concrete

Size of the nodal spacing Δx = 10 mm and the time increment Δt = 2 min is specified in the computation of the proposed method and the FEM. For the proposed method, the stable condition at the fire exposed surface in (18) is checked at each time step. If the dissatisfaction exists in a time step, such step is neglected and postponed to the next time step.

The comparisons of the temperature profile in the sections between the FEM and the proposed method with different values of α are illustrated in Fig 6. It is found that the temperature profiles can be approximately represented by the power function. Furthermore, the good agreements between the temperatures at the fire exposed surface obtained from FEM and the proposed method are observed. The value of α less affects the temperature of the fire exposed surface. However, the value of α is not constant but approximately in range of 2 to 3.5.

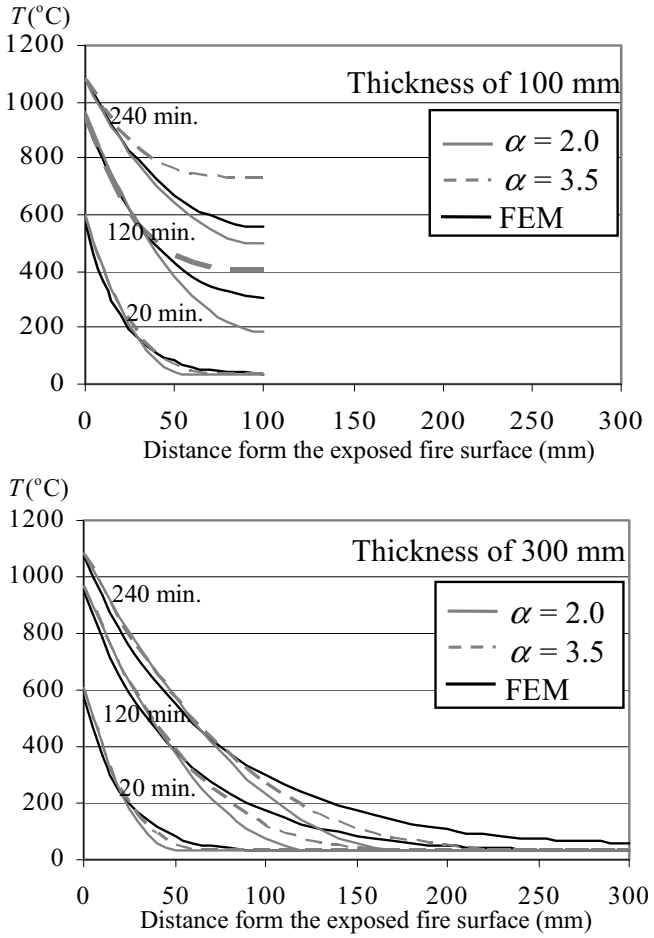

Fig. 6 comparison of the temperature profile between the FEM and the proposed method with different values of α

TABLE I
POSITIONS OF THE COMPARED TEMPERATURE AND THEIR SYMBOLS

Position	Symbol	
	Section of 100 mm thickness	Section of 300 mm thickness
Fire exposed surface	F-100	F-300
42 mm from the fire exposed surface	M-100	M-300
Non-fire exposed surface	N-100	N-300

To simply apply the energy based temperature profile for the heat transfer analysis, the α value is assumed to be a constant value of 2.7. Accuracy of the temperature predicted with the α assumption is investigated by comparing with the FEM. The temperature profiles of the sections (in Fig. 4) exposed to the standard fire of ASTM E 1529 [16], the standard fire of ASTM E 119 [5] and the temperature of 550 °C are investigated. The comparisons as shown in Fig 7 are illustrated in terms of the temperature variation with time at the specific points in the sections as described in Table 1. Note

that the temperature of 550 °C represents cases of low fire load. The position of 30 mm is specified as the general position of the reinforcing steel in RC members.

The good agreements of the temperature variation at the fire exposed surface are observed. Comparing with the FEM, the temperature variations of the proposed method at the other points, except the case of N-300, tends to slightly overestimate. In an overall picture, the proposed method with the α value of 2.7 can be used to predict the temperature profile of concrete sections under various fire exposures.

IV. Validation

The proposed method is validated by comparing its prediction of the temperature variations with the experimental variation [17], the analytical variation of the FEM and the analytical variation of the FDM. The previous research [17] investigated the temperature in post-tensioned concrete slabs having a thickness of 160 mm and exposed to the standard fire of BS EN 1991-1-2 [15] on their one side. Thermocouples were used to measure temperature at the fire exposed surface, the non-fire exposed surface and the positions of 42 mm from fire exposed surface. The comparison of the temperature variation with time is illustrated in Fig. 8. From the illustration, it is seen that the results of the proposed method only slightly deviate from the results of the experiment, the FEM and the FDM. The energy based temperature profile can thus be used to approximate the temperature variation in concrete sections exposed to fire loads.

V. Conclusion and Discussion

This paper simplifies the FDM to predict the temperature profile within concrete sections exposed to a fire on their one side. The proposed method is based on the energy conservation principle and a pre-determined shape function of the temperature profile. According to the energy conservation principle, the provided heat energy from the boundary balances the received heat energy in a fire-exposed section. The heat energy in the section is to take into consideration the heat capacity of the system and the temperature profile function. In the study, the shape function is assumed to be a power function. The specific function is derived based on the energy conservation principle.

To investigate the suitable value of the power α for concrete sections, the temperature profiles of the concrete sections computed by the proposed method using different power number is compared with those computed by the FEM. It is found that the value of α less affects the predicted temperature at fire exposed surface. The value of α is not constant but approximately in range of 2 to 3.5. However, the temperature profiles of the proposed method with the α value of 2.7 slightly deviate from those of the experiment, the FEM and the FDM for various fire loads.

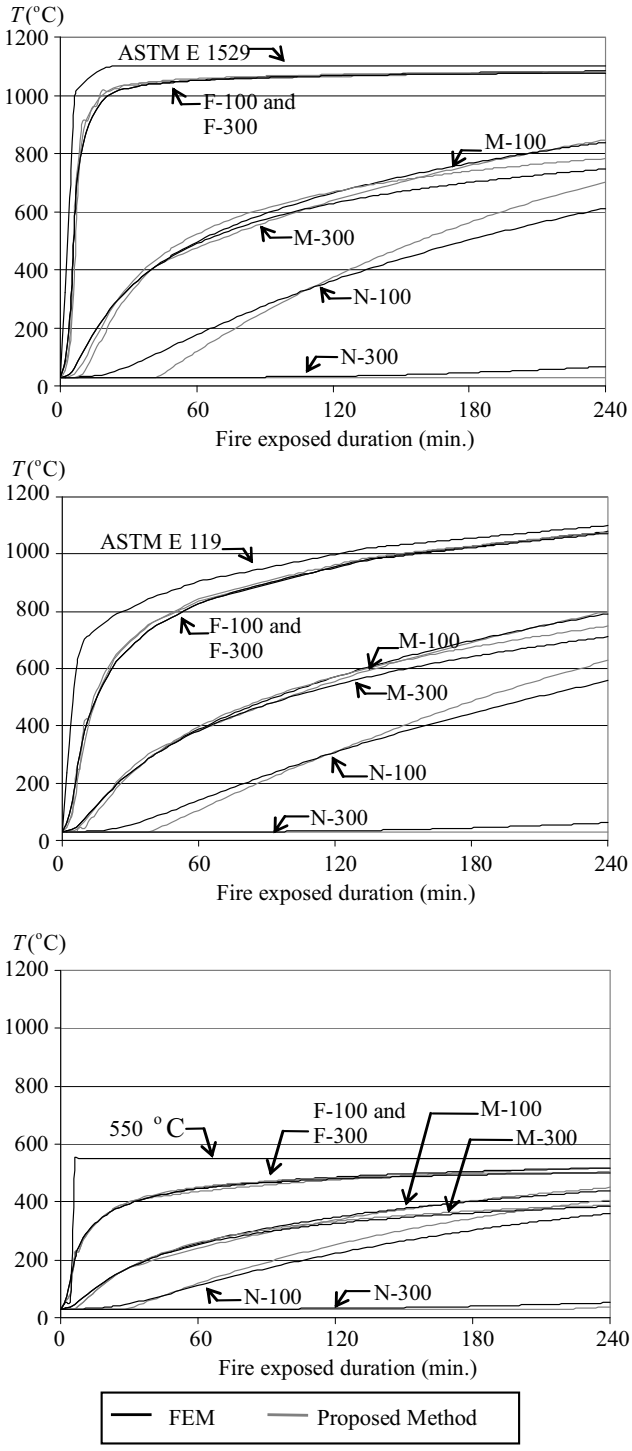

Fig. 7 Comparison of the temperature profile between the proposed method with the α value of 2.7 and the FEM

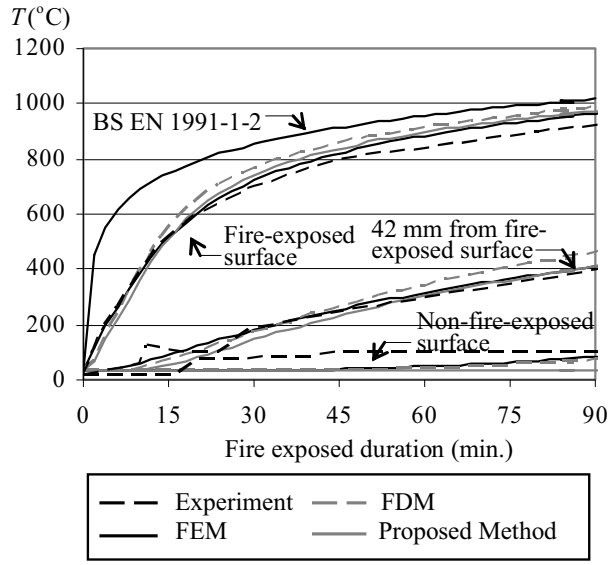

Fig. 8 Comparison of the predicted temperature variation with the experiments, the FEM and the FDM

By using the energy based temperature profile, the temperature matrix of the FDM nodal network can be avoided. The method is also useful to manipulate the stable conditions of the FDM in the section and at the fire exposed surface. Therefore, design engineers can simply apply the proposed method to evaluate the temperature profile by using regular spreadsheet software. The proposed method facilitates design engineers analyzing the heat transfer which is a necessary part to investigate the fire resistance and the structural behavior of concrete structures under fire scenarios. The proposed method is potential to develop for other cases of fire exposure.

REFERENCES

[1] O. M.A. Youssef, M. Moftah, "General stress–strain relationship for concrete at elevated temperatures", Eng. Struct., 29(10), 2007, 2618–2634.
[2] AS 3600, Concrete structures. Australia: Committee BD-002, 2001.
[3] BS EN 1991-1-2, Actions on structures: Part 1-2 General actions—structures exposed to fire. Brussels (Belgium): European Committee for Standardization, 2002.
[4] ACI 216.1-07, Standard method for determining fire resistance of concrete and masonry construction assemblies. Detroit: American Concrete Institute; 2007.
[5] ASTM E 119, Standard methods of fire test of building construction and materials, Test Method E119a -08. American Society for Testing and Materials, West Conshohocken, PA, 2008.
[6] ISO 834, Fire-resistance tests—elements of building construction—Part 1: General requirements. International Standard, Geneva, 1999.
[7] S. Bratina, M. Saje, I. Planinc, "The effects of different strain contributions on the response of RC beams in fire", Eng. Struct., 29(3), 2007, 418–430.
[8] A. Law, J. Stern-Gottfried, M. Gillie, G. Rein, "The influence of travelling fires on a concrete frame", Eng. Struct., 33, 2011, 1635–1642.
[9] T.T. Lie, Structural fire protection. ASCE Manuals and Reports on Engineering Practice, No. 78, New York, NY, USA, 1992.
[10] V.R. Kodur, T.C. Wang, F.P. Cheng, "Predicting the fire resistance behaviour of high strength concrete columns", Cem. Concr. Compos., 26, 2004, 141–153.
[11] V.K.R. Kodur, M. Dwaikat, "A numerical model for predicting the fire resistance of reinforced concrete beams", Cem. Concr. Compos., 30, 2008, 431–443.
[12] S.F. El-Fitiany, M.A. Youssef, "Assessing the flexural and axial behaviour of reinforced concrete members at elevated temperatures using sectional analysis", Fire Saf. J., 44, 2009, 691–703.
[13] K. V. Wong, Intermediate Heat Transfer. New York: Marcel Dekker, INC., 2003, ch. 5.
[14] ANSYS, ANSYS multiphysics. Version 11.0 SP1. ANSYS Inc., Canonsburg (PA), 2007.
[15] BS EN 1992-1-2, Design of concrete structures. General rules. Structural fire design. Brussels (Belgium): European Committee for Standardization, 2004.
[16] ASTM E 1529, Standard Test Methods for Determining Effects of Large Hydrocarbon Pool Fires on Structural Members and Assemblies. ASTM Intl., West Conshohocken, PA., 2000.
[17] C.G. Bailey, E. Ellobody, "Fire tests on bonded post-tensioned concrete slabs", Eng. Struct., 31, 2009, 686-696.

Praise Worthy Prize

International Review of Civil Engineering (I.RE.C.E.), Vol. 3, N. 5
ISSN 2036 - 9913 *September 2012*

Spreadsheet Calculation of Energy Based Method to Predict Temperature in Concrete Slabs

P. Panedpojaman

Abstract – *Under various fire scenarios, both heat transfer analysis and structural analysis are required to assess fire resistance of reinforced concrete member. For heat transfer analysis, Finite element method and Finite difference method are complicate for practical use. To simply predict temperature in concrete slab, the energy based method is a simplified FDM based on the predetermined temperature profile and the energy conservation. However, the method provides an inaccurate temperature prediction. To improve the prediction accuracy, this study reformulates the energy based method and investigates a suitable predetermined temperature profile. Furthermore, to facilitate design engineers, the method is proposed as a simple spreadsheet calculation. Through the empirical study of the FEM temperature profile, the exponent is found to be logarithmic proportional to the ratio of the lowest temperature to the highest in concrete slabs. The power function with variation of the exponent provides the better accurate temperature prediction. Comparing with FEM analysis and experimental results, the spreadsheet calculation is validated for temperature prediction of concrete slab under various fire loads.*

Keywords: *Concrete Slab, Energy Based Method, Fire Loads, Spreadsheet Calculation, Temperature Prediction*

Nomenclature

A	Surface area
b	Slab thickness
b'	Effective thickness
c	Specific heat
ε	Resultant emissivity
h	Coefficient of heat transfer convection
i	Subscript which denotes the number of a grid point
k	Thermal conductivity
n	Subscript which denotes the number of a time step
q	Heat flux
Q_I^n	Heat energy in the section
Q_T^n	Heat transfer energy from fire load
s	Location of i at the fire exposed surface
t	Fire duration
T	Temperature
$T^n(x)$	Concrete temperature profile at time step n
T_f	Fire temperature
$T_{f,EX}$	Fire temperature of the external fire curve (EX)
$T_{f,HY}$	Fire temperature of the hydrocarbon curve (HY)
$T_{f,ST}$	Fire temperature of the standard temperature-time curve (ST)
T_0	Lowest temperature in the section
T_r	Room temperature
T_s	Fire exposed surface temperature
α	Power of the function
Δx	Small intervals in the slab
Δt	Time increment
σ	Stefan Boltzmann constant
ρ	Material density

I. Introduction

To design fire resistance of reinforced concrete (RC) members, the prescriptive methods [1]-[3] specify minimum cross-section dimensions and minimum clear cover to the reinforcing bars. However the methods are limited to experimental results or predetermined analysis under standard temperature-time curves such as BS 476 [4] ASTM E 119 [5], ISO 834 [6]. For different temperature-time curves as in the performance-based approach, the methods cannot be applied to fire safety design. Heat transfer analysis and structural analysis are required to evaluate a structural capacity of RC members under various fire loads.

As a simple RC design under fire loads, spreadsheet calculation of the structural analysis based on the cross sectional approach [7], [8] can be applied. To use the simple calculations, temperature profiles in RC cross

Manuscript received and revised August 2012, accepted September 2012

section must be predetermined to specify mechanical properties of the section corresponding to its temperature. Structural designers can apply the predetermined temperature profiles of the fire safety standards such as BS EN 1992-1-2 [2]. However, the predetermined temperature profiles cover only some cross-section dimensions under a standard temperature-time curve. Without a convenient temperature prediction, the simple RC design under fire loads is limited.

Even though, temperature in a structural steel member can simply be computed through the iterative calculation method [9], [10], the method is only suitable for high thermal conductivity such as steel material. The iterative calculation method cannot be applied for concrete section due to its much lower thermal conductivity. To conduct heat transfer analysis, the finite element method (FEM) and the finite difference method (FDM) are powerful for concrete sections. The FEM and the FDM are a numerical technique for finding approximate solutions to partial differential equations (PDE) including the heat transfer equation. The FEM is considered as the most accurate tool to predict the temperature profile whereas the FDM is a simplified form of the FEM.

However, cost of their software as well as their requirement of expertise users makes both methods impractical for normal design. Both methods are complicate to be developed by design engineers, but normally limited for research works.

Simplified methods to predict the temperature profile is very limited. Wickstrom [11] proposed a simplified method to predict temperature in concrete slab based on predetermined temperature variation derived from computer-based thermal analysis. However, the method provides its accurate predictions for the fire load of ISO 834 [6]. Panedpojaman [12] established a modified FDM to predict temperature in concrete slabs under various fire loads. The method is based on the predetermined shape function of the temperature profile and the energy conservation. Inconvenience of the large FDM matrix to solve the temperature profile at each time step can be avoided by using the energy based method. However, inaccuracy of the temperature prediction is its disadvantage. Therefore, this study is aimed to improve the accuracy of the energy based method. The method is reformulated whereas a suitable predetermined shape function of the temperature profile is investigated. The method is proposed as a simple spreadsheet calculation to facilitate design engineers. The research conducted in this study is limited to concrete sections exposed to monotonically increasing fire curves on their one side such as slabs or walls.

II. Finite Difference Method

Due to the energy based method is a modified FDM, brief concepts of the FDM is described in this section.

Consider a system exposed to a fire on their one side which is finite in direction of the x-coordinate as shown in Fig. 1. For a system with one dimensional thermal load with the constant thermal properties and without the heat generation in the system, unsteady-state conduction problem is governed by:

$$\frac{\partial^2 T}{\partial x^2} = \frac{\rho c}{k}\frac{\partial T}{\partial t} \tag{1}$$

where T is the temperature; ρ is the density; c is the specific heat; k is the thermal conductivity; and t is the fire duration. The equation is employed to compute temperature profiles in the analyzed section as a function of time. At the fire-exposed surface, a convection and radiation boundary condition exists. For the one dimensional system, the boundary condition at the fire-exposed surface, $x = b$, is expressed in (2). The non fire-exposed surface is considered as insulation or zero heat flux, q, boundary condition as expressed in (3). Such condition is also a mathematical expression of this thermal symmetry in direction of the x-coordinate:

$$k\frac{\partial T}{\partial x} = q\left(x = b\right) = h\left(T_f - T_s\right) + \varepsilon\sigma\left(T_f^4 - T_s^4\right) \tag{2}$$

$$k\frac{\partial T}{\partial x} = q\left(x = 0\right) = 0 \tag{3}$$

where T_f is the fire temperature (^{o}K) which is a function of time; T_s is the temperature (^{o}K) at the fire exposed surface; h is the coefficient of heat transfer convection; and ε and σ are the resultant emissivity and Stefan Boltzmann constant, respectively.

To solve the partial differential equation in (1), the finite difference method as a numerical technique can be applied. The finite difference of derivatives involves the approximation of a differential equation by algebraic equations. The equations are pointwise continuous which is applicable throughout the region and space considered.

A network of grid points by dividing x and t domains into small intervals of Δx, as shown in Fig. 1, and Δt is applied. T_i^n represents the temperature at location $x = i\Delta x$ at $t = n\Delta t$. i is the number of a grid point and n is the number of a time step.

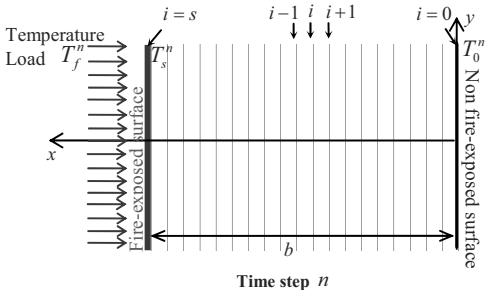

Fig. 1. Nodal network of a section exposed to a fire on its one side

Based on the forward-difference approximation, (1) used to solve the temperature at the internal grid points is represented in (4). Corresponding to (2) and (4), the temperature at the fire-exposed surface is represented in (5) which takes the heat capacity of the interval next to the boundary into account [13]. Therefore, T_s^{n+1} can be solved based on the temperature of the previous step.

Note that due to (5) is related to T_s^{n+1} and T_s^n, q^n in (5) is replaced by $q^{n+1/2}$ given by (6) to provide a neutral approximation and T_s^{n+1} is rewritten in (7):

$$\frac{T_{i+1}^n + T_{i-1}^n - 2T_i^n}{(\Delta x)^2} = \frac{\rho c}{k}\frac{T_i^{n+1} - T_i^n}{\Delta t} \tag{4}$$

$$T_s^{n+1} = \frac{2\Delta t}{\rho c \Delta x}\left[q^n - k\frac{T_s^n - T_{s-1}^n}{\Delta x}\right] + T_s^n \tag{5}$$

$$q^{n+1/2} \approx h\left(T_f^{n+1/2} - T_s^n\right) + \varepsilon\sigma\left(\left(T_f^{n+1/2}\right)^4 - \left(T_s^n\right)^4\right) \tag{6}$$

$$T_s^{n+1} = \frac{2\Delta t}{\rho c \Delta x}\left[q^{n+1/2} - k\frac{T_s^n - T_{s-1}^n}{\Delta x}\right] + T_s^n \tag{7}$$

To provide stable solutions and avoidance to violation of the second law of thermodynamics, (4) and (7) must be satisfied the stability condition in (8) and (9), respectively:

$$(k/\rho c)\left(\Delta t/\Delta x^2\right) \le 0.5 \tag{8}$$

$$q^{n+1/2} - k\frac{T_s^n - T_{s-1}^n}{\Delta x} > 0 \tag{9}$$

The FDM is solved in terms of the nodal temperature matrix at each time step. The method is more complicated to solve the temperature corresponding to the stability condition when the fire curves and variation of the thermal properties with temperature are involved.

III. Energy Based Method

The energy based method, EBM, [12] is a simplified FDM to predict the temperature in concrete slabs under various monotonically increasing fire curves. The method is established based on the energy conservation principle and a predetermined shape function of the temperature profile in concrete sections. However accuracy of the temperature prediction is its disadvantage. The surface temperature equation and the predetermined temperature profile are reformulated in this study.

Based on the empirical investigation as described in the next section, the concrete temperature profile, $T^n(x)$, within concrete sections exposed to fire on their one direction at a time step n is considered as the power function with exponent variation as follows:

$$T^n(x) = C^n x^{\alpha^n} + T_0^n \tag{10}$$

where:

$$C^n = \frac{T_s^n - T_0^n}{\left(b'^n\right)^{\alpha^n}} \tag{11}$$

α^n is the power of the function; T_0 is the lowest temperature in the section; and b'^n is the effective thickness as described in Figs. 2 in which temperatures in this zone is higher than the room temperature, T_r. To specify the temperature profile function at a time step n, T_s^n, T_0^n and b'^n are the key parameters.

Through the predetermined temperature profile, T_s^{n+1} in (7) can be modified by substituting the term of $\left(T_{s-1}^n - T_s^n\right)/\Delta x$ with the derivative function of $T^n(x)$ in (10) at the mid point of the edge interval as given in (12). The equation of T_s^{n+1} in (7) and the stability condition in (9) can be reformulated in (13) and (14), respectively:

$$\frac{T_{s-1}^n - T_s^n}{\Delta x} \approx \left.\frac{dT^n(x)}{dx}\right|_{x=b'^n-\Delta x/2} = C^n\alpha^n\left(b'^n - \Delta x/2\right)^{\alpha^n-1} \tag{12}$$

$$T_s^{n+1} = \frac{2\Delta t}{\rho c \Delta x}\left[\begin{array}{l} q^{n+1/2} + \\ -kC^n\alpha^n\left(b'^n - \Delta x/2\right)^{\alpha^n-1}\end{array}\right] + T_s^n \tag{13}$$

$$q^{n+1/2} - kC^n\alpha^n\left(b'^n - \Delta x/2\right)^{\alpha^n-1} > 0 \tag{14}$$

Note that the EBM of [12] assumed the α^n value to be constant as 2.7 whereas the derivative term in (15) was applied:

$$\frac{T_{s-1}^n - T_s^n}{\Delta x} \approx \left.\frac{dT^n(x)}{dx}\right|_{x=b} = \alpha\frac{T_s^n - T_0^n}{b} \tag{15}$$

The derivative term in (15) is suitable only for a very small Δx. However, through the empirical investigation as described in the next section, it is found that a very

small value of Δx cannot be satisfied the stability condition in (14).

T_0^n can be computed through the energy conservation in which the heat transfer energy from fire load Q_T^n in (16) balances the heat energy in the section Q_I^n in (17).

The heat energy in the section is to take the heat capacity of the system and the temperature profile into consideration as shown in Figs. 2:

$$Q_T{}^n = \sum_{m=1}^{n} A\left(-q^m\right)\Delta t \tag{16}$$

$$\begin{aligned} Q_I{}^n &= \int_0^{b''} \rho cA\left(T^n(x) - T_r\right)dx = \\ &= \rho cAb'^n\left[\frac{\left(T_s^n - T_0^n\right)}{\left(\alpha^n + 1\right)} + \left(T_0^n - T_r\right)\right] \end{aligned} \tag{17}$$

where A is the surface area. Due to a uniform temperature load throughout the fire-exposed surface is assumed, the surface area can be considered as a unit area (i.e., $A = 1$). The energy conservation equation (i.e., $Q_T^n = Q_I^n$) is rearranged as:

$$Q_T{}^n = \rho cb'^n\left[\frac{\left(T_s^n - T_0^n\right)}{\left(\alpha^n + 1\right)} + \left(T_0^n - T_r\right)\right] \tag{18}$$

As shown in Figs. 2, two cases of the energy based temperature profile are considered: the low energy case and the high energy case. For the low energy case, the heat energy does not affect throughout the slab thickness b.

The effective heat transfer thickness b'^n is less than b and T_0^n is equal to T_r. b'^n can be computed based on (18) as:

$$b'' = \frac{Q_T{}^n\left(\alpha^n + 1\right)}{\rho c\left(T_s^n - T_r\right)} \tag{19}$$

For the high energy case, the heat energy affect throughout the slab thickness b, that is $b'^n = b$ and $T_0^n > T_r$. T_0^n can be computed based on (18) as:

$$T_0^n = \frac{1}{\alpha^n}\left[\left(\alpha^n + 1\right)\left(\frac{Q_T{}^n}{\rho cb} + T_r\right) - T_s^n\right] \geq T_r, T_0^{n-1} \tag{20}$$

By substituted the computed value of T_s^n, b'^n and T_0^n in (10) and (11), the temperature profile $T^n(x)$ in concrete slabs under various fire load can be predicted.

Due to the predetermined temperature profile is highest at the fire-exposed surface and decrease in the inner, the profile cannot violate the second law of thermodynamics. The stability condition in (8) is omitted in the EBM.

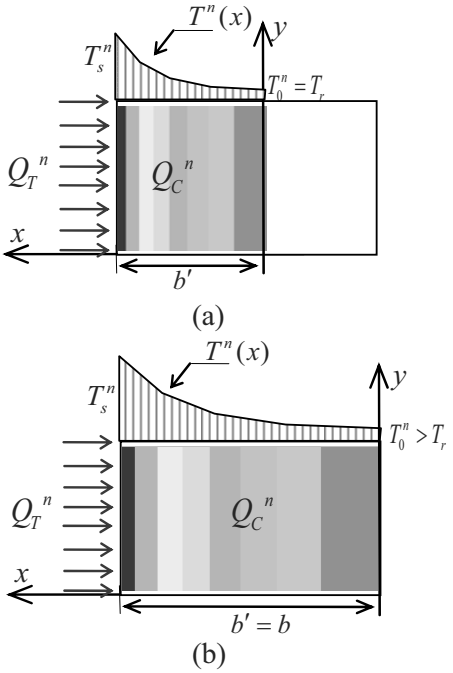

Figs. 2. Energy conservation of the fire-exposed section: (a) Low energy case; (b) High energy case

However, the stability condition in (14) must be checked. Due to variation of T_f^n with time, the dissatisfaction of the stability condition can be occurred in any time step in both typical FDM and The spreadsheet calculations. The dissatisfaction causes $T_s^{n+1} \leq T_s^n$ which is incorrect for the slab under monotonically increasing fire curves. Normally, Δx and Δt must be resized to satisfy the stability condition.

However, to simply implement in regular spreadsheet software, this study assumes T_s^n in the dissatisfied step equal to T_s^{n-1}. The procedure to predict the temperature profile in the fire-exposed section under a fire load can be summarized as illustrated in Fig. 3.

IV. Investigation of Predetermined Temperature Profile

To determine the predetermined temperature profile of concrete slabs, variation of the temperature profile with time analyzed by the FEM [14], ANSYS software, is investigated. The FEM models as shown in Fig. 4 are concrete slabs with thickness of 100, 300 and 500 mm.

The slab is modeled with Solid70, three-dimensional solid elements, having eight nodes with a single degree of freedom (i.e., temperature) at each node. The surface element at the fire-exposed surface is modeled with Surf152. The surface element is capable to account for heat convection and radiation of the fire temperature.

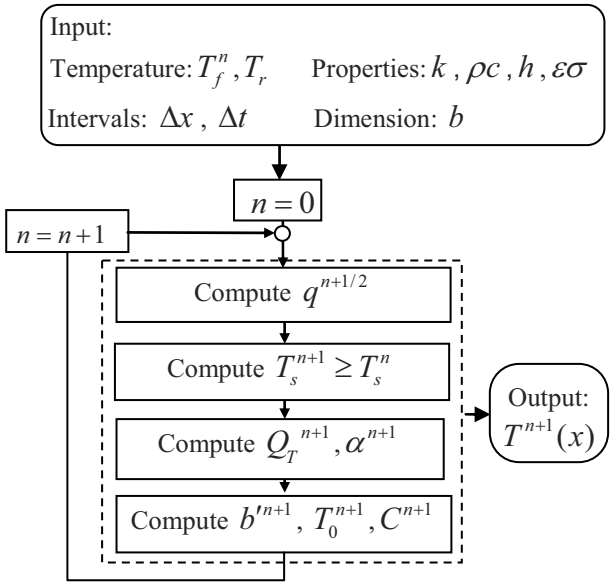

Fig. 3. Procedure to predict the temperature profile

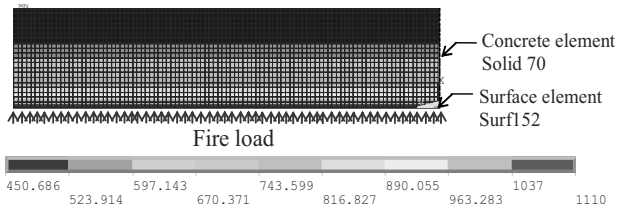

Fig. 4. FEM model

The nominal temperature-time curves [2] include the external fire curve (EX), the standard temperature-time curve (ST) and the hydrocarbon curve (HY) are used as fire loads in the slab model as shown in Fig. 5.

The functions of the curves are given as follows:

$$T_{f,EX} = 660\left(1 - 0.687e^{-0.32t} - 0.313e^{-3.8t}\right) + 20 \quad (21)$$

$$T_{f,ST} = 20 + 345\log_{10}\left(8t + 1\right) \quad (22)$$

$$T_{f,HY} = 1080\left(1 - 0.325e^{-0.167t} - 0.675e^{-2.5t}\right) + 20 \quad (23)$$

where $T_{f,EX}$, $T_{f,ST}$ and $T_{f,HY}$ are the temperature (^{o}C) of EX, ST and HY fire, respectively; and t is the time in minute.

The thermal properties of concrete are in accordance with BS EN 1992-1-2 (2004) [2]. Density and specific heat of concrete with siliceous or calcareous aggregates described in Table I are used in the FEM model. The thermal conductivity (W/m°K) as given in (24) is based on the lower limit of thermal conductivity of concrete which gives more realistic temperatures for concrete structures [2].

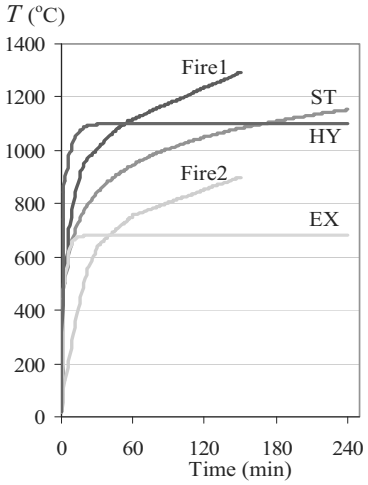

Fig. 5. Temperature-time curve

The coefficient of heat transfer-convection h is 25 W/m^2°K for the ST and EX temperature-time curve and 50 W/m^2°K for the HY curve. Stefan Boltzmann constant of 5.67×10^{-8} W/m^2°K^4 and the resultant emissivity of 0.7 are specified according to BS EN 1991-1-2 (2002) [15]. The normal concrete density of 2300 kg/m^3 at the room temperature is assumed in the model:

$$k = 1.36 - 0.136\left(T/100\right) + 0.0057\left(T/100\right)^2 \quad (24)$$

However, to simplify the EBM computation, the value of ρc is conservatively assumed to be a constant value of 2.1x10^6 J/m^3°K.

TABLE I
VARIATION DENSITY AND SPECIFIC HEAT OF CONCRETE WITH TEMPERATURE

T (°C)	ρ (kg/m^3)	c (J/kg°K)	ρc (J/m^3°K)
20	2.30E+3	9.00E+2	2.07E+6
100	2.30E+3	9.00E+2	2.07E+6
200	2.25E+3	1.00E+3	2.25E+6
300	2.22E+3	1.05E+3	2.33E+6
400	2.19E+3	1.10E+3	2.40E+6
600	2.14E+3	1.10E+3	2.36E+6
800	2.10E+3	1.10E+3	2.31E+6
1000	2.06E+3	1.10E+3	2.27E+6
1200	2.02E+3	1.10E+3	2.23E+6

The analyzed temperature profile under the three fire loads at fire duration of 0.5, 1, 1.5, 2, 2.5, 3, 3.5 and 4 hr is recorded to investigate the predetermined profile.

The maximum fire duration of 4 hr refers to the maximum required fire-resistance of structural members.

As a result, 72 temperature profiles (3 sections × 3 fire curves × 8 fire durations) are considered.

The FEM temperature profiles of the various fire loads are partly shown in Fig. 6. The power function is empirically found to be fit to the FEM profile. The best fit power value of each FEM profile is computed by the regression analysis.

Through the empirical investigation, the logarithmic relationship between the power value and the value of $\Delta T_0^n / T_s^n$ is observed as shown in Fig. 7.

The logarithmic function of the power value is suggested as:

$$\alpha^n \approx -0.7\, ln\left(\Delta T_0^{n-1} / T_s^{n-1}\right) + 1.4 \tag{25}$$

where:

$$\Delta T_0^{n-1} = T_0^{n-1} - T_r + 10^{-4} \tag{26}$$

The logarithmic function is corresponding to the high conductive heat flux in the concrete slab.

The EBM temperature profile with the proposed α^n function is computed and compared with the FEM temperature as shown in Fig. 6. Size of the interval Δx of 10 mm and the time increment Δt of 60 s is specified in the EBM computation.

The accuracy of the predict temperature profile is observed in the figure. The example of the EBM spreadsheet calculation for the slab with 100 mm thickness under the ST fire curve is shown in Table II.

To illustrate the accuracy improvement of the proposed method, variation of the temperature with time of the 100mm thick slab at 25 mm 50 mm and 100 mm from fire-exposed surface is investigated. Comparison of the FEM variation with those obtained from the proposed and original method is shown in Figs. 8.

Comparing with the FEM variation, the original method slightly underestimates the temperature at the near fire-exposed surface but significantly deviate at the non fire-exposed surface. The proposed method clearly provides the predicted variation very fit to the FEM profile for various fire durations.

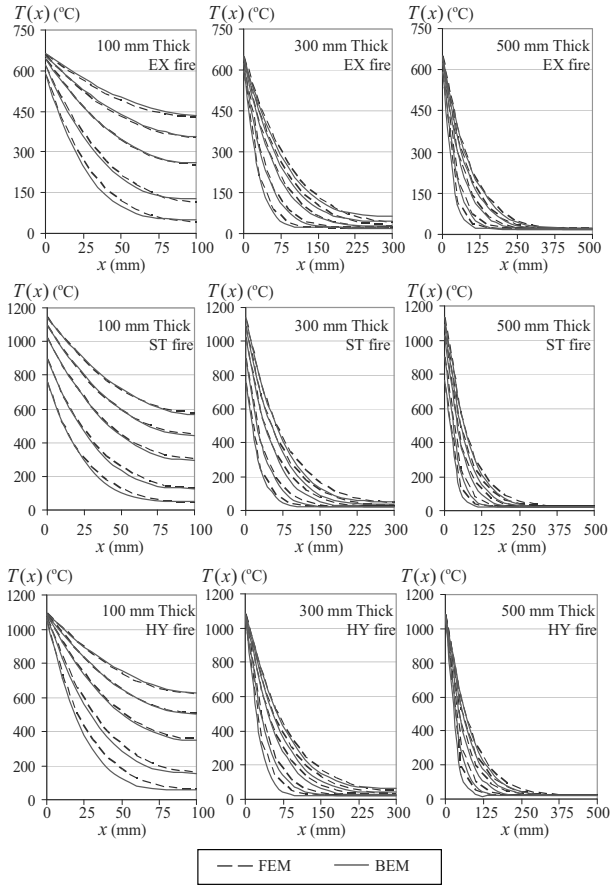

Fig. 6. FEM profile and EBM profile under various fire loads

TABLE II
EXAMPLE OF THE SPREADSHEET CALCULATION

Step n	t	$T_{f,ST}^n$	$q^{n+1/2}$	k	T_s^n	${Q_p}^n$	α^n	b'^n	T_o^n	C^n	T^n
	(s)	(°C)	(W/m^2)	(W/m°K)	(°C)	(J)		(m)	(°C)	(°C/m$^\alpha$)	(.05m)
0	0	20	5.6×10^3	1.33	20				20		20
1	60	349	1.6×10^4	1.31	52	3.1×10^5	9.9	0.05	20	2.7×10^{14}	20
2	120	445	2.0×10^4	1.25	123	1.2×10^6	9.9	0.06	20	1.2×10^{14}	20
3	180	502	2.3×10^4	1.21	177	2.4×10^6	9.9	0.08	20	1.5×10^{13}	20
4	240	544	2.5×10^4	1.16	228	3.7×10^6	9.9	0.09	20	4.1×10^{12}	20
5	300	576	2.6×10^4	1.12	276	5.1×10^6	9.9	0.10	21	2.2×10^{12}	21
.											
.											
30	1800	842	1.8×10^4	0.72	764	3.7×10^7	3.8	0.10	48	4.2×10^6	101
.											
.											
60	3600	945	1.3×10^4	0.64	901	6.4×10^7	2.9	0.10	129	6.1×10^5	232
.											
.											
120	7200	1049	9.5×10^4	0.58	1025	1.0×10^8	2.3	0.10	295	1.5×10^5	440
.											
.											
180	10800	1110	7.3×10^3	0.56	1093	1.3×10^8	2.1	0.10	442	7.7×10^4	597
.											
.											
240	14400	1153	6.0×10^3	0.56	1141	1.6×10^8	1.9	0.10	567	4.7×10^4	719

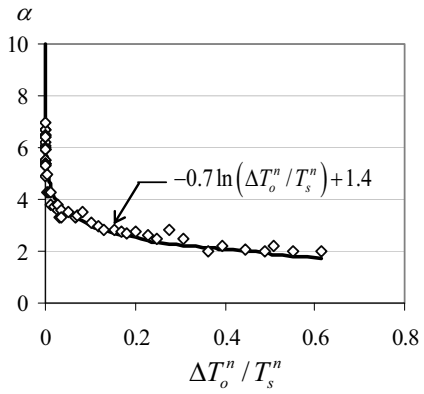

Fig. 7. Logarithmic relationship between the power value and the value of T_0^n / T_s^n

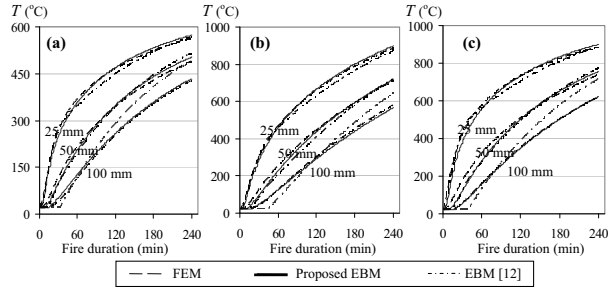

Figs. 8. Comparison of the FEM variation with those obtained from the proposed and original method: (a) under EX fire, (b) under ST fire and (c) under HY fire

V. Sensitivity and Validation of the Energy Based Method

In addition to the suitable α function, the prediction accuracy of the energy based method is also depended on accuracy of the slab heat energy Q_T and the heat flux q which relates to T_s^n. Based on the temperature of the previous step, size of Δx and Δt, T_s^n in (13) can be computed. Therefore, size of Δx and Δt dose not only affect the stability condition, but the temperature accuracy as well. To describe influence of Δx and Δt on the temperature prediction, the temperature computation of the 100mm thick slab under the ST fire curve with various Δx and Δt conducted as shown in Fig. 9. The temperatures are investigated at 0 mm (T_s^n), 25 mm and 100 mm (T_0^n) from the fire-exposed surface.

Comparing with the FEM temperature, Fig. 9 illustrates that the predicted temperature is accurate for the computation with the small value of Δx and Δt.

The value of Δx and Δt less affects T_s^n. The large value of Δx and Δt trends to provide the underestimated temperature, especially near the non fire-exposed surface. However, it is found that the temperature cannot be computed for very small value of Δx due to the dissatisfaction of the stability condition for all steps. Furthermore, for the larger value of Δt, the larger value of Δx is required to satisfy the stability condition. In the computation with Δt of 300 s, Δx of 10 mm cannot be satisfied the stability computation along the process.

Through the various slab models, the Δx value of 10 mm and the Δt value of 60 s are suitable to provide the accurately predicted temperature as well as the satisfaction of the stability condition.

The spreadsheet calculation of the EBM are validated by comparing its computed temperature with those of the previous researches [2], [16], [17] and the FEM profile as shown in Figs. 10 and 11.

Details of concrete slabs in the comparison are described in Table III. Note that Fire 1 and Fire 2 in Table III is a parametric temperature–time curve [18] based on compartment properties such as the fuel load, ventilation opening and wall linings [19].

The parametric fire consists of a growth phase and a decay phase.

However, the study is limited to the growth phase as a monotonically increasing function.

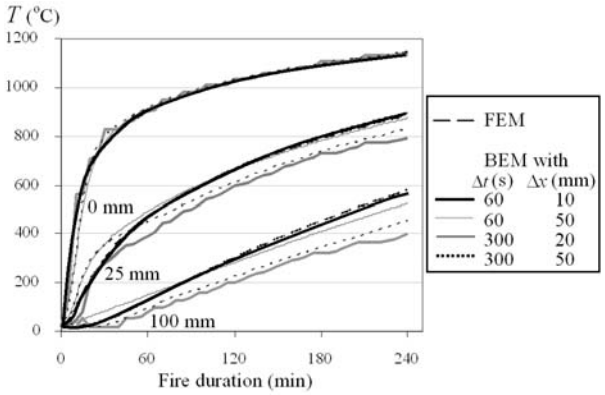

Fig. 9. Sensitivity of Δx and Δt on the predicted temperature

TABLE III
DETAILS OF CONCRETE SLABS IN THE COMPARISON

Case symbol	Thick. (mm)	Location of recorded Temp. from fire surface (mm)	Fire curve	Reported by
ST-90	90	20, 40, 60, 80	ST	[16]
ST-100	100	30, 55, 80, 95		
ST-160	160	0, 42, 160	ST	[17]
ST-200	200	-	ST	[2]
F1-120	120	0, 30, 50, 120	Fire1 [19] (Fig. 5)	-
F1-180	180	0, 30, 50, 180		
F2-120	120	0, 30, 50, 120	Fire2 [19] (Fig. 5)	-
F2-180	180	0, 30, 50, 180		

It is observed in Fig. 10 that the results of the spreadsheet calculation agree well with the FEM temperature and slightly deviate from the results of the previous researches.

As shown in Fig. 11, the predicted temperature of concrete slab under parametric temperature–time curves also agrees well with the FEM temperature.

The spreadsheet calculation can thus be used to approximate the temperature profile in concrete slab exposed to various fire loads.

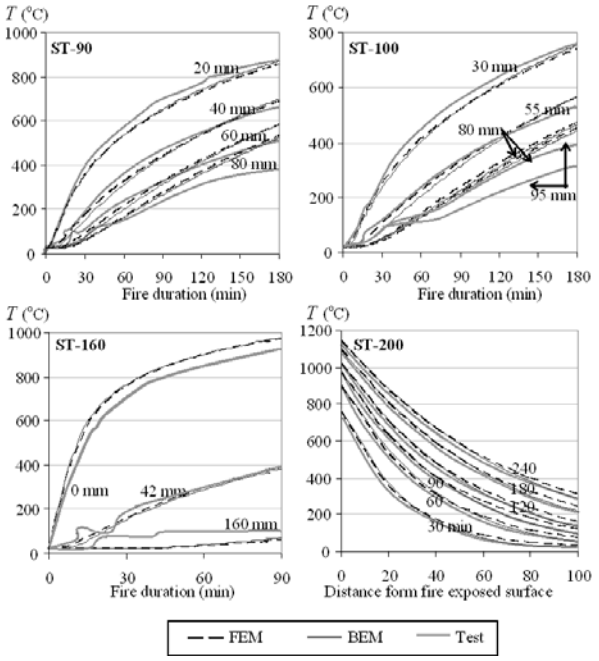

Fig. 10. Comparison of the predicted slab temperature under ST fire with the FEM temperature and the experimental results

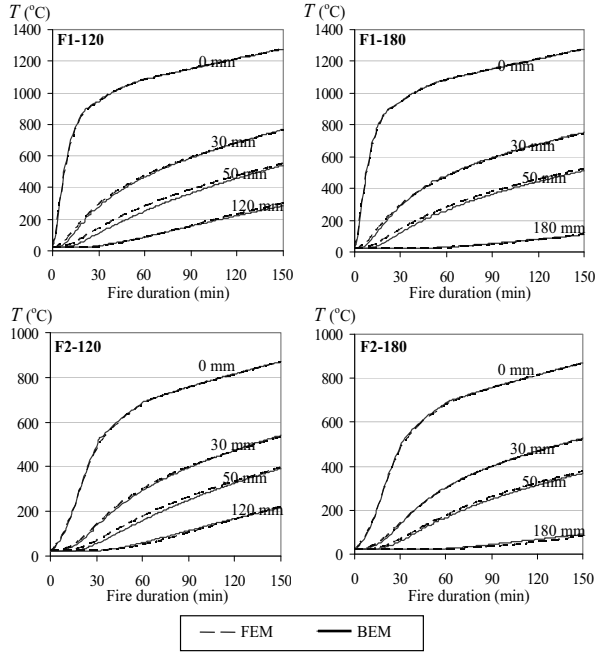

Fig. 11. Comparison of the predicted slab temperature under the parametric temperature–time curves with the FEM temperature

VI. Conclusion

To improve the temperature prediction within concrete slabs, the energy based method is reformulated whereas the suitable predetermined temperature profile is investigated. Furthermore, the method is proposed as a spreadsheet calculation for practical use.

The method as a simplified finite difference method is derived based on the energy conservation principle and a predetermined temperature profile. The equation of the fire surface temperature is reformulated to be more reasonable based on the derivative of the suitable profile function. Comparing with the FEM analysis, the power function is found to be a suitable predetermined shape function of the profile. By using the regression analysis of the various FEM temperature profile, the power value of the predetermined function is suggested to be a logarithmic function of the ratio of the lowest temperature in slabs to the highest.

In addition to the suitable predetermined shape function, the accuracy of the method also depends on the interval size and the time increment. The computation with the interval size of 10 mm and the time increment of 60 second provides the accurate temperature prediction as well as the stable computation along the process. The spreadsheet calculation is validated by comparing its temperature prediction with those of the previous researches and the FEM profile.

By using the spreadsheet calculation, the complicated temperature matrix of the FDM nodal network can be avoided. The method is also useful to manipulate the stability conditions of the FDM. Design engineers can simply evaluate the temperature profile by using regular spreadsheet software. The method facilitates design engineers analyzing the heat transfer which is a necessary part to investigate the fire resistance and the structural behavior of concrete structures under various fire scenarios. The spreadsheet calculation is potential to develop for concrete sections with two direction fire loads such as column and beam cases.

Acknowledgements

The authors would like to acknowledge Faculty of Engineering, Prince of Songkla University, Thailand for providing the financial support for this research project (contract no. ENG-55-2-7-02-0139-S).

References

[1] AS 3600, *Concrete structures* (Committee BD-002, Australia, 2001).

[2] BS EN 1992-1-2, *Design of concrete structures: General rules—Structural fire design* (European Committee for Standardization, Brussels, Belgium, 2004).

[3] ACI 216.1-07, *Standard method for determining fire resistance of concrete and masonry construction assemblies* (American Concrete Institute, Detroit, 2007).

[4] BS 476, *Fire tests on building materials and structures—Part 20: method from determination of the fire resistance of elements of construction (general principles)* (BSi, UK, 1987).

[5] ASTM E 119, *Standard methods of fire test of building construction and materials, Test Method* (American Society for Testing and Materials, West Conshohocken, PA, 2008).

[6] ISO 834, *Fire-resistance tests—elements of building construction—Part 1: General requirements* (International Standard, Geneva, 1999).
[7] S.F. El-Fitiany and M.A. Youssef, Assessing the flexural and axial behaviour of reinforced concrete members at elevated temperatures using sectional analysis, *Fire Safety Journal, Vol. 44:691–703, July 2009*.
[8] P. Panedpojaman, Predicting Moment Capacity of RC Beams under Fire by Using Two-dimensional Sectional Analysis, *The 4th KKU International Engineering Conference, pp. 93-99 2012, Khonkaen, Thailand, May 2012.*
[9] ENV 1993-1-2, *Design of steel structures—part 1-2. General rules—structural fire design* (European Committee for Standardization, Brussels, Belgium, 1995).
[10] W.L. Gamble, Predicting Protected Steel Member Fire Endurance Using Spread-sheet Programs, Technical Note, *Fire Technology*, *Vol. 25(*Issue 3*):256-273, 1989*.
[11] U. Wickstrom, *Fire Technology Technical Report SP-RAPP 1986A very simple method for estimating temperature in fire exposed concrete structures* (Swedish National Testing Institute, 1986, pp. 186–194).
[12] P. Panedpojaman, Energy Based Temperature Profile for Heat Transfer Analysis of Concrete Section Exposed to Fire on One Side, *World Academy of Science, Engineering and Technology (*Issue 65*):897-902, 2012*.
[13] K. V. Wong, *Intermediate Heat Transfer* (New York, Marcel Dekker Inc., 2003, pp. 83-125).
[14] ANSYS, *ANSYS multiphysics. Version 11.0 SP1* (Canonsburg (PA), ANSYS Inc., , 2007).
[15] BS EN 1991-1-2, *Actions on structures: Part 1-2 General actions—structures exposed to fire* (European Committee for Standardization, Brussels, Belgium, 2002).
[16] L. Lim and C. Wade, *Fire Engineering Research Report 02/12: Experimental Fire Tests of Two-Way Concrete Slabs*, (New Zealand, BRANZ Limited, 2012).
[17] C.G. Bailey and E. Ellobody, Fire tests on bonded post-tensioned concrete slabs, *Engineering Sericulture*, *Vol. 45(*Issue 3*):686–696, March 2009*.
[18] V.K.R. Kodur, P.Pakala and M.B.Dwaikat, Energy based time equivalent approach for evaluating fire resistance of reinforced concrete beams, *Fire Safety Journal, Vol. 45(*Issue 4*):211–220, June 2010.*
[19] R. Feasey and A.H. Buchanan, Post-flashover fires for structural design, *Fire Safety Journal, Vol. 37(*Issue 1*):83–105, February 2002*.

Authors' information

Prince of Songkla University, Faculty of Engineering, Civil Engineering Department, Hat-Yai, Songkhla, Thailand, 90110.

Pattamad Panedpojaman was born on the 8th October, 1980 at Songkhla, Thailand. In 2005 he took Master degree in Civil Engineering at Chulalongkorn University, Thailand. In 2011 he took Ph.D. degree in Civil Engineering at Chulalongkorn University.
His recent publications include: Effects of tensile softening on the cracking resistance of FRP reinforced concrete under thermal loads, published in Structural Engineering and Mechanics; Fire resistance evaluation for the steel roof structure of a typical warehouse, published in ASEAN Engineering Journal; Modeling of bonding between steel rebar and concrete at elevated temperatures, published in Construction and Building Materials; and Modified Quasi-static, Elastic-plastic Analysis for Blast Walls with Partially Fixed Support, published in Engineering Journal. His research focuses on a simplified method to evaluate fire resistance of structural member, design of cellular beams and blast wall systems, and fire modeling for structural analysis.
Dr. Panedpojaman is member of Council of Engineers, Thailand and the Engineering Institute of Thailand.

Energy Based Method for Heat Transfer Analysis of Rectangular Concrete Sections

Pattamad Panedpojaman[1,*] and Passagorn Chaiviriyawong[2]
[1]Lecturer, Department of Civil Engineering, Faculty of Engineering,
Prince of Songkla University, Songkhla 90110, Thailand.
[2]Assistant Professor, Department of Civil Engineering, Faculty of Engineering,
Prince of Songkla University, Songkhla 90110, Thailand.

* Corresponding author. Pattamad Panedpojaman, Department of Civil Engineering,
Faculty of Engineering, Prince of Songkla University, Songkhla 90110, Thailand.
Tel. (6674) 28-7140, Fax (6674) 45-9396, E-mail address: ppattamad@eng.psu.ac.th

Abstract
In addition to the prescriptive method used in design, the fire resistance of reinforced concrete structures under various fire scenarios needs to be assessed by combined heat transfer and structural analysis. The available numerical simulations of heat transfer analysis are complicated techniques and require an expert user. To simply predict temperature within rectangular concrete sections subjected to various fire loads in two directions, the energy based method is proposed for practical use. The method is based on a pre-determined power function as the temperature profile, and conservation of energy: it can be implemented in a spreadsheet. The power function is suitable for monotonically increasing fire curves such as the nominal temperature-time curves. The analysis of two dimensional heat transfer is approximated by superposition of one-dimensional solutions. Benchmarking against FEM analysis of various sections shows that an exponent 2.6 performs well to predict the temperature. By comparing the temperature prediction with the previous experimental and FEM results, the method is validated. However, the method has its limitations; in particular the lowest temperature needs to remain less than 0.2 times the highest, or the energy estimated becomes inaccurate. The method is used to predict the temperature profile as well as the temperature at the reinforcing location: knowledge of these is necessary for fire safety design.

Keywords: Energy based method; Fire; Heat transfer analysis; Rectangular concrete section; Temperature prediction.

1. Introduction

Under fire exposure, structural members including reinforced concrete (RC) members lose both strength and stiffness. A high temperature significantly degrades the mechanical properties of concrete and steel [1]. To ensure fire safety, RC members are to be designed against fire load. In the prescriptive design method, fire resistance is pursued with prescribed minimum cross-section dimensions and minimum clear cover to the reinforcing bars, as in AS 3600 [2], BS EN 1992-1-2 [1] and ACI 216.1 [3]. These provisions are based on prior analysis under a specific fire curve, and do not match general fire scenarios and conditions.

The fire resistance or behavior of RC structures under different fire scenarios must be investigated through both heat transfer analysis and structural analysis. A detailed structural analysis is normally done with the finite element method (FEM), or other numerical packages. However, for simplified calculations such as the 500°C

isotherm method [1], and a sectional analysis method, no expensive software is needed as a regular spreadsheet program suffices.

For the heat transfer analysis, various formulations of transient conduction in sections have been proposed by a number of researchers [4-7]. The formulations are more complicated when the thermal properties vary and fire curves are involved. As a result, there are sophisticated numerical codes for solving the transient heat conduction problems of concrete section exposed to fire, including the use of finite difference method, FDM, [8] and finite element method, FEM, implemented in packages such as SAFIR [9] and ANSYS [10]. However, these methods are rather complicated for normal design, especially the FEM. Usually the FDM is considered simpler to adopt in research [8, 11-13]. In the FDM, a nodal network replaces the continuum of points, and a set of algebraic equations replaces the differential equations. To compute the temperature in sections, a large matrix of the temperatures of all nodal points at each time step is required. There are also stability conditions, relating the time step to the spatial grid. To manipulate these problems, El-Fitiany and Youssef [13] implemented the FDM as C++ code to predict temperature profiles.

Due to the complexity of the FDM and the FEM, requiring an expert user, a simplified method to predict the temperature is useful for practice. However, the availability of simplified methods is poor. Wickstrom [14] proposed an empirical hand calculation method to predict the temperature in a concrete slab under a specific fire curve. The method is derived from one dimensional heat transfer analysis and a pre-determined temperature variation. The method provides its accurate prediction only for a specific fire [13] and cannot be applied to concrete sections with heat conduction in two directions [15]. Panedpojaman [16] proposed the energy based method (EBM) to simply predict temperature in concrete slabs under various thermal loads. The EBM is a modified FDM by using a pre-determined shape function for the temperature profile and conservation of energy. However, the EBM [16] cannot also be used to predict temperature of concrete sections with heat conduction in two directions.

Therefore, we develop the EBM to predict the temperatures during two-dimensional heat conduction, as in the case of rectangular beams and columns. A suitable pre-determined shape function for rectangular concrete sections is investigated by comparing with the temperature profiles from the FEM for various sections. The predicted temperature is validated by comparing with previous experimental results. The method can be implemented in a regular spreadsheet program.

2. Finite Difference Method and Energy Based Method for One-dimensional Heat Transfer Analysis

We shall develop a simplified two-dimensional heat transfer analysis, based on the one-dimensional energy based method which is related to the finite difference method. The main concepts of both methods are described in this section.

Consider a section with thickness b in x-direction, exposed to fire on one side as shown in Fig. 1. The surface not exposed to fire could also be a line of symmetry in the x direction, or an insulated surface. For isotropic and homogeneous media, the heat conduction equation is derived from Fourier's law of heat conduction. A one dimensional unsteady conduction problem with constant thermal properties and without heat generation is governed by Eq. (1). This equation is solved

computationally for internal temperature profiles as functions of time t. In the case of fire, convection and radiation boundary conditions at $x = b$ determine the surface heat flux q in the x direction as in Eq. (2).

$$\frac{\partial^2 T}{\partial x^2} = \frac{\rho s_p}{k}\frac{\partial T}{\partial t} \tag{1}$$

$$k\frac{\partial T}{\partial x} = q = h\left(T_f - T_s\right) + \varepsilon\sigma\left(T_f^4 - T_s^4\right) \tag{2}$$

Here, k and s_p are the thermal conductivity and the specific heat; T, T_f and T_s are the temperature, the fire temperature and the fire-exposed surface temperature (^{o}K); ρ is the material density; h is the coefficient of heat transfer by convection; and ε and σ are the emissivity and Stefan Boltzmann constant that determine radiative heat transfer rates.

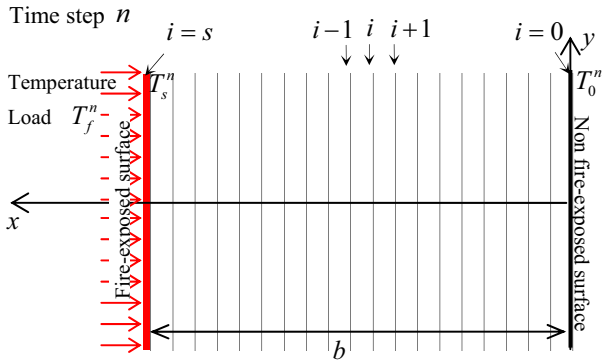

Fig. 1. The node indexing scheme for the one dimensional problem of a section exposed to a fire on one side.

2.1 The Finite Difference Method

The finite difference method is a numerical technique which can be applied to solve partial differential equations. The finite difference approximations of derivatives convert differential equations to algebraic equations. The approximations use uniform grids for each coordinate, including time, as illustrated in Fig. 1. As a convenient shorthand notation, T_i^n represents the temperature at location $x = i\Delta x$ at $t = n\Delta t$: so i is the index for location whereas n is the index for time. If the forward-difference approximation is used in Eq. (1), the finite-difference equation is represented as

$$\frac{T_{i+1}^n + T_{i-1}^n - 2T_i^n}{\left(\Delta x\right)^2} = \frac{\rho s_p}{k}\frac{T_i^{n+1} - T_i^n}{\Delta t} \tag{3}$$

The finite difference form of the boundary condition at $i = s$, Eq. (2), can be expressed as

$$k\frac{T_s^n - T_{s-1}^n}{\Delta x} = q^n = h\left(T_f^n - T_s^n\right) + \varepsilon\sigma\left(\left(T_f^n\right)^4 - \left(T_s^n\right)^4\right) \tag{4}$$

Due to the intervals of Δx in the FDM, the effect of the heat capacity of the system next to the boundary must be included in Eq. (4) [17] as

$$q^{n+1/2} - k\frac{T_s^n - T_{s-1}^n}{\Delta x} = \rho s_p \frac{\Delta x}{2}\frac{T_s^{n+1} - T_s^n}{\Delta t} \tag{5}$$

Note that to achieve symmetry in Eq. (5) relative to the time points T_s^{n+1} and T_s^n, q^n in Eq. (4) is replaced by $q^{n+1/2}$ of Eq. (6). Eq. (5) is rearranged in Eq. (7). Therefore, T_s^{n+1} can be solved based on temperature of the previous step.

$$q^{n+1/2} \approx h\left(T_f^{n+1/2} - T_s^n\right) + \varepsilon\sigma\left(\left(T_f^{n+1/2}\right)^4 - \left(T_s^n\right)^4\right) \quad (6)$$

$$T_s^{n+1} = \frac{2\Delta t}{\rho s_p \Delta x}\left[q^{n+1/2} - k\frac{T_s^n - T_{s-1}^n}{\Delta x}\right] + T_s^n \quad (7)$$

To avoid violating the second law of thermodynamics in Eq. (3), the stability condition $\left(k/\rho s_p\right)\left(\Delta t/\Delta x^2\right) \le 0.5$ has to be satisfied: for finer spatial resolution also smaller time steps are necessary, and the computational cost increases rapidly with spatial resolution. Furthermore, for increasing functions T_f, the value of T_s^{n+1} must be larger than the value of T_s^n. As a result, another stability condition has to be satisfied:

$$q^{n+1/2} - k\frac{T_s^n - T_{s-1}^n}{\Delta x} > 0 \quad (8)$$

To compute the temperature profiles, a matrix of the temperatures of all nodal points is computed at each time step. Δx and Δt must be manipulated to satisfy the stability conditions during the numerical solution.

2.2 Energy Based Temperature Profile Method, EBM

To simplify the FDM of the 1D analysis, the energy conservation principle and a pre-determined shape function of the temperature profile is adopted in [16]. The amount of energy transfer to a section under fire exposure, Q_{T1}^n, can be approximated as in Eq. (9) [18]. The amount of heat energy in that section, Q_{I1}^n, is computed taking into account the heat capacity of the system, and the temperature profile as shown in Fig. 2. Q_{I1}^n can be approximated as in Eq. (10). Based on the energy conservation principle, the cumulative energy transfer Q_{T1}^n equals the accumulated heat energy Q_{I1}^n as in Eq. (11)

$$Q_{T1}^n = \int_0^{t^n} qA\,dt \approx \sum_{m=0}^{n} A\left(q^m\right)\Delta t \quad (9)$$

$$Q_{I1}^n = \int_0^b \rho s_p A\left(T^n(x) - T_r\right)dx \quad (10)$$

$$Q_{T1}^n = Q_{I1}^n \text{ or } \sum_{m=1}^{n} A\left(q^m\right)\Delta t = \int_0^b \rho s_p A\left(T^n(x) - T_r\right)dx \quad (11)$$

where T_r is the room temperature; A is the surface area; and $T^n(x)$ is the temperature profile within the cross section. Assuming uniform temperature of the fire-exposed surface, the surface area can be replaced with unit area (i.e., $A = 1$).

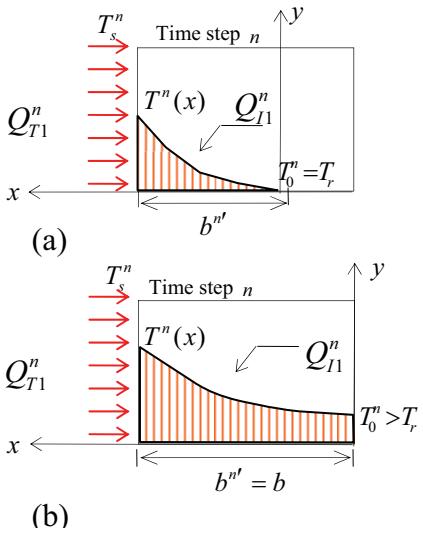

Fig. 2. Heat energy in the section: (a) Low energy case; (b) High energy case

Through the energy conservation principle, T_s^{n+1} in Eq. (7) and the temperature in the section can be solved when the shape function of $T^n(x)$ is pre-determined. We postulate the shape function to be a power function as in Eq. (12). This is suitable for monotonically increasing fire curves. The temperature is always maximum at the fire exposed surface and decreases inwards within the section.

$$T^n(x) = C^n x^\alpha + T_0^n \tag{12}$$

where

$$C^n = \left(T_s^n - T_0^n\right) / \left(b^{n'}\right)^\alpha \tag{13}$$

α is the power of the function; $b^{n'}$ is the effective depth in which the temperature is higher than the room temperature as described in Fig. 2; and T_0^n is the temperature at $b^{n'}$.

Two cases of temperature profile are shown in Fig. 2: the low energy case in which $T_0^n = T_r$ and $b^{n'} < b$. $b^{n'}$ can be computed through the energy conservation Eq. (11).

$$b^{n'} = \frac{Q_{T1}^n (\alpha + 1)}{\rho s_p \left(T_s^n - T_r\right)} \tag{14}$$

the high energy case in which $T_0^n > T_r$ and $b^{n'} = b$. T_0^n can also be computed through the energy conservation Eq. (11).

$$T_0^n = \frac{1}{\alpha}\left[(\alpha+1)\left(\frac{Q_{T1}^n}{\rho s_p b} + T_r\right) - T_s^n\right] \geq T_r \tag{15}$$

By substituting the term $\left(T_{s-1}^n - T_s^n\right)/\Delta x$ with the derivative from Eq. (12) at $x = b^{n'} - \Delta x/2$, T_s^{n+1} in Eq. (7) and the stability condition (8) can be rewritten as (16) and (17):

$$T_s^{n+1} = \frac{2\Delta t}{\rho s_p \Delta x}\left[q^{n+1/2} - kC^n \alpha \left(b^{n\prime} - \Delta x/2 \right)^{\alpha-1} \right] + T_s^n \qquad (16)$$

$$q^{n+1/2} - kC^n \alpha \left(b^{n\prime} - \Delta x/2 \right)^{\alpha-1} > 0 \qquad (17)$$

The difference between T_f^n and T_s^n depends on the time, it is not constant. When the difference is small, the value of $q^{n+1/2}$ in Eq. (5) may not satisfy Eq. (17). This condition could occur at any time step in both typical FDM and the proposed method. Once the dissatisfaction occurs, T_s^{n+1} is lower than T_s^n. By using the FDM, Δt and Δx must be resized to satisfy the stability condition. However, to simplify the calculation, this study assumes $T_s^{n+1} = T_s^n$ at a dissatisfied step $n+1$. Note that, as an increasing function, the pre-determined shape function cannot violate the second law of thermodynamics within the sections exposed to a monotonically increasing function of fire curves. The stability condition $(k/\rho c)\left(\Delta t/\Delta x^2\right) \le 0.5$ is redundant and is omitted in the EBM.

When the value of α is pre-determined, the temperature profiles of sections exposed to a fire can be solved. The value $\alpha = 2.7$ is suggested in [16]. By using the EBM, the large matrix system of regular FDM can be avoided. The procedure to predict the temperature profile is summarized in Fig. 3.

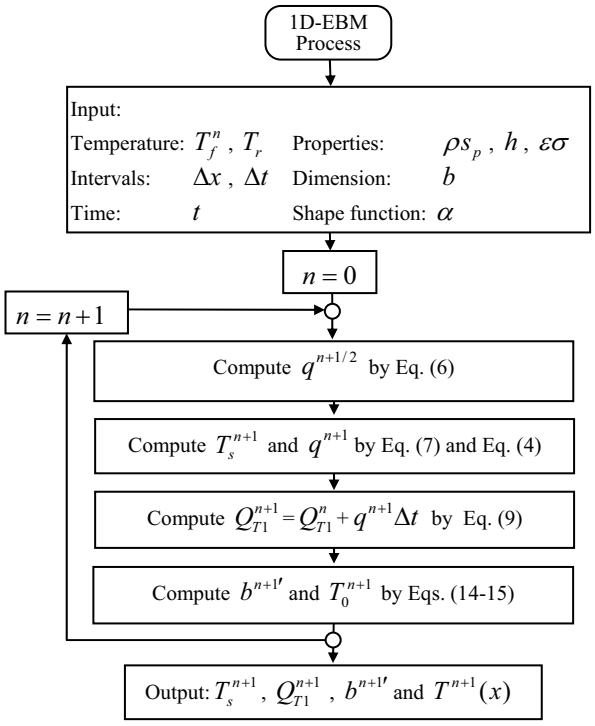

Fig. 3. Procedure to predict the one-dimensional temperature profiles in a section at step n

3. Simplified 2D Heat Transfer Analysis

Consider a cross section with dimension of $2d \times 2c$ exposed to a uniform fire on its four sides. Due to symmetry of the cross section, the analysis involves only a quarter of the section exposed to a fire in two directions as shown in Fig. 4. The decomposition shown in Fig. 4 is applied to approximate the two dimensional problem as a superposition of two one-dimensional problems. The temperature profile, $T^n(x)$, and the effective depth, $b^{n\prime}$, in each direction are computed by using the 1D procedure in Fig. 3. The subscripts V and H represent the vertical and horizontal direction, respectively.

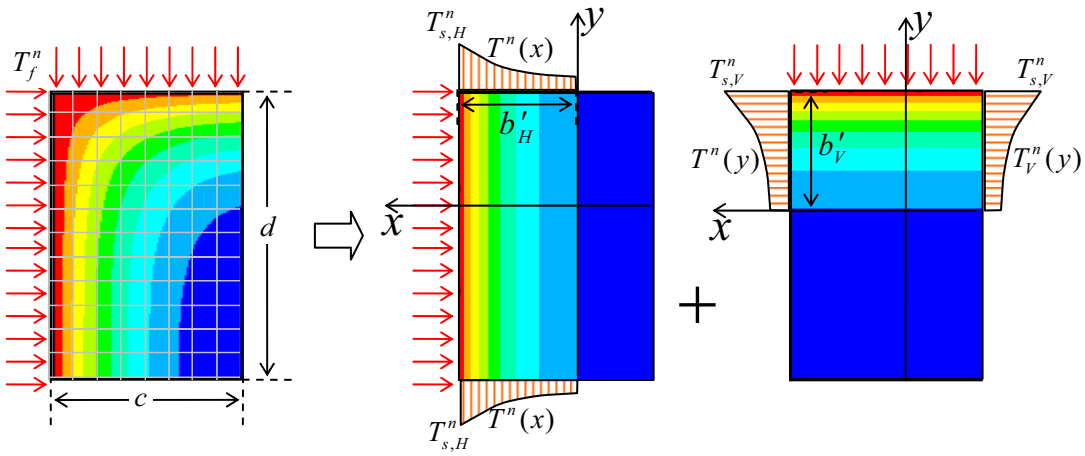

Fig. 4. Quarter of a section exposed to fire in two directions and its decomposition model

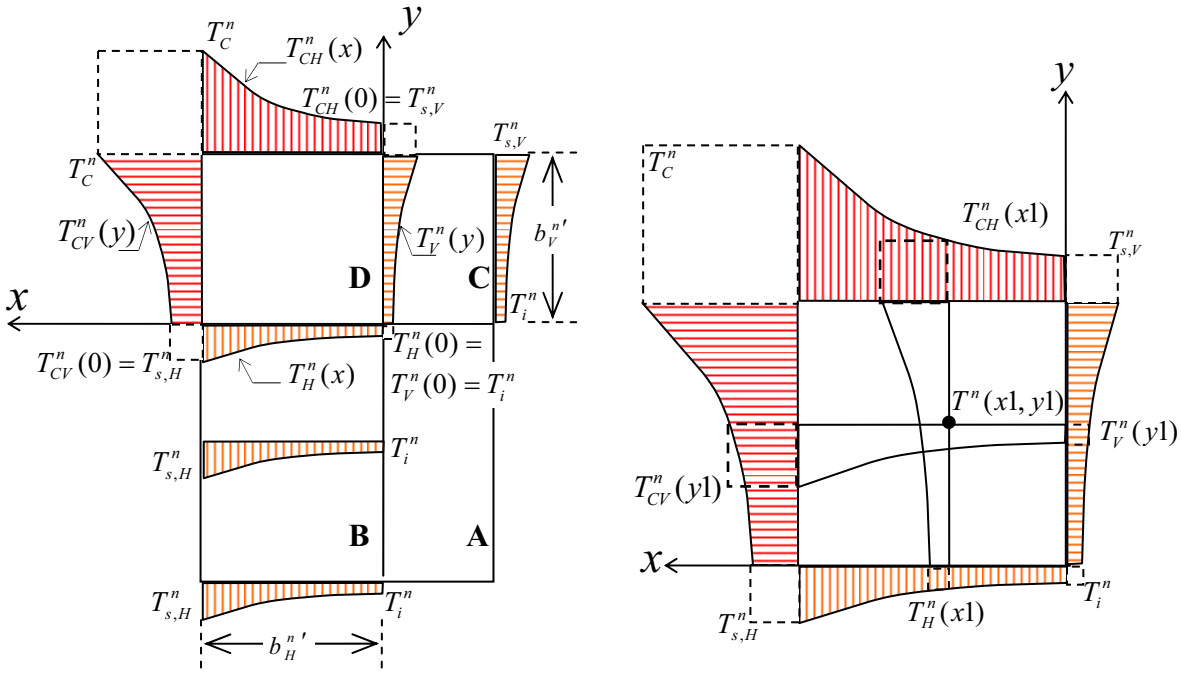

Fig. 5. Temperature profiles: (a) overall temperature profile and (b) temperature profile in Zone D

The overall temperature profile is divided into four zones as shown in Fig. 5(a), labeled with A, B, C and D. Zone A is out of the effective area of the heat transfer analysis for both horizontal and vertical analysis. The temperature in this

zone, the inner temperature T_i^n, is a constant. T_i^n is the minimum temperature of the section. Zone B is only in the effective area of the horizontal analysis. The temperature profile in this zone, $T_H^n(x)$, varies directly with x, independent of y. Conversely, Zone C is in the effective area of the vertical analysis. The temperature profile in Zone C, $T_V^n(x)$, varies directly with y but is independent of x.

In Zone D we have both horizontal and vertical heat transfer. The temperature profile in this zone varies with both x and y. Non-homogeneous boundary conditions are given by $T_H^n(x)$, $T_V^n(y)$, $T_{CH}^n(x)$ and $T_{CV}^n(y)$, as shown in Fig. 5(a) and Fig. 5(b). The $T_{CH}^n(x)$ and $T_{CV}^n(y)$ are the surface temperatures in the horizontal and vertical direction of the corner. Note that all functions are based on the trial function in Eq. (12). The continuity conditions are, $T_{CV}^n(b_V^{n\prime}) = T_{CH}^n(b_H^{n\prime}) = T_C^n$, $T_{CH}^n(0) = T_{s,V}^n$, $T_{CV}^n(0) = T_{s,H}^n$ and $T_V^n(0) = T_H^n(0) = T_i^n$. As a result, $T_H^n(x)$, $T_V^n(y)$, $T_{CH}^n(x)$ and $T_{CV}^n(y)$ can be described as follows:

$$T_H^n(x) = \left(T_{s,H}^n - T_i^n\right)\left(x / b_H^{n\prime}\right)^\alpha + T_i^n \tag{18}$$

$$T_V^n(y) = \left(T_{s,v}^n - T_i^n\right)\left(y / b_V^{n\prime}\right)^\alpha + T_i^n \tag{19}$$

$$T_{CH}^n(x) = \left(T_C^n - T_{s,V}^n\right)\left(x / b_H^{n\prime}\right)^\alpha + T_{s,V}^n \tag{20}$$

$$T_{CV}^n(y) = \left(T_C^n - T_{s,H}^n\right)\left(y / b_V^{n\prime}\right)^\alpha + T_{s,H}^n \tag{21}$$

Based on the overall character of Zone A to Zone C in Fig. 5(a) and the temperature profile in Zone D as shown in Fig. 5(b), the temperature function in the overall section is approximated by

$$T^n(x,y) = \left(T_C^n - T_{s,H}^n - T_{s,V}^n + T_i^n\right)\left(\frac{x'y'}{b_H^{n\prime} b_V^{n\prime}}\right)^\alpha + \left(T_{s,H}^n - T_i^n\right)\left(\frac{x'}{b_H^{n\prime}}\right)^\alpha + \left(T_{s,V}^n - T_i^n\right)\left(\frac{y'}{b_V^{n\prime}}\right)^\alpha + T_i^n \tag{22}$$

where $x' = \max(x, 0)$ and $y' = \max(y, 0)$. The overall temperature profile in Eq. (22) is controlled by six key variables, i.e. $b_V^{n\prime}$, $b_H^{n\prime}$, $T_{s,V}^n$, $T_{s,H}^n$, T_C^n and T_i^n. Through the horizontal and vertical analysis, the values of $b_V^{n\prime}$, $b_H^{n\prime}$, $T_{s,V}^n$ and $T_{s,H}^n$ can be computed.

Consider a diagonally symmetric temperature in the corner section, as shown in Fig. 6. The EBM can also be applied to such symmetric cases. The T_C^n is computed by using Eq. (16) in which the analyzed thickness, b, is assumed to be a small value, that is $b = \Delta x$.

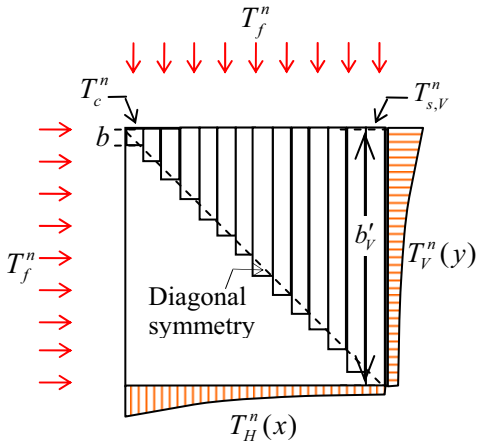

Fig. 6. Diagonally symmetric temperature

Based on the decomposition model in Fig. 4, the 2D heat transfer energy of the quarter section with a unit length, Q_{T2}^n, is approximated in Eq. (23). Whereas the heat energy in the section exposed to a fire in two directions, Q_{I2}^n, in Eq. (10) can be rewritten to correspond with the 2D temperature profile in Eq. (24). As a result, T_i^n can be derived, as done in Eq. (25), from the energy conservation principle, $Q_{T2}^n = Q_{I2}^n$.

$$Q_{T2}^n = cQ_{T1,H}^n + dQ_{T1,V}^n \tag{23}$$

$$Q_{I2}^n = \int_{\left(b_V^{n\prime}-d\right)}^{b_V^{n\prime}} \int_{\left(b_H^{n\prime}-c\right)}^{b_H^{n\prime}} \rho s_p \left(T^n(x,y) - T_r\right) dxdy \tag{24}$$

$$T_i^n = \frac{Q_{T2}^n / \rho s_p + T_r cd - \left(T_C^n - T_{s,H}^n - T_{s,V}^n\right)\lambda_1 - T_{s,H}^n \lambda_2 - T_{s,V}^n \lambda_3}{\left(\lambda_1 - \lambda_2 - \lambda_3 + cd\right)} \tag{25}$$

where

$\lambda_1 = b_H^{n\prime} b_V^{n\prime} / (\alpha+1)^2$

$\lambda_2 = b_H^{n\prime} d / (\alpha+1)$

$\lambda_2 = b_V^{n\prime} c / (\alpha+1)$

Note that, for the low energy case in which $b_H^{n\prime} < c$ and $b_V^{n\prime} < d$, $b_H^{n\prime} = b_V^{n\prime}$ and $T_{s,H}^n = T_{s,V}^n$, the temperature profile does not depend on the section dimension. The procedure to predict the 2D temperature profile is summarized as illustrated in Fig. 7. The EBM is considered as a spreadsheet calculation procedure.

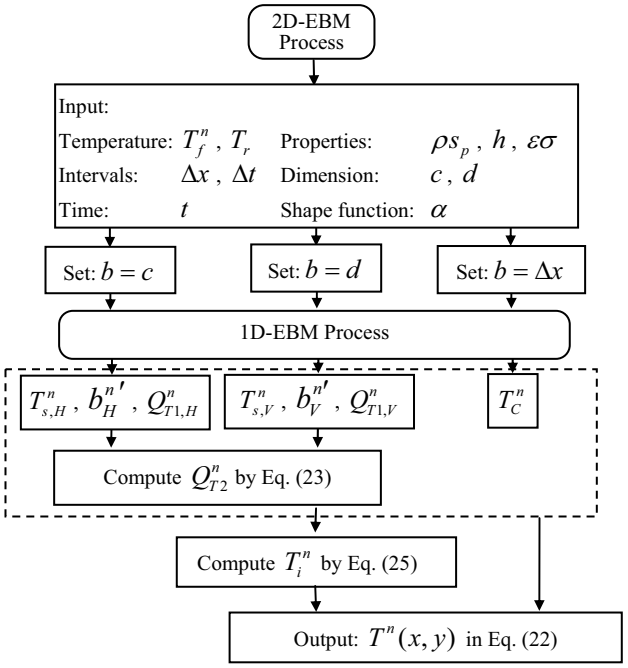

Fig. 7. Procedure to predict the 2D temperature profile

4. Investigation of Suitable Exponent for the Temperature Profile

Rectangular concrete sections are considered in the study. To investigate suitable values of the exponent α, the temperature profiles in concrete sections computed by FEM, using ANSYS software, are compared with the proposed method using different exponents. The concrete sections in the comparison are exposed to the nominal temperature-time curves of BSEB 1992-1-2:2004 [1] on their four sides. All the nominal temperature-time curves are monotonically increasing. Due to symmetry, only one quarter of the section exposed to fire on two sides needs to be solved as shown in Fig. 4. The nominal temperature-time curves include the standard temperature-time curve (ST), the external fire curve (EX) and the hydrocarbon curve (HY), shown in Fig. 8. We investigates 6 different sizes in this study: 300 mm × 300 mm ($2c \times 2d$), 300mm × 600 mm, 400mm × 400 mm, 500mm × 800 mm, 600mm × 600 mm, and 800mm × 800 mm. The temperatures for 8 different fire durations, which are 30, 60, 90, 120, 150, 180, 210 and 240 minutes, are scoped in the comparison. The maximum fire resistance in codes is normally 240 minutes. As a result, there are 144 (3x6x8) data sets in the comparison.

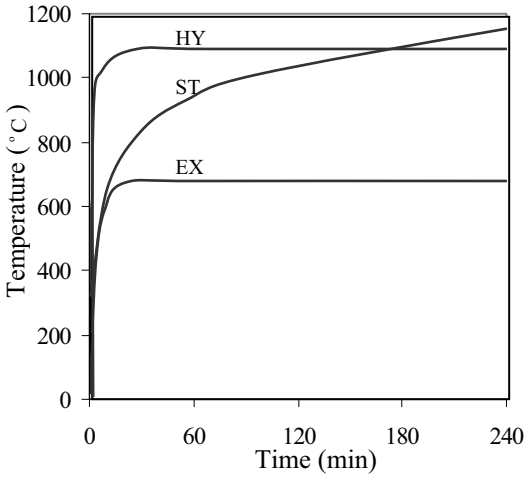

Fig. 8. Nominal temperature-time curves of BSEB 1992-1-2:2004 [1]

The thermal properties of concrete in accordance with BS EN 1991-1-2 (2002) [19] and BS EN 1992-1-2 (2004) [1] are specified in the computation. The variations of the thermal conductivity k and the product of the density and the specific heat ρs_p with temperature are described in Fig. 9. The specific heat capacity with moisture content of 1.5% is applied in the FEM analysis. The thermal conductivity used is a lower bound for concrete, which gives realistic temperatures for concrete structures [1]. To simplify the computation of the EBM, the value of ρs_p is assumed to be constant at $2{,}300\times10^3$ J/m^{3o}K J, about the average value of ρs_p. The coefficient of heat transfer-convection h is of 25 W/m^2°K for the standard temperature-time and external fire curves and 50 W/m^2°K for the hydrocarbon curve. Stefan Boltzmann constant and the resultant emissivity related to the concrete surface are 5.67 x 10^{-8} W/m^2°K^4 and 0.7, respectively.

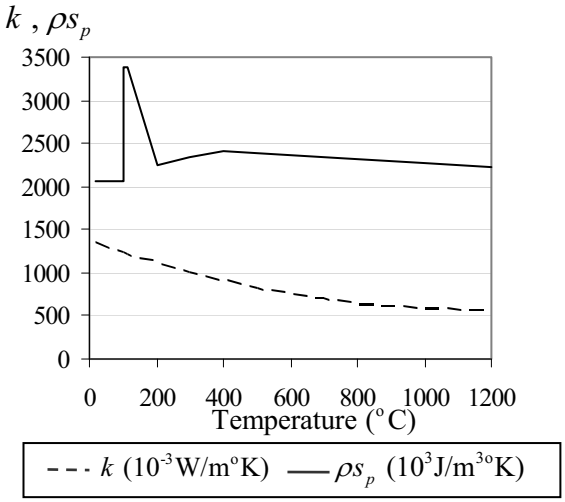

Fig. 9. Thermal properties of concrete

To analyze the temperature profile in the section by ANSYS [10], the sections are modeled with three-dimensional solid elements, Solid70, having eight nodes with a single degree of freedom (i.e., temperature) at each node. The surface element, Surf152, is used to account for heat convection and radiation of the fire temperature.

The element size of $c/20 \times d/20$ is specified for the FEM model whereas Δx of 10 mm is specified for the EBM analysis. The time increment Δt of 60 s is used in both methods.

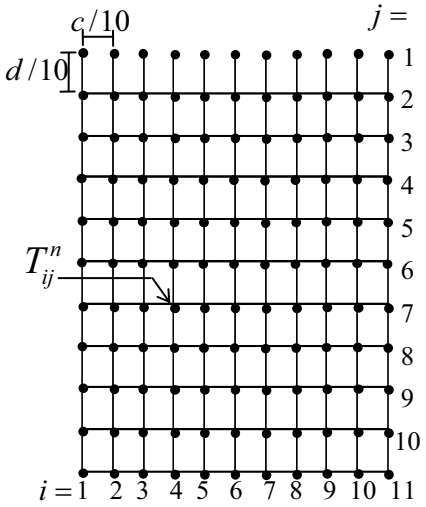

Fig. 10. Nodal points for the error investigation

The temperatures obtained from the FEM and the EBM with different α values are recorded for the 121 nodal points shown in Fig. 10. An error between the nodal temperatures obtained from the EBM, $T_{EBM,ij}^n$, and the nodal temperatures obtained from the FEM, $T_{FEM,ij}^n$, is characterized by the normalized absolute error:

$$\varepsilon_{ij}^n = \frac{\left| T_{EBM,ij}^n - T_{FEM,ij}^n \right|}{\max\left(T_{FEM,ij}^n \right)} \tag{26}$$

The variation of the average normalized absolute error, ε_{av}, with α value is described in Fig. 11. ε_{av} is the average value of ε_{ij}^n throughout all 144 data sets which is normally 17,424 (121x144) nodal temperatures. However, the data sets with ε_{av} larger than 0.10 are not included in the averaging, because the EBM is not an appropriate approximation in those cases. The value α = 2.6 minimizes ε_{av} and is optimal in this test panel, as illustrated in Fig. 11.

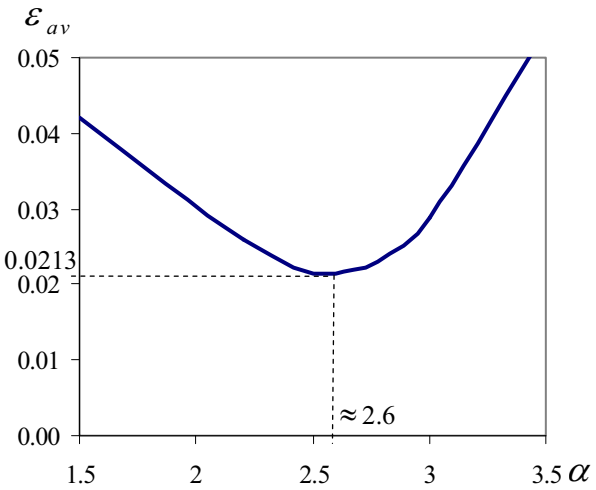

Fig. 11 Variation of the average error with α value

An example of the temperature profiles from the FEM and the EBM, with α = 2.6 for the 300 mm × 600 mm cross section at 90-min fire exposure, is shown in Fig. 12. The fast approximate solutions are comparatively accurate near the fire exposed surface, giving results very similar to the FEM, but the accuracy diminishes inwards. Another illustration of the accuracy of the EBM is in Fig. 13 and Fig. 14, showing the variation of the temperature distribution along the diagonal line with duration of fire exposure.

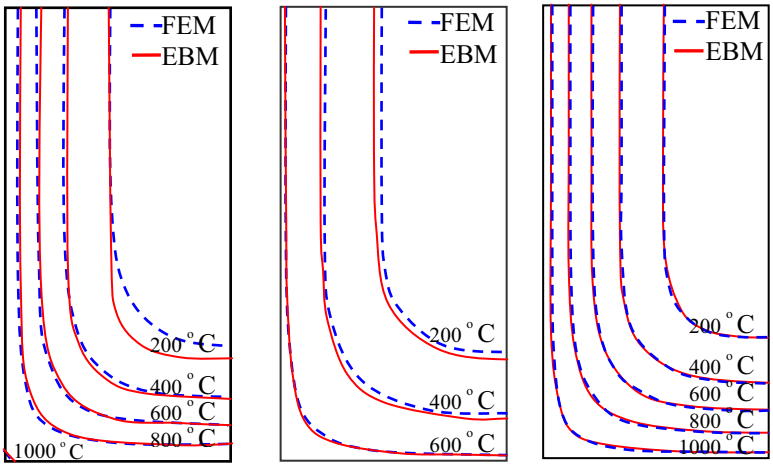

ST Exposure EX Exposure HY Exposure

Fig. 12 Temperature profiles in the 300 mm × 600 mm cross section at 90-min fire exposure

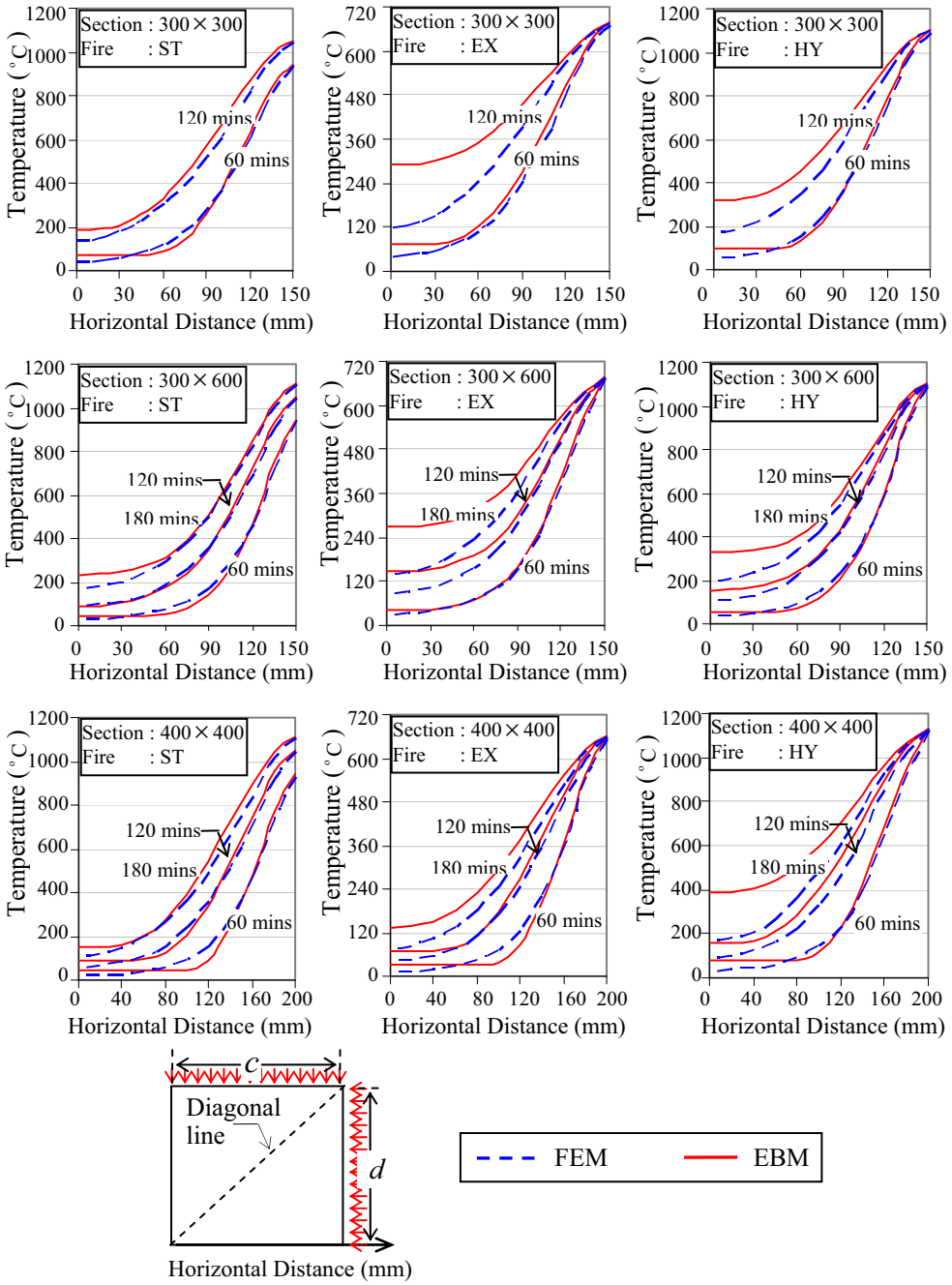

Fig. 13 Variation of the temperature distribution with fire exposure duration along the diagonals of small size sections

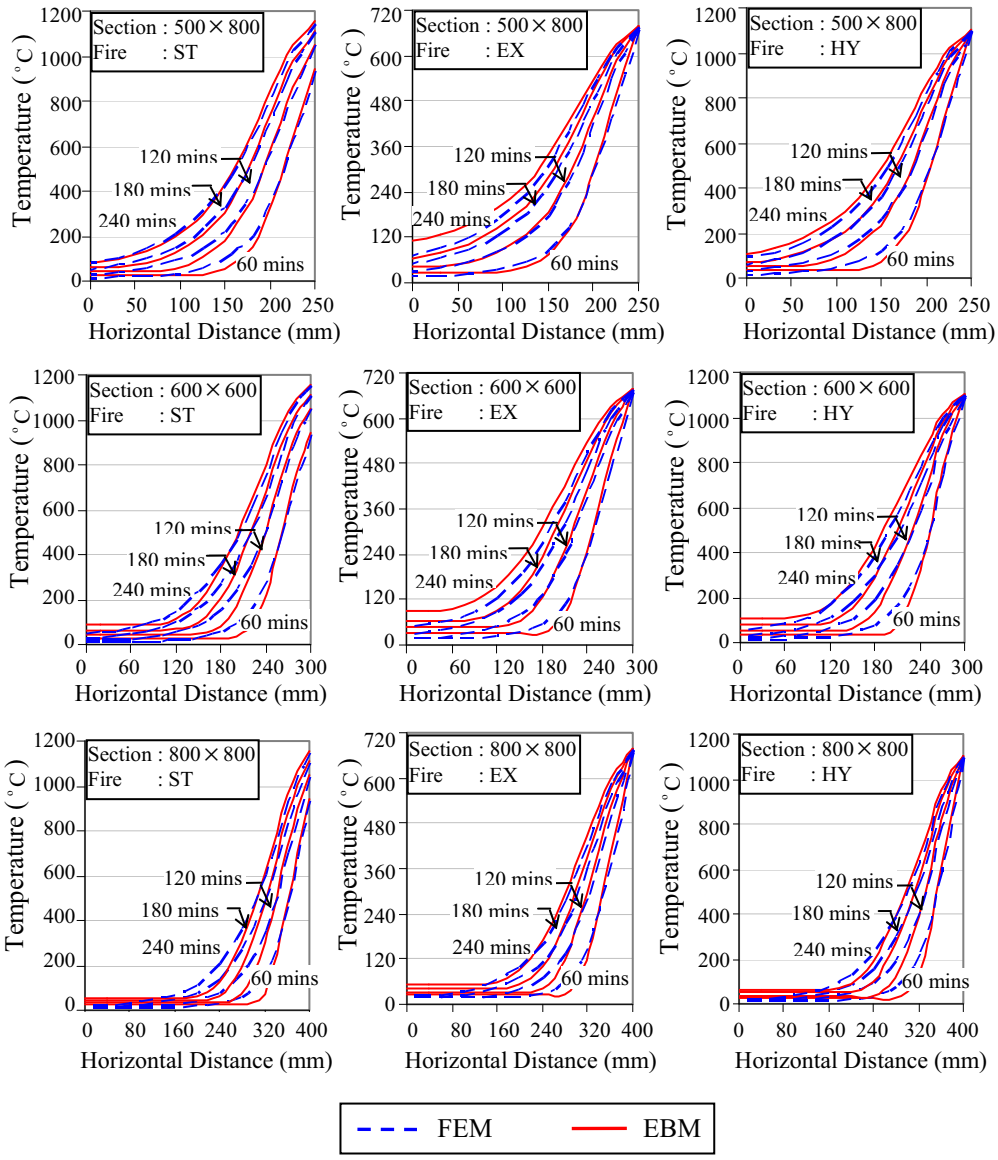

Fig. 14 Variation of the temperature distribution with fire exposure duration along the diagonals of large size sections

Even though the α value of 2.6 provides the minimum ε_{av}, large values of ε_{av} ($\varepsilon_{av} \geq 0.05$) and significantly overestimated heat energy ($Q^n_{T2,EBM} / Q^n_{T2,FEM} \geq 1.10$) are still typical of the EBM for small size sections with long fire durations, as shown in Fig. 13. $Q^n_{T2,EBM}$ is the accumulated heat energy according to the EBM, and $Q^n_{T2,FEM}$ is similar according to the FEM. In such cases, the heat transfer energy is high compared with the heat capacity of the sections. T^n_i / T^n_c can be used to indicate the local variation in heat energy of each section. For example, under the same amount of heat transfer energy, T^n_i of a small sized section is higher than that of larger section, due to lower heat capacity. As a result, under the same amount of heat transfer energy, T^n_i / T^n_c is higher in smaller size sections.

The variations of ε_{av} and $Q^n_{T2,EBM}/Q^n_{T2,FEM}$ with T^n_i/T^n_c are shown in Fig. 15(a) and 15(b), respectively. The figures show that the temperature accuracy of the EBM relates to the accuracy of the energy. Large values of ε_{av} are found in the cases with significantly overestimated heat energy. The assumption that the decomposition to one dimensional models is a good approximation to Q^n_{T2} in Eq. (23), no longer holds. Note that underestimated heat energy for low T^n_i/T^n_c is shown in Fig 15(b), and they normally occur at the early times of fire exposure. The cumulative heat energy is low, and the magnitude of error in the energy is small giving also accurate estimates of the temperature.

Fig. 15 suggests that the data sets with $T^n_i/T^n_c < 0.20$ (109 data sets) can be considered acceptable cases, with $\varepsilon_{av} < 0.05$, as summarized in Table 1. In the case of $T^n_i \geq 0.2T^n_c$, the approximate temperatures are significantly overestimated in the inner area as shown in Fig. 13. However, the approximate temperatures are still close to the FEM analysis near the surface exposed to fire.

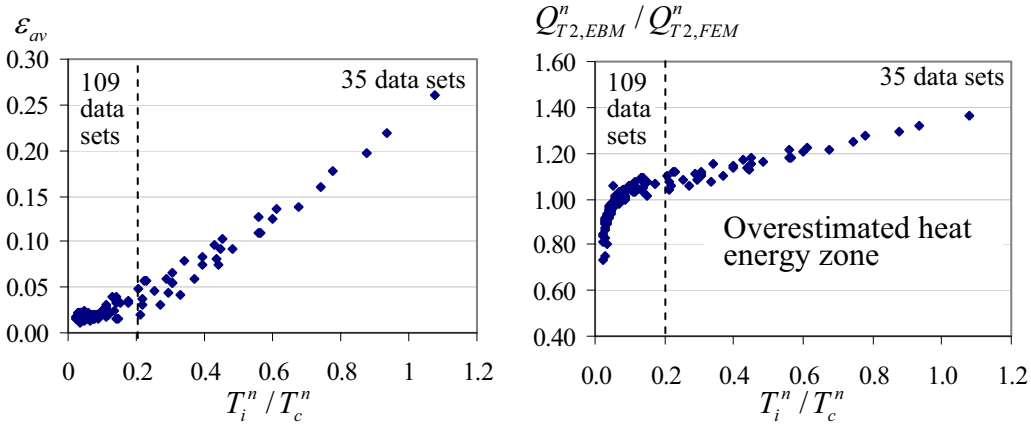

Fig. 15 Variation of ε_{av} and $Q^n_{T2,EBM}/Q^n_{T2,FEM}$ with T^n_i/T^n_c

Table 1 Acceptable cases for the EBM analysis

Section (mm)	Acceptable fire duration (min) for EBM analysis ($T^n_i \leq 0.2T^n_c$)		
	ST	EX	HY
300×300	<150	<90	<120
300×600	<180	<120	<150
400×400	<240	<150	<180
500×800		>240	
600×600		>240	
800×800		>240	

5. Validation of the EBM

The EBM is validated by comparing the predicted temperature with the data of experiments and the FEM analysis. The experimental temperatures of RC sections under fire exposure from Lie et al. [20] reported in [13], Jau and Huang [21], Abbasi and Hogg [22], and Dwaikat and Kodur [23] are used in the comparison. Details of the dimensions, the fire load (ASTM E119 [24], BS 476 [25] and ISO 834 [26]) and the location of temperature measurement are described in Fig. 16. The thermal properties are assumed to be in accordance with BS EN 1991-1-2 [19] and BS EN 1992-1-2 [1]. The effects of reinforcing steel in RC sections on the heat transfer analysis are neglected, due to its relatively small area [8]. Points D and E are at the reinforcing locations.

The comparisons of the experimental temperature–fire duration relationship at the measured points and the temperature profiles with those of the EBM and the FEM are shown in Fig. 17 and Fig. 18, respectively. Note that, to limit the influence zone of unexpected fire [21], the temperature profile in Fig. 18 is described in the dimension of 250mm × 300 mm. A good agreement between the EBM and the other methods is observed in the figures. The EBM temperatures are slightly low at early times, compared with both experimental results and FEM analysis.

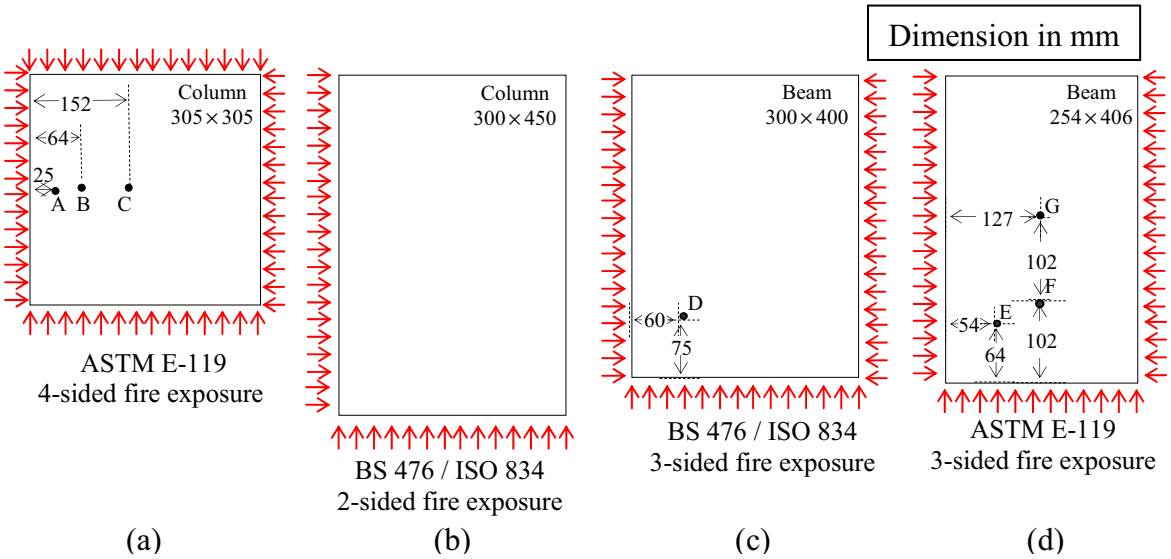

Fig. 16 Details of the experiments and the locations of temperature measurement: (a) Lie et al. [20], (b) Jau and Huang [21], (c) Abbasi and Hogg [22], and Dwaikat and Kodur [23]

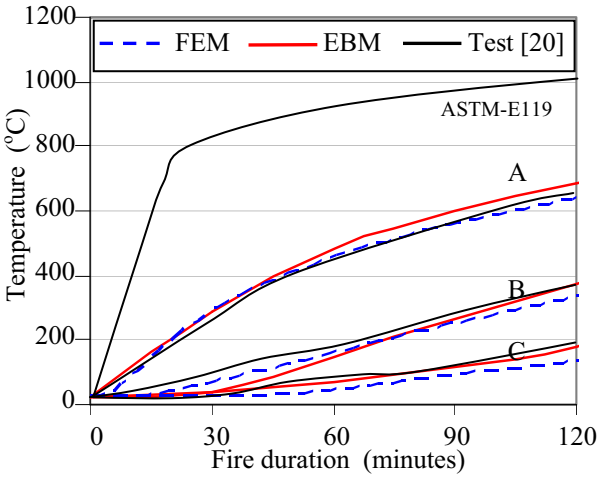

(a)

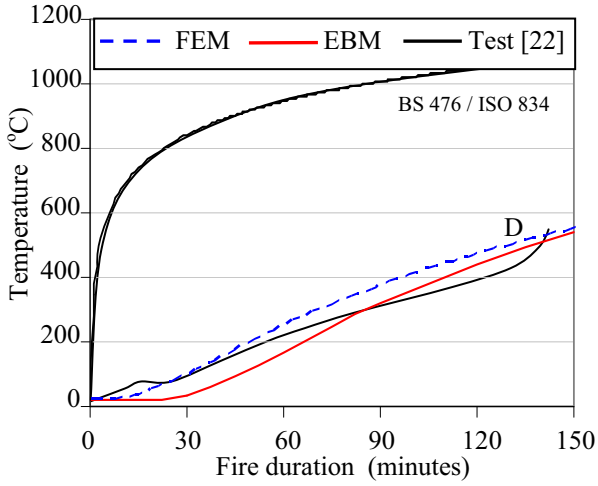

(b)

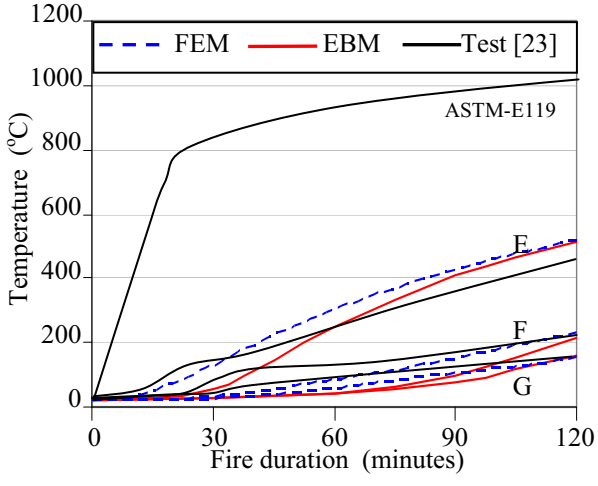

(c)

Fig. 17 Comparison of experimental temperature–fire duration relationship at the measured points with the EBM and the FEM: (a) the experiment of Lie et al. [20], (b) the experiment of Abbasi and Hogg [22], and (c) the experiment of Dwaikat and Kodur [23].

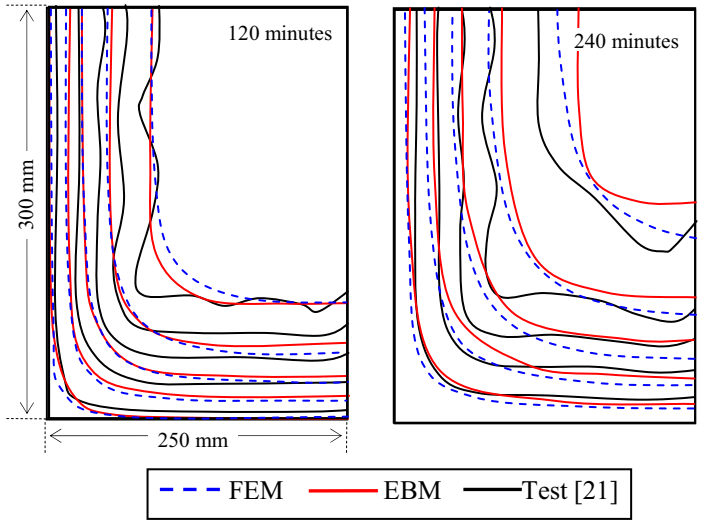

Fig. 18 Comparison of experimental temperature profiles from Jau and Huang [21] with the EBM and the FEM

6. Discussion and Conclusion

An energy based method for heat transfer analysis is developed based on the energy conservation principle and a pre-determined power function for temperature profiles in concrete sections. The power function is suitable for monotonically increasing fire curves. According to the energy conservation principle, the cumulative heat energy transferred from the boundary equals the heat energy accumulated within a fire-exposed section. The heat energy within the section is computed based on the heat capacity and the temperature profile. As a result, the temperature function in the section can be computed.

The heat transfer energy of a rectangular section exposed to fire from two directions is evaluated based on decomposition to superposed one dimensional models, in which the energy can be computed by one-dimensional heat transfer analysis. Through the energy conservation principle, the temperature function in the overall section is evaluated. The temperature profile of a rectangular section is controlled by six key variables that are the horizontal and vertical surface temperature, the horizontal and vertical effective depth, the corner temperature, and the inner temperature.

On comparing the EBM approximation with the FEM computations for various concrete sections and fire loads, the exponent = 2.6 minimizes the average error. However, the EBM approximation significantly overestimates the energy if the predicted minimum temperature exceeds 0.2 times the predicted maximum temperature. In such cases, the decomposition to one dimensional problems is a poor approximation. This characterizes the limitation of the EBM approximation in practical use.

The EBM is validated by comparing the predicted temperature with the experimental and FEM results. Even though the FEM analysis includes non-constant thermal properties, the simplified EBM approximation still delivers closely similar results.

The energy based method can be implemented as a spreadsheet calculation, and the complications of using FEM or FDM can be avoided. Design engineers can simply apply the proposed method to evaluate the temperature profile in a regular

spreadsheet program. The proposed method facilitates analysis of heat transfer, necessary to ensure fire resistance of concrete structures under various fire scenarios.

Acknowledgment

This research was financially supported by Faculty of Engineering, Prince of Songkla University, contract no. ENG-55-2-7-02-0139-S. We would like to sincerely thank the copy-editing service of Research and Develop Office and Assoc. Prof. Dr. Seppo Karrila who dedicated their time to provide valuable comments. These supports are gratefully acknowledged

Reference

[1] British Standards Institution, Eurocode 2: design of concrete structures– Part 1–2: general rules- structural fire design, BS EN1992-1-2, BSI, London, 2004.
[2] AS 3600, Concrete structures. Australia: Committee BD-002, 2001.
[3] ACI Committee 216.1, Standard Method for Determining Fire Resistance of Concrete and Masonry Construction Assemblies, American Concrete Institute, Detroit, 2007.
[4] A. Haji-Sheikh, J.V. Beck, Temperature solution in multi-dimensional multilayered bodies, Int. J. Heat Mass Transfer 45 (2002) 1865–1877.
[5] F. de Monte, Unsteady heat conduction in two-dimensional two slab-shaped regions. Exact closed-form solution and results, Int. J. Heat Mass Transfer 46 (2003) 1455–1469.
[6] D. Di Capua, A.R. Mari, Nonlinear analysis of reinforced concrete cross-sections exposed to fire, Fire Saf. J. 42 (2007) 139–149.
[7] Z.H. Wang, K.H. Tan, Temperature Prediction of Concrete-Filled Rectangular Hollow Sections in Fire Using Green's Function Method, J. Eng. Mech. 133 (2007) 688-700.
[8] T.T. Lie (Ed.), Structural Fire Protection, in: ASCE Manuals and Reports of Engineering Practice, No. 78, American Society of Civil Engineers, New York, 1992.
[9] J.M. Franssen, V.K.R. Kodur, J. Mason, User's Manual for SAFIR 2004. A Computer Program for Analysis of Structures Subjected to Fire, University of Liege, Liege, 2005.
[10] ANSYS, ANSYS multiphysics. Version 11.0 SP1. ANSYS Inc., Canonsburg (PA), 2007.
[11] E. Chowdhury, L. Bisby, M. Green, Heat transfer and structural response modelling of FRP confined rectangular concrete columns in fire, Constr. Build. Mater. 32 (2012) 77–89.
[12] K.S Chung, S. Park, S.M. Choi, Material effect for predicting the fire resistance of concrete-filled square steel tube column under constant axial load, J. Constr. Steel Res. 64 (2008) 1505–1515.
[13] S.F. El-Fitiany, M.A. Youssef, Assessing the flexural and axial behaviour of reinforced concrete members at elevated temperatures using sectional analysis, Fire Saf. J. 44 (2009) 691–703.
[14] U. Wickstrom, A very simple method for estimating temperature in fire exposed concrete structures, Fire Technology Technical Report SP-RAPP 1986, 46, Swedish National Testing Institute, 1986, pp. 186–194.
[15] A.H. Buchanan, Structural design for fire safety, 1st edn., John Wiley and Sons Ltd., Chichester, 2001.

[16] P. Pattamad, Energy Based Temperature Profile for Heat Transfer Analysis of Concrete Section Exposed to Fire on One Side, World Academy of Science, Engineering and Technology 65 (2012) 897-902.

[17] K.V. Wong, Intermediate Heat Transfer. New York: Marcel Dekker, INC., 2003.
[18] V.K.R. Kodur, P.Pakala, M.B.Dwaikat, Energy based time equivalent approach for evaluating fire resistance of reinforced concrete beams, Fire Saf. J. 45 (2010) 211–220.
[19] British Standards Institution, Eurocode 1: actions on structures – Part 1–2: general actions – actions on structures exposed to fire, BS EN 1991-1-2, BSI, London, 2002.
[20] T.T. Lie, T.D. Lin, D.E. Allen, M.S. Abrams, Fire resistance of reinforced concrete columns, Technical Paper No. 378, Division of Building Research, National Research Council of Canada, Ottawa, ON, Canada, 1984.
[21] W.C. Jau, K.L. Huang , A study of reinforced concrete corner columns after fire, J. Cem. Concr. compos. 30 (2008) 622–638.
[22] A. Abbasi, P.J. Hogg, Fire testing of concrete beams with fibre reinforced plastic rebar, Composites: Part A 37 (2006) 1142–1150.
[23] M. B. Dwaikat, V. K. R. Kodur, Response of Restrained Concrete Beams under Design Fire Exposure, J. Struct. Eng. 135 (2009) 1408-1417.
[24] ASTM, Standard methods of fire test of building construction and materials, Test Method E119a -08, American Society for Testing and Materials, West Conshohocken, PA, 2008.
[25] BS. Fire tests on building materials and structures—Part 20: method from determination of the fire resistance of elements of construction (general principles), BS 476-3:1987, BSi, UK, 1987
[26] ISO 834-1975, Fire resistance tests- elements of building construction, Int. Org. Stand. (1975).

The 4th KKU International Engineering Conference 2012 (KKU-IENC 2012)
"Driving together towards ASEAN Economic Community"
Faculty of Engineering, Khon Kaen University, Thailand, May 10-12, 2012

Predicting Moment Capacity of RC Beams under Fire by Using Two-dimensional Sectional Analysis

Pattamad Panedpojaman
Department of Civil Engineering, Faculty of Engineering,
Prince of Songkla University, Songkhla 90110, Thailand.
E-mail: ppattamad@eng.psu.ac.th

Abstract— **Under elevated temperatures, reinforced concrete (RC) structures are affected by variation of the mechanical properties with temperature. Simplified and practical approaches which enable engineers to design RC structures accounting for the mechanical variation are required. The study develops a cross sectional analysis to predict the moment capacity of RC beams. The two-dimensional temperature distribution is used in the analysis. The capacity is computed based on the force equilibrium corresponding to the assumed element strain and the pre-determined element temperature. The variation of nonlinear stress-strain relationship with temperature is adopted in the analysis. The developed method is limited to under or normal-reinforced beams. The predicted moment capacity is validated with the finite element analysis. The cross sectional approach is found to be a potential method to predict the moment capacity under fire.**

Keywords: Cross sectional analysis, Moment capacity, RC beams, Elevated temperatures.

I. INTRODUCTION

Mechanical properties of concrete and steel significantly reduce under elevated temperatures such as in Fire [1,2]. For safety reasons, structures must be designed to resist effect of fire. Reinforced concrete (RC) structures under fire are currently designed by using prescribed methods. The methods specify minimum cross-section dimensions and minimum clear cover to the reinforcing bars. The methods are limited to pre-determined dimensions and fire scenarios. To design different fire conditions, other design or analysis methods are required.

As an alternative method, the finite element method (FEM) has been proven to be an efficient method to design RC structures during exposure to fire [3,4]. The finite element analysis of structures under fire consists of heat transfer analysis and structural analysis. Evaluated through the heat transfer analysis, temperature profile of structure members is used as a factor to define material properties in the structural analysis. However, using the approach requires a detailed finite element program as well as an expertise user.

To facilitate structural designers, a sectional analysis has been proposed. The temperature profile within a concrete cross-section must be pre-determined before a sectional analysis. Generally, in addition to the FEM, evaluating the temperature profile can be computed based on the finite difference method [5], or the given temperature profile of EN 1992-1-2 [1]. By using a cross sectional analysis, a RC cross section is divided into finite elements or fibers. Based on a simple equilibrium and compatibility equations, structural behavior of a RC section is evaluated. The method can easily be applied in regular spreadsheet softwares. Therefore, a sectional analysis is an alternative method in addition to an expensive finite element software.

A few researchers have been adopted a sectional analysis to predict structural behavior of RC members under fire. Rigberth [6] computed the moment capacity of RC beams by summarizing force in each horizontal concrete element of the beam section until the force was equal to the summarized yield force of the reinforcing steel. The concrete elements were assumed to be in the compression strength. Rigberth did not consider the stress and strain distribution in the cross section. El-Fitiany [7] studied the moment capacity and the curvature of a RC section. His concrete sections were considered as horizontal discrete fibers and assumed linear strain relationship along its depth. Temperature of each fiber layer was based on an average value of its temperature distribution and used to compute the corresponding stress. The average temperature of the fibers affects accuracy to predict the structural behavior.

The current study proposes a sectional analysis to predict the moment capacity of RC beams under fire. The analysis is developed by dividing the concrete section into horizontal and vertical discrete elements. The discrete element causes more accuracy to compute its corresponding stress. The scope of study is limited to under or normal-reinforced beams exposed to fire only on its three sides, no fire load on its top surface. The three-side fire exposure is as a general case of an interior beam in a typical building. Induced thermal, transient creep strains, coefficient of thermal expansion and tensile strength of concrete is not considered based on the simplified calculation methods of EN 1992-1-2 [1]. Fire load is considered as time-temperature curve such as the standard fire curve ASTME119 [8]. The proposed method for calculating the moment capacity of fire-exposed RC beams is verified against a finite element program.

Failures of RC beams can be considered as compression failure (over-reinforced beams), tension failure (under-reinforced beams) and balanced Failure (balanced reinforcement). The beam is known as an over-reinforced beam when the concrete crushes before the tension rebars yield. This type of failure is a sudden failure. For under-reinforced beams, the tension rebars yield before the concrete crushes. The beam is considered as a balanced-reinforced

beam when concrete crushes and the tension rebar yields simultaneously. However, the beam failure caused by fire is difficult to identify the stage of reinforcement, i.e. over, under or normal reinforcement since variation of the stress-strain relationships of concrete and steel with temperature. Due to the steel strength decreases much faster with temperature than the concrete strength, the over-reinforced beams may turn into the under or normal-reinforced beams under fire. Most failures are the tension failure or the balanced failure [6]. Therefore, the limitation of the under or normal-reinforced beams is adopted in the study.

II. MECHANICAL OF CONCRETE AND STEEL

The sectional analysis of a RC concrete section under elevated temperatures is based on simple force equilibrium and compatibility equations. Variation of the stress-strain relationship with temperature is used to evaluate force profile of the cross section before an equilibrium check. Several researchers [9-11] have referred to the Eurocodes to assess behaviors of RC structures under and after fire. The current study also adopts the mechanical properties of steel and concrete at elevated temperatures based on the Eurocodes.

The stress-strain relationship for concrete and hot rolled reinforcing steel is assumed to follow the stress-strain relationship of BS EN 1992-1-2 [1] up to the peak stress and perfectly plastic thereafter. The perfectly plastic is generally assumed for structural analysis under elevated temperatures [12] and imply used in the sectional analysis [6].

A. Compressive stress-strain relationship of concrete

The compressive stress $\sigma_{c,T}$ -strain $\varepsilon_{c,T}$ relationship of concrete under elevated temperatures [1] is

$$\sigma_{c,T} = \frac{3\varepsilon_{c,T} f_{c,T}}{\varepsilon_{c1,T}\left[2 + \left(\varepsilon_{c,T} / \varepsilon_{c1,T}\right)^3\right]} \quad (1)$$

in which $f_{c,T}$ is the compressive strength of concrete under elevated temperatures referred to Table I; $\varepsilon_{c1,T}$ and $\varepsilon_{cu,T}$ are the peak strain and the ultimate strain of concrete under elevated temperatures also referred to Table I.

B. Stress-strain relationship of steel

The stress $\sigma_{s,T}$ -strain $\varepsilon_{s,T}$ relationship of the reinforcing steel under elevated temperatures [1] is

$$\sigma_{s,T} = \varepsilon_{s,T} E_{s,T} \quad \text{for } \varepsilon < \varepsilon_{sp,T}$$

$$\sigma_{s,T} = f_{sp,T} - c + (b/a)\left[a^2 - \left(\varepsilon_{sy,T} - \varepsilon_{s,T}\right)^2\right]^{0.5} \quad \text{for } \varepsilon_{sp,T} < \varepsilon < \varepsilon_{sy,T} \quad (2)$$

where

$$a^2 = \left(\varepsilon_{sy,T} - \varepsilon_{sp,T}\right)\left(\varepsilon_{sy,T} - \varepsilon_{sp,T} + c / E_{s,T}\right)$$

$$b^2 = c\left(\varepsilon_{sy,T} - \varepsilon_{sp,T}\right) E_{s,T} + c^2$$

$$c = \left(f_{sy,T} - f_{sp,T}\right)^2 / \left(\left(\varepsilon_{sy,T} - \varepsilon_{sp,T}\right) E_{s,T} - 2\left(f_{sy,T} - f_{sp,T}\right)\right)$$

in which $E_{s,T}$ is the slope of the linear elastic range under elevated temperatures; $f_{sp,T}$ and $f_{sy,T}$ are the proportional-limit stress and the yield stress under elevated temperatures; and $\varepsilon_{sp,T}$ and $\varepsilon_{sy,T}$ ($\varepsilon_{sy,T}$=0.02) are the proportional-limit strain and the yield strain under elevated temperatures. Variation of the mechanical properties of the steel with temperature is shown in Table II.

TABLE I. VARIATION OF COMPRESSIVE STRENGTH, PEAK STRAIN AND ULTIMATE STRAIN OF CONCRETE WITH TEMPERATURE [1]

Temperature, T (°C)	Calcareous Concrete		
	$\frac{f_{c,T}}{f_{c,20\ °C}}$	$\varepsilon_{c1,T}$	$\varepsilon_{cu,T}$
20	1.00	0.0025	0.0200
100	1.00	0.0040	0.0225
200	0.97	0.0055	0.0250
300	0.91	0.007	0.0275
400	0.85	0.010	0.0300
500	0.74	0.015	0.0325
600	0.60	0.025	0.0350
700	0.43	0.025	0.0375
800	0.27	0.025	0.0400
900	0.15	0.025	0.0425
1000	0.06	0.025	0.0475

TABLE II. VARIATION OF MECHANICAL PROPERTIES OF STEEL WITH TEMPERATURE [1]

Temperature, T (°C)	$\frac{E_{s,T}}{E_{s,20\ °C}}$	$\frac{f_{y,T}}{f_{y,20\ °C}}$	$\frac{f_{p,T}}{f_{p,20\ °C}}$
30	1.00	1.00	1.00
100	1.00	1.00	1.00
200	0.90	1.00	0.81
300	0.80	1.00	0.61
400	0.70	1.00	0.42
500	0.60	0.78	0.36
600	0.31	0.47	0.18
700	0.13	0.23	0.07
800	0.09	0.11	0.05
900	0.07	0.06	0.04
1000	0.04	0.04	0.02

III. SECTIONAL ANALYSIS

For the current study, RC beams are divided into horizontal and vertical discrete elements as shown in Figure 1(a). The beam dimension is defined by the beam width b and the distance between the tension bars and the top surface of the RC section d. The subscript of i and j is used to denote row i and column j of the element, respectively. The subscript of k and l is used to denote number of the compression and tension bars, respectively. Temperature of the concrete element $T_{c,ij}$, the compression bars $T_{s',k}$ and the

tension bars $T_{s,l}$ are pre-determined before the sectional analysis.

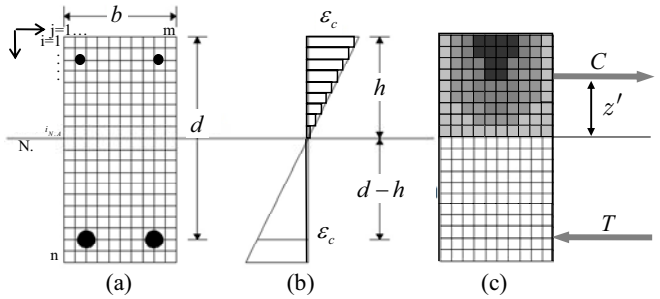

Figure 1. Discrete elements for the sectional analysis approach

The strain distribution is assumed to be linear along the beam depth as described in Figure 1(b) but constant along the beam width. Due to the scope of an under or normal-reinforced beam, the yield strain of the tension rebars controls the strain distribution of the cross section. Slope of the strain distribution ϕ depends on the yield strain $\varepsilon_{sy,T}$, the location of the tension rebars d and a trial distance of the neutral axial h as

$$\phi = \frac{\varepsilon_{sy,T}}{d-h} \tag{3}$$

The strain of each element is considered based on the average value. The strain of the concrete element $\varepsilon_{c,i}$ and the compression bars $\varepsilon_{s',k}$ are computed as follows:

$$\varepsilon_{c,i} = z_{c,i}\phi \tag{4}$$

$$\varepsilon_{s',k} = z_{s',k}\phi \tag{5}$$

in which $z_{c,i}$ and $z_{s',k}$ are the distance from the neutral axial N.A. to center of the concrete element row i, and to center of the compression bars k, respectively.

Based on concept of the under or normal-reinforced beams, tensile stress of the tension rebars reach the yield stress $f_{sy,T}$ corresponding to its temperature. Compressive stress of the concrete element $\sigma_{c,ij}$, and stress of the compression rebars $\sigma_{s',k}$ are a function of the corresponding strain and element temperature (see in Figure 1(b) and Figure 1(c)) as described in Section II.

Summation of the compression force in the compressive zone C and the tension force T of the rebars can be computed as follows

$$C = \sum_{i=1}^{i_{N.A}}\sum_{j=1}^{all}\sigma_{c,ij}A_{c,ij} + \sum_{k=1}^{all}\sigma_{s',k}A_{s',k} \tag{8}$$

$$T = \sum_{l=1}^{all} f_{sy,T}A_{s,l} \tag{9}$$

in which $A_{c,ij}$, $A_{s',k}$ and $A_{s,k}$ are the area of the concrete element, the compression rebars and the tension rebars, respectively. The force equilibrium, i.e. $C = T$, is used to identify acceptable location of the neutral axial.

The moment capacity of the beams at failure is computed as

$$M = CL \tag{10}$$

where

$$L = d - h + z' \tag{11}$$

$$z' = \frac{\sum_{i=1}^{i_{N.A}} z_{c,i}\sum_{j=1}^{m}\sigma_{c,ij}A_{c,ij} + \sum_{k=1}^{all} z_{s',k}\sigma_{s',k}A_{s',k}}{C} \tag{12}$$

in which L is the lever arm of the resultant force between C and T; and z' is the distance between the neutral axial and the resultant force C as described in Figure 1(c). The process to compute the moment capacity is also summarized in the flow chart as shown in Figure 2.

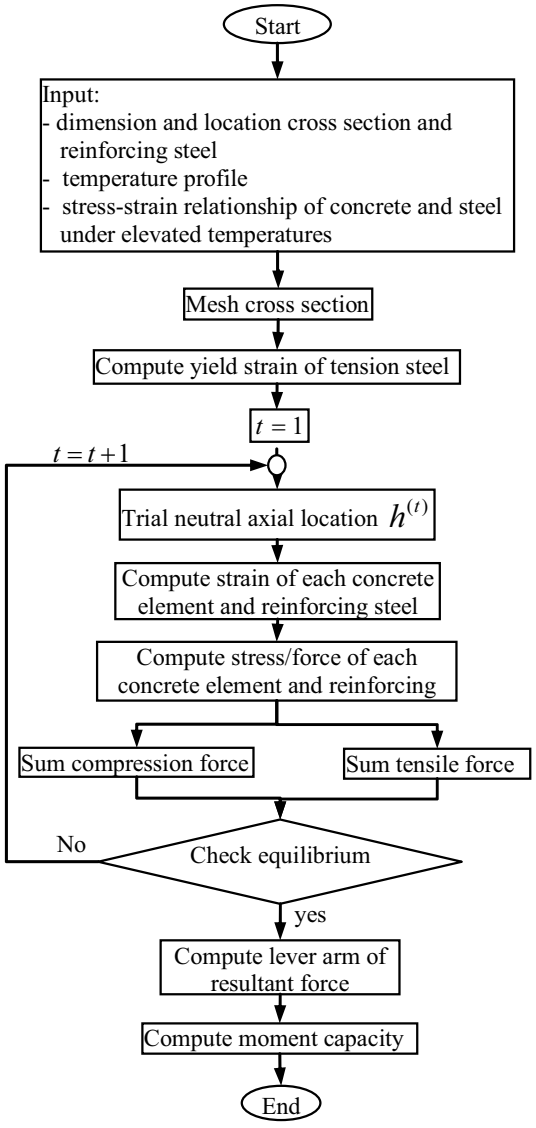

Figure 2. Process to compute the moment capacity

IV. COMPARISON WITH FINITE ELEMENT ANALYSIS

The proposed method is validated by comparing the predicted moment capacity under elevated temperatures with that of a finite element model. The beams as shown in Figure 3 are used in the comparison. Beam 1 and Beam 2 are designed as an under-reinforced beam and a normal-reinforced beam, respectively. Dimensions of the beams are 200 mm x 300 mm in the cross-section, and 4000 mm in the supported span. To simulate a finite element model of the load-bearing beams under elevated temperatures, the commercial finite element software ANSYS is used. Due to symmetry of the investigated beams, the finite element model involves only a quarter of the beam as shown in Figure 4.

The element size of about 20 mm is meshed in the finite element analysis and the cross sectional analysis. The compressive strength of calcareous concrete and the yield stress of the reinforcing bars are 24 MPa and 475 MPa, respectively. The beams are reinforced by 20 mm-diameter and 12 mm-diameter deformed bars and subjected to the standard fire curve of ASTM-E119 [8] as shown in Figure 5. The fire exposure only on three sides as the normal fire exposure is simulated. The thermal and mechanical properties of the reinforcing steel and concrete in accordance with BS EN 1992-1-2 [1] are employed in the analysis.

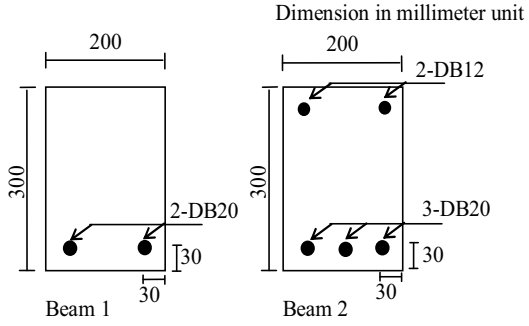

Figure 3. Beams used in the comparison

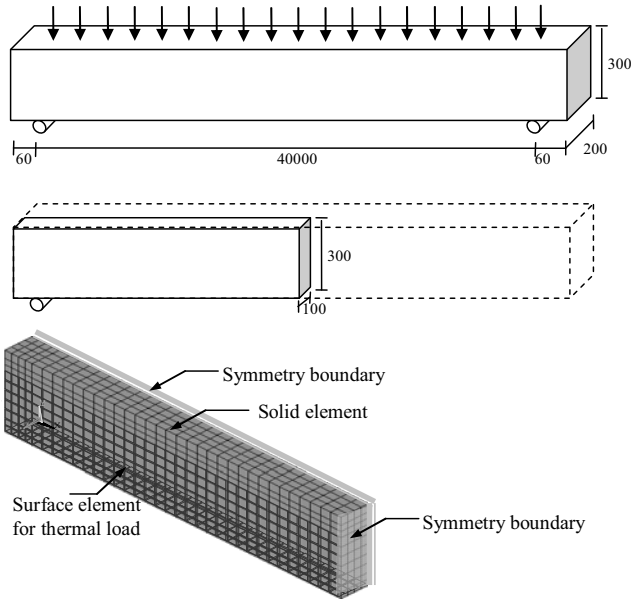

Figure 4. Finite element model of the beam

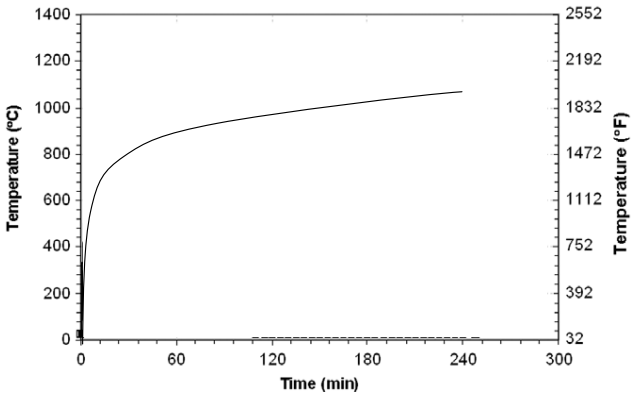

Figure 5. Standard fire curve of ASTM-E119 [8]

For the thermal analysis, the beam is modeled with three-dimensional solid elements [13], Solid70, having eight nodes with a single degree of freedom (i.e., temperature) at each node. To simulate temperature profile of the section induced by the ambient temperature, the surface element, Surf152, is used to account for heat convection and radiation. The steel rebars do not significantly influence the temperature distribution of the beam cross-section [14]. Therefore, the rebars are not included in the heat transfer analysis. The analyzed temperature profile of the heat transfer analysis is described in Figure 6 and inputted in the cross sectional analysis. Note that, without the finite element analysis, the finite difference method [5] or the given temperature profile of EN 1992-1-2 [1] can also be used to predict the temperature profile.

Before the structural analysis, the rebar elements are added in the model. The rebar temperature is defined to be equal to the temperature of concrete at the same location. A solid element, Solid65, to model concrete and a bar element, Link8, to model the steel rebar are adopted in the structural model. The solid element is capable of modeling concrete cracking in tension based on the smear crack theory. The load at the yield strain of the reinforcing steel, $\varepsilon_{sy,T}$=0.02, is used to identify the moment capacity of the beam.

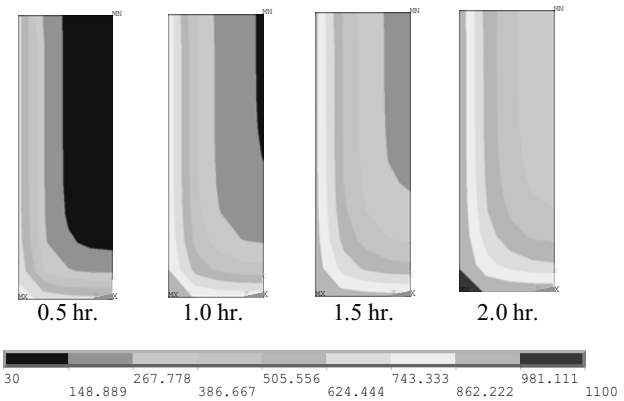

Figure 6. Temperature profile of the heat transfer analysis for the half-width of the beams

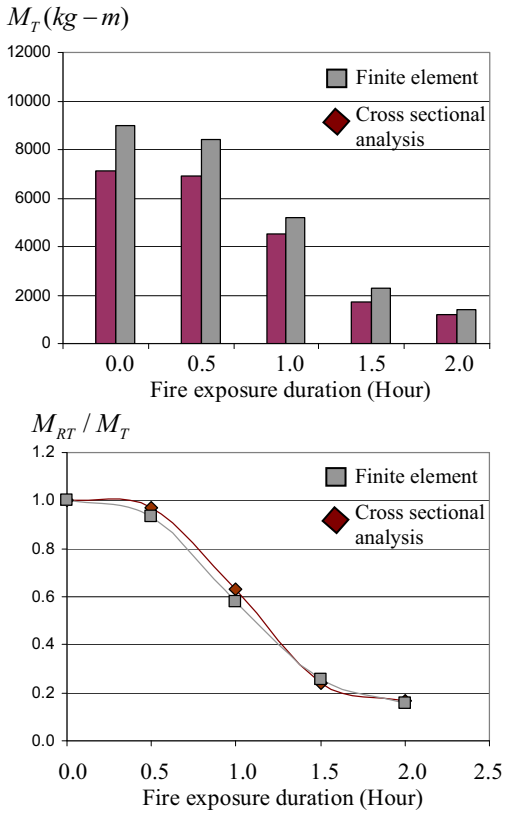

Figure 7. Comparison of the moment capacity between the finite element and cross sectional analysis for Beam 1

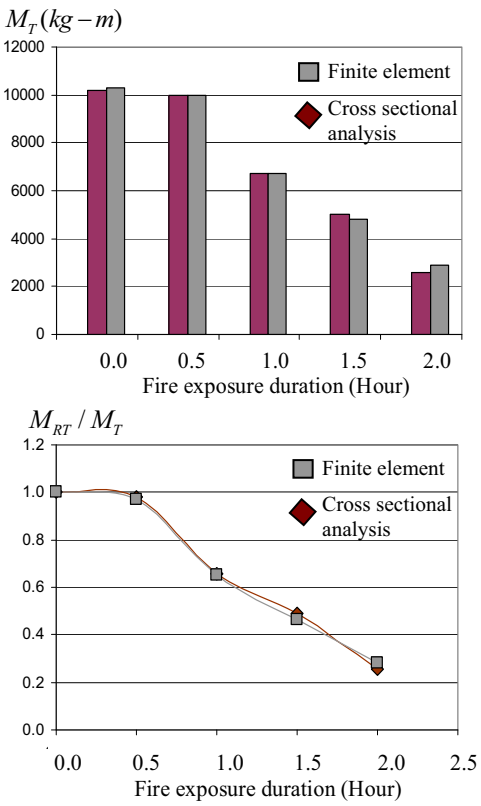

Figure 8. Comparison of the moment capacity between the finite element and cross sectional analysis for Beam 2

Comparisons between the finite element and the cross sectional analysis of the moment capacity under elevated temperatures M_T and degradation ratio of M_T to the moment capacity at room temperatures M_{RT} is shown in Figure 7 and Figure 8. It is described that the cross sectional analysis can accurately be used to predict the capacity degradation comparing with the finite element analysis. The predicted moment capacity of the cross sectional analysis is very accurate for Beam 2, the normal reinforced beam. The moment capacity of Beam 1 is lower than that of the finite element analysis about 15-20%. Under the 3-D finite element analysis, the strain profile of the beam section at the mid span differs from the assumption of the linear strain distribution. The different strain profile causes the difference of the moment capacity. However, the cross sectional analysis tends to provide the conservative capacity comparing with the finite element analysis.

V. CONCLUSIONS

The cross sectional approach is developed to analyze the moment capacity of RC beams under elevated temperatures. The concrete section is divided into discrete elements in horizontal and vertical direction. The strain distribution is assumed to be linear along the beam depth but constant along the beam width. The moment capacity is computed based on the force equilibrium which is corresponding to the element strain and the element temperature. By using the sectional analysis, the element temperature must be pre-determined. The analysis considers the stress-strain relationship for concrete and the reinforcing steel. Induced thermal, transient creep strains, coefficient of thermal expansion and tensile strength of concrete is not included in the analysis. The scope of study is limited to the under or normal-reinforced beams.

Accuracy of the proposed method in terms of the predicted moment capacity and the degradation ratio is found in the validation of the proposed method against a finite element analysis, especially for the normal-reinforced beam, However, for the under-reinforced beam, the predicted capacity is less accurate and more conservative. Effect of the reinforcing level and the assumption of the linear strain distribution should be further investigated to remind the limit of the sectional analysis. However, the cross sectional approach is a potential method to predict the moment capacity under fire and can be simply applied by design engineers.

ACKNOWLEDGMENT

This research was financially supported by Faculty of Engineering, Prince of Songkla University, contract no. ENG-55-2-7-02-0139-S. This support is gratefully acknowledged.

REFERENCES

[1] EC2, Eurocode 2: design of concrete structures—part 1.2: general rules- structural fire design, BS EN 1992-1-2. London (UK): British Standards Institution, 2004

[2] M.A. Youssef and M. Moftah, "General stress–strain relationship for concrete at elevated temperatures," Engineering Structures, vol. 29 (10), pp. 2618–2634, 2007.

[3] S. Bratina, M. Saje and I. Planinc, "The effects of different strain contributions on the response of RC beams in fire," Engineering Structures, vol. 29 (3), pp. 418–430, 2007.

[4] V.K.R. Kodur, and M. Dwaikat, "A numerical model for predicting the fire resistance of reinforced concrete beams," Cement & Concrete Composites, vol. 30, pp. 431-443, 2008.

[5] T.T. Lie, Structural fire protection, ASCE Manuals and Reports on Engineering Practice, No. 78. New York, NY, USA, 1992.

[6] J. Rigberth, Simplified design of fire exposed concrete beams and columns. An evaluation of Eurocode and Swedish building code against advanced computer models, Rep. 5063. Dept. of Fire Safety Engineering, Lund Univ., Lund, Sweden, 2000.

[7] S.F. El-Fitiany and M.A. Youssef , "Assessing the flexural and axial behaviour of reinforced concrete members at elevated temperatures using sectional analysis," Fire Safety Journal , vol: 44, pp. 691–703, 2009.

[8] ASTM, American Society of Testing and Materials, Standard Test Methods For Fire Tests of Building Construction and Material, ASTM E119. West Conshohocken, PA, 2001.

[9] V.K.R. Kodur, M.B. Dwaikat , "Design equation for predicting fire resistance of reinforced concrete beams," Engineering Structures, Vol. 33, pp. 602–614, 2011.

[10] V.K.R. Kodur, M.B. Dwaikat , "A numerical model for predicting the fire resistance of reinforced concrete beams," Cement & Concrete Composites, Vol. 30, pp. 431–443, 2008

[11] Z. Huang, " Modelling the bond between concrete and reinforcing steel in a fire," Engineering Structures, vol. 32, pp. 3660–3669, 2010.

[12] M. A. Ibrahim and S. M. Mahmood, "Finite element modeling of reinforced concrete beams strengthened with FRP laminates," European Journal of Scientific Research, vol. 30(4), pp. 526-541, 2009.

[13] ANSYS, *ANSYS multiphysics. Version 11.0 SP1*, ANSYS Inc., Canonsburg (PA), 2007.

[14] T.T. Lie and R.J. Irwin, "Method to calculate the fire resistance of reinforced concrete columns with rectangular cross section," ACI Structural Journal, vol. 90(1), pp. 52–60, 1993.

SIMPLIFIED COMPUTATION AND FINITE ELEMENT INVESTIGATION OF FIRE EXPOSED CONCRETE BEAMS

Pattamad Panedpojaman
Department of Civil Engineering, Faculty of Engineering
Prince of Songkla University, Songkhla, Thailand
E-mail: ppattamad@eng.psu.ac.th

Passagorn Chaiviriyawong
Department of Civil Engineering, Faculty of Engineering
Prince of Songkla University, Songkhla, Thailand

ABSTRACT

For fire safety, the moment capacity of RC beams under fire load can be simply computed by using such as the 500 °C isotherm method and the two dimensional sectional analysis. The 500 °C isotherm method recommended by Eurocode is a handy simplified method. Whereas the two dimensional sectional analysis can simply be implemented in a spreadsheet program. To suggest fire safety engineers, this study evaluates the accuracy to predict the moment capacity of both methods against 3D FE models. Different cross-section dimensions of RC beams under various fire load including standard fire and parametric fire curve are investigated. It is found that the moment capacity obtained from the isotherm method is significantly conservative. The capacity of the isotherm method is lower than that of the sectional analysis up to 17%. The moment capacity of the sectional analysis is agree well with the capacity of the FE models at which the tension reinforcements reach the yield stress about 10% of their beam length. However, the ultimate capacities of the FE model are normally higher than the capacity of the sectional analysis. It implicitly describes the safety of the sectional analysis. Therefore, for economy design, fire safety engineers may apply the sectional analysis to evaluate the moment capacity.

Keywords:500 °C isotherm, sectional analysis, moment capacity, FE model, RC beam.

I. Introduction

Under fire scenarios, mechanical properties of concrete and steel significantly degrade. For safety purposes, fire resistance of structural members must be evaluated based on fire loads, fire durations and sectional details. Fire resistance of reinforced concrete (RC) members can be identified in terms of their fire resistance duration or their load capacity.

The fire resistance duration of RC beams is defined as the length of time which the member can retain structural stability criteria of in fire safety codes and standards [1, 2]. As prescribed methods in the fire safety standards, the fire resistance duration is specified based on minimum cross-section dimensions and minimum clear cover to the reinforcements for the predetermined fire loads. By using the prescribed methods, structural and thermal analysis of the beams can be avoided. However, the methods are limited to predetermined dimensions and fire loads. Even though, there are number of methods and formulae for evaluating the fire resistance duration of various RC section and fire load [3-5], the methods do not clearly consider effect of service or design load on the fire resistance.

To clearly determine the fire resistance, engineers are required to compute load capacity of RC beams under fire for their specific design. The load capacity must be conducted through heat transfer analysis and structural analysis. The heat transfer analysis provides temperature profile of the beam section which is used to define corresponding material properties in the following structural analysis. In addition to the finite element (FE) method, the temperature profile can also be obtained by using the predetermined temperature profile of BS EN 1992-1-2 [6], the finite difference method [7], the energy based temperature profiles as a simplified of the FDM [8], etc.

For the structural analysis, the FE method has been proven to be an efficient method to evaluate the load capacity [9, 10]. The FE method can be used instead of real beam experiments. Due to its complicate use, the method is generally applied in research works. The 500 °C isotherm method [6] and the two dimensional sectional analysis [11] are alternative computation methods. As a handy simplified computation method recommended by BS EN 1992-1-2 [6], the 500 °C isotherm method has been widely applied to design the load capacity. The method assumes zero concrete strength for all concrete above 500 °C but full concrete strength for all concrete below 500 °C. Effect of the temperature profile is just partly considered and may affect accuracy to predict the capacity. To fully consider the temperature profile, the two dimensional sectional analysis was developed [11]. The load capacity of the sectional analysis is computed based on the force equilibrium accounting for element strain and the relative strength of the concrete and steel as a function of the temperature. The sectional analysis can simply be implemented in a regular spreadsheet program [11].

The accuracy investigation of the simplified computation methods is limited. Comparing with computer program of a simplified two dimensional sectional analysis, Reference

[12] found the slightly conservative accuracy of the 500 °C isotherm method. The investigated beams [12] are only under groups of fire loads in which their heating phases are very similar to the ISO-834 standard fire [2]. Therefore, this study is aimed to clearly evaluate the accuracy to predict the moment capacity of both methods for various cross-section dimensions of RC beams and fire loads including standard fire curves and parametric fire curve. The fire exposure only on three sides of the beams as the normal fire exposure is simulated. The capacity of the simplified computation is compared with of three dimensional FE models.

II. Simplified Computation Method

RC Beams carrying load under normal temperature causes bending moments and shear force. This study focuses on the moment capacity of under-reinforced beams as practical design. For under-reinforced beams, the concrete crushes after the tension reinforcement yields.

To compute the moment capacity, the stress-strain distribution in a beam cross-section is graphically described in Fig. 1. The ultimate moment capacity, M_U, consists of the capacity corresponding to the force of compression reinforcement, M_{U1}, and the force of concrete in compression zone, M_{U2}.Where d, d' and z is the effective depth of the beam, the effective depth of the compression reinforcement and the lever arm between centroid of the tension and compression reinforcement, respectively; b is the width of effective cross-section; x is the depth of the compression zone; A_s and $A_{s'}$ are the area of tension and compression reinforcements; ε and σ are the strain and the stress of materials; and the subscript of c, s and s' represents concrete, tension reinforcements and compression reinforcements. Note that the tension stress in concrete is neglected due to its very low tensile strength comparing with the reinforcement.

Under high temperature, the strength degradation with temperature of concrete and steel affects the ultimate moment capacity. In this study, temperature profile of the beam section is predetermined by using the heat transfer analysis of the FE method. The structural analysis of the 500 °C isotherm method and the two dimensional sectional analysis are described as follows:

A. 500 °C Isotherm Method

The 500 °C isotherm method is valid for a given minimum width of cross-section under a standard fire curve and a parametric fire exposure with an opening factor ≥ 0.14 $m^{1/2}$ [6]. The method simply reduces the cross-section size with respect to the temperature profile. The average depth of the 500 °C isotherm in the cross-section is determined. Concrete with a temperature over 500°C is assumed to have no the compressive strength whereas concrete with a temperature under 500 °C is assumed to retain its initial values of the strength and modulus of elasticity.

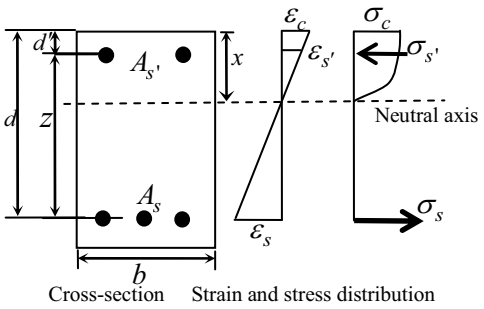

Figure 1. Stress-strain distribution in RC beam sections.

Fig. 2 (a) illustrates an example of the effective cross-section with the effective width, b_{fi}, under fire. The temperature of all reinforcements in the tension and compression zones is used to specify the corresponding strength for the computation. Even though, some of the reinforcements may fall outside the 500 °C isotherm, they are still included in the computation.

The method applies the conventional computation method [13] to determine the ultimate moment capacity of the reduced cross-section, $M_{U,ISO}$, in (1) to (6). The compressive stress distribution is assumed to be a rectangular stress distribution at the compressive strength of normal temperature (20 °C), $f'_{c,RT}$, as described in Fig. 2 (b). The factor λ and η define the effective height of the compression zone and the effective strength, respectively. For normal strength concrete, the factor λ and η are 0.8 and 1 [13]. F_s, $F_{s'}$ and F_c are the ultimate force of the tension reinforcements, the compression reinforcement and the concrete in compression zone, respectively. Due to the force equilibrium in the section, $F_s = F_{s'} + F_c$.

$$M_{U,ISO} = M_{U1} + M_{U2} \quad (1)$$

$$M_{U1} = F_{s'} z \quad (2)$$

$$M_{U2} = F_c z' \quad (3)$$

$$F_{s'} = \sum A'_{s,k} f_{y,k}(T) = F_{s1} \quad (4)$$

$$F_c = \eta f'_{c,RT} \lambda x b_{fi} = F_{s2} \quad (5)$$

$$F_s = \sum A_{s,l} f_{y,l}(T) = F_{s1} + F_{s2} \quad (6)$$

z' is the lever arm between centroid of the tension reinforcements and compression concrete; the subscript of k and l represents number of the compression and tension reinforcements; and $f_y(T)$ is the yield stress of reinforcements at temperature T.

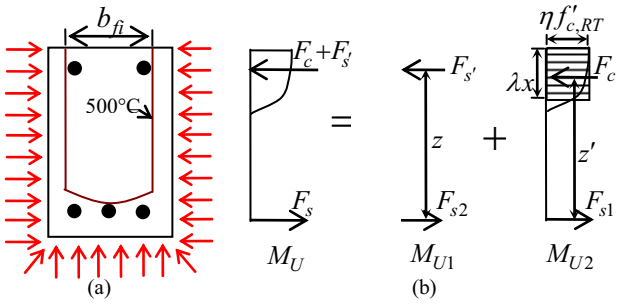

Figure 2. Principle of 500 °C isotherm method: (a) 500 °C isotherm in the cross-section and (b) conventional computation method [6].

B. Two Dimensional Sectional Analysis

The beam cross-section with their horizontal and vertical discrete elements is used in the computation as shown in Fig. 3(a). The element size of $b/10$ is used in this study. The subscript of i and j represent number of row and column of each element. The strain distribution is assumed to be linear along the beam depth but constant along the beam width as described in Fig. 3(b). For an under-reinforced beam, the yield strain of the tension reinforcements, $\varepsilon_{sy}(T)$, = 0.02 controls the strain distribution of the cross-section. Slope of the strain distribution ϕ, the strain of the concrete element $\varepsilon_{c,ij}$ and the strain of the compression bars $\varepsilon_{s',k}$ are computed in (7), (8) and (9).

$$\phi = \frac{\varepsilon_{sy}(T_l)}{d-x} \tag{7}$$

$$\varepsilon_{c,ij} = z_{c,i}\phi \tag{8}$$

$$\varepsilon_{s',k} = z_{s',k}\phi \tag{9}$$

x is the trial distance of the neutral axial; $z_{c,i}$ and $z_{s',k}$ are the distance from the neutral axis, N.A., to center of the concrete element row i, and to center of the compression bars k, respectively.

Stress of the concrete elements $\sigma_{c,ij}(T)$, the compression reinforcements $\sigma_{s',k}(T)$ and the tension reinforcements $\sigma_{s,l}(T)$ is determined corresponding to their strain and temperature (see in Fig. 3(b) to 3(c)). Summation of compression force in the compressive zone, C, and the tension force, T, of the reinforcements can be computed as follows:

$$C = \sum_{i=1}^{i_{N.A}} \sum_{j=1}^{all} \sigma_{c,ij}(T) A_{c,ij} + \sum_{k=1}^{all} \sigma_{s',k}(T) A_{s',k} \tag{10}$$

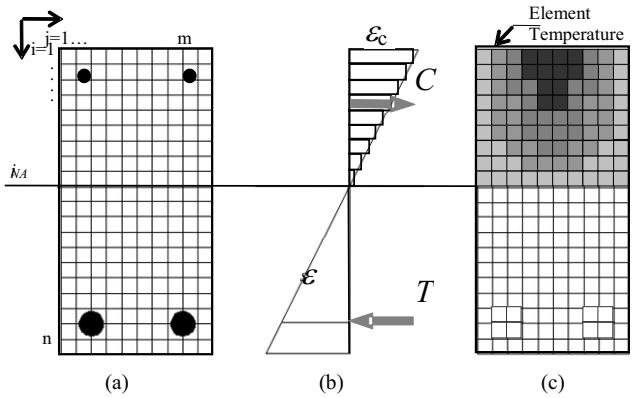

Figure 3. Discrete elements for the sectional analysis [11].

$$T = \sum_{l=1}^{all} f_{sy,T} A_{s,l} \tag{11}$$

The force equilibrium, i.e. $C = T$, is used to identify acceptable location of the neutral axis based on trial and error process. The ultimate moment capacity of the sectional analysis, $M_{U,SA}$, is computed as

$$M_{U,SA} = CL \tag{12}$$

in which L is the lever arm between the centriod of C and T as described in Fig. 3(b).

III. Investigated Beam and Mechanical Property

The 4 beam sections named as B1 to B4, as shown in Fig. 4 are used in the investigation. The stirrup and the beam length are not used in the simplified computations but required in the 3D FE model. The beams are exposed to fire loads of the nominal temperature-time curves [6] and a parametric temperature-time curve [5] as shown in Fig. 5. The nominal temperature-time curves include the external fire curve (EX) and the standard temperature-time curve (ST). Fire 1 and Fire 2 as a parametric temperature-time curve are derived based on compartment properties such as the fuel load, ventilation opening and wall linings [14]. The fire loads of Ex and Fire 2 represent less severe fire scenarios whereas the others represent severe fire scenarios. The 48 cases are investigated and described in Table 1.

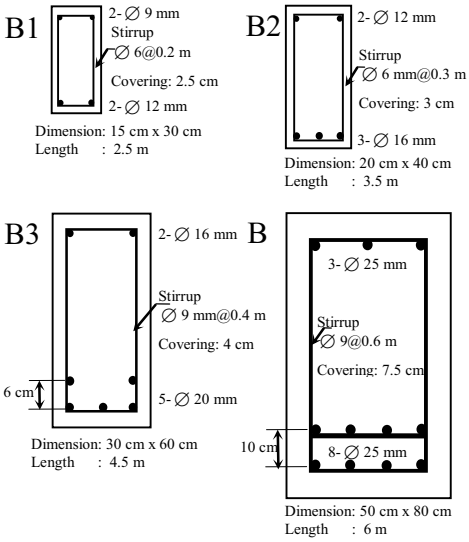

Figure 4. Investigated beams.

Table 1 Investigated Cases

Beam	Fire duration (min) for fire load					
	ST and EX			***Fire 1 and Fire 2***		
B1	30	60	90	30	60	90
B2	60	90	120	60	90	120
B3	60	120	180	60	120	150
B4	120	180	240	90	120	150

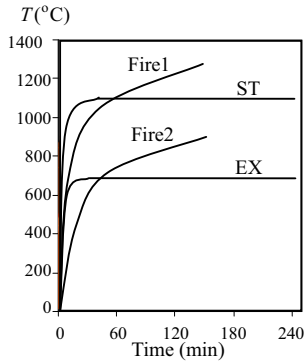

Figure 5. Temperature-time curve.

To compute the moment capacity by using the sectional analysis and the FE method, the variation of stress-strain relationship with temperature is required. This study applies the normalized stress-strain relationship for calcareous concrete and hot rolled reinforcing steel of BS EN 1992-1-2 [6] as shown in Fig. 6. After the peak stress, the perfectly plastic is generally assumed for the structural analysis under elevated temperatures [15]. At normal temperature 20 °C, concrete with the compressive strength f_c' of 24 MPa are assumed. Based on their steel grade, the yield stress of steel reinforcement f_y are 475 MPa for the bars with $\varnothing \geq$ 12 mm and 320 MPa for all stirrups and the rests.

IV. Finite Element Model

The accuracy of the simplified computations is validated by comparing with a 3D finite element model. The model is simulated by the commercial finite element software ANSYS. The beams in Fig. 4 are modeled as a cantilever beam with load at their end as shown in Fig. 7. The beam length and the stirrups are designed and modeled to prevent the shear failure in the analysis. The fire load as the temperature-time curve is applied on the three sides of the beam model. Due to symmetry of the beams, the finite element model involves only the half section. Similar to the sectional analysis, the element size of about $b/10$ is also meshed in the finite element model. The thermal and mechanical properties of the steel reinforcement and concrete in accordance with BS EN 1992-1-2 [6] are employed in the analysis. To evaluate the moment capacity, both thermal and structural analysises are conducted.

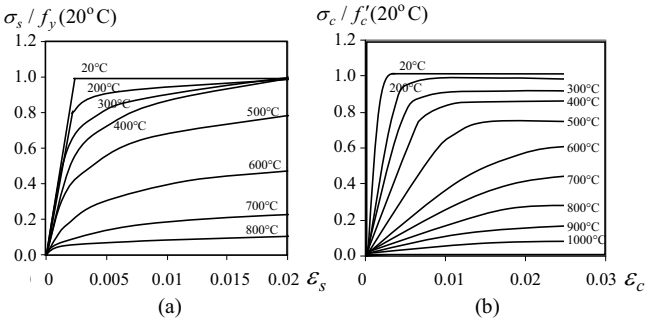

Figure 6. Normalized stress-strain relationship: (a) for hot rolled reinforcing steel and (b) for concrete .

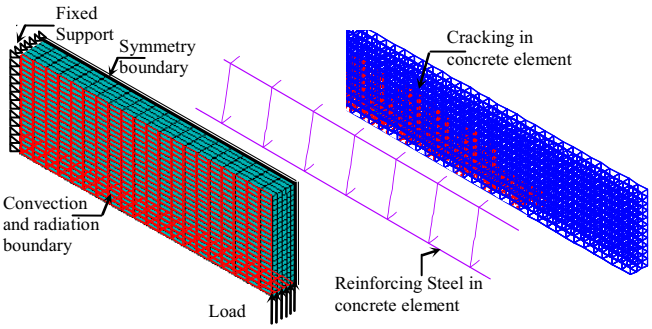

Figure 7. Finite element model.

As shown in Fig. 7, a solid element capable of concrete cracking in tension is used to model the concrete elements. The reinforcements and stirrups are modeled with a bar element. The thermal analysis accounts for heat convection and radiation. The element temperature is used to determine the corresponding mechanical properties of each element in the following structural analysis. The load at the reinforcement yield strain, $\varepsilon_{sy}(T)$, of 0.02 is specified to identify the moment capacity of the beams. A detailed description of the FE model is given by [11].

V. Moment Capacity Investigation

The moment capacity of all beams are computed by using the 500 °C isotherm method, the two dimensional sectional analysis and the 3D FE analysis. The temperature profiles used in all computations are derived by the heat transfer analysis of the FE model. Therefore, each case of the computation has the same temperature profile.

The simplified methods compute the ultimate moment capacity with the yield stress of the tension reinforcements. However, in the 3D FE model, the reinforcements do not simultaneously yield. As an example, consider the yielding in Beam1 under ST load at 30-min fire duration shown in Fig. 8. The results obtained from the FE models reveals that the tension reinforcements initially yield at the maximum moment location, that is near the support. However, the beam failure is still not occurred. Once the applied load is increased, the tensile force is transferred to the adjacent rebar element. The yielding gradually extends to the reinforcement element far the support. Note that the tensile force induced in the reinforcements is also transferred to the surrounding concrete causing cracking of the surrounding concrete elements along the length of the reinforcements.

Because the analysis involves many crack elements, it is time consuming to determine the ultimate load of the 3D FE model. The FE moment capacity M_{FE} is determined when the yielding length of the tension reinforcements is about 10% of the beam length. Normally, the ultimate moment capacity is higher that the determined M_{FE} about 15 - 20%.

Consider accuracy to evaluate the moment capacity of the simplified methods against the FE method for all beam cases as shown in Fig. 9(a). The graph shows the ratios of $M_{U,ISO}/M_{FE}$ and $M_{U,SA}/M_{FE}$ over the value of M_{FE}. The value of $M_{U,SA}/M_{FE}$ ratio is mostly close to 1 whereas the value of $M_{U,ISO}/M_{FE}$ is mostly lower than 0.87. That is the sectional analysis accurately provides the moment capacity comparing with the FE method. The 500 °C isotherm method tends to provide the very conservative capacity. $M_{U,SA}$ and $M_{U,ISO}$ are lower than M_{FE} up to 10% and 21%, respectively.

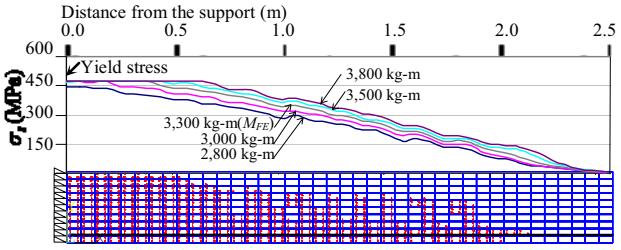

Figure 8. Variation of the tensile stress in the tension reinforcements with moment load.

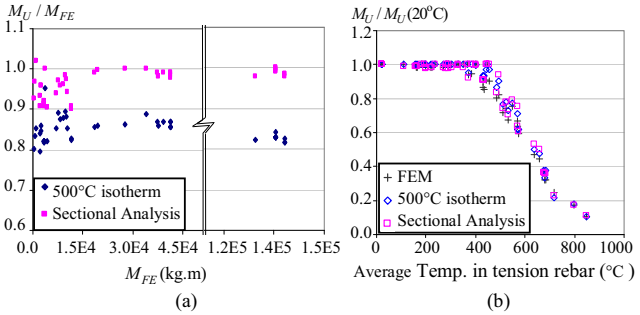

Figure 9. Comparison of the moment capacity: (a) moment capacity ratio of the simplified method to the FEM, and (b) degradation ratio of the moment capacity.

Note that fire loads and fire duration do not clearly affect the difference between $M_{U,ISO}/M_{FE}$ and $M_{U,SA}/M_{FE}$. However, the difference tends to be larger for the large section such as the 50 cm x 80 cm beam. M_{FE} of the beam is about 140,000 kg-m. The maximum difference between the simplified methods is about 17% or 26,000 kg-m. The characteristics may be due to enlargement of the temperature profile effect in the large section.

The degradation ratio of the moment capacity over the average temperature of the tension reinforcements is described in Fig. 9(b). All methods provide similar degradation ratios in each case. The moment capacity is normally not degraded when the reinforcement temperature lower than 400 °C. At this stage, the yield strength of steel and the compressive strength of concrete are less damaged. Similar to the mechanical properties, the moment capacity are significantly degraded when the reinforcement temperature higher than 400 °C.

VI. Conclusion

As a simplified method to compute the moment capacity of RC beams, the 500 °C isotherm method and the two dimensional sectional analysis are evaluated against the 3D FE analysis. The moment capacity of the FEM is determined when the yielding length of the tension reinforcements reaches about 10% of the beam length. It is found that the sectional analysis provides the moment capacity close to the FE method. The 500 °C isotherm method provides the very conservative moment capacity up to 21% comparing that of the FE method. The large cross-section tends to cause the larger capacity difference between the simplified methods. However, the degradation ratios of all methods are slightly deviate from each other. Note that the ultimate moment capacity of the FE method is higher than the determined capacity about 15 - 20%. Therefore, the moment capacity of the sectional analysis is still safe and more economy to be used.

Acknowledgment

This research was financially supported by Faculty of Engineering, Prince of Songkla University, contract no. ENG-55-2-7-02-0139-S. This support is gratefully acknowledged.

References

[1] ASTM, American Society of Testing and Materials, Standard test methods for fire tests of building construction and material, ASTM E119. West Conshohocken, PA, 2001.

[2] International Standard, Fire-resistance tests—elements of building construction—Part 1: General requirements, ISO 834. Geneva, 1999.

[3] A.H. Buchanan, "Structural Design for Fire Safety", John Wiley & Sons Ltd., Chichester, England, 2002.

[4] P. Pakala, "Energy based equivalent approach for evaluating fire resistance of reinforced Concrete Beams," MS Thesis, Michigan State University, East Lansing, Michigan, USA,2009.

[5] V.K.R. Kodur, P.Pakala and M.B.Dwaikat, "Energy based time equivalent approach for evaluating fire resistance of reinforced concrete beams," Fire Safety Journal, vol. 45, pp.211–220, 2010.

[6] EC2, Eurocode 2: Design of concrete structures—part 1.2: general rules- structural fire design, BS EN 1992-1-2. London (UK): British Standards Institution, 2004.

[7] T.T. Lie, Structural fire protection, ASCE Manuals and Reports on Engineering Practice, No. 78. New York, NY, USA, 1992.

[8] P. Panedpojaman, "Spreadsheet calculation of energy based method to predict temperature in concrete slabs," International Review of Civil Engineering, vol. 3(5), pp. 403-411, 2012

[9] S. Bratina, M. Saje and I. Planinc, "The effects of different strain contributions on the response of RC beams in fire," Engineering Structures, vol. 29(3), pp. 418-430, 2007.

[10] V.K.R. Kodur, and M. Dwaikat, "A numerical model for predicting the fire resistance of reinforced concrete beams," Cement & Concrete Composites, vol. 30, pp. 431-443, 2008.

[11] P. Panedpojaman, "Predicting moment capacity of RC beams under fire by using two-dimensional sectional analysis," The 4th KKU International Engineering Conference 2012, Khon Kaen, Thailand, May 10-12, 2012.

[12] J. Rigberth, Simplified design of fire exposed concrete beams and columns. An evaluation of Eurocode and Swedish building code against advanced computer models, Rep. 5063. Dept. of Fire Safety Engineering, Lund Univ., Lund, Sweden, 2000.

[13] EC2, Eurocode 2: design of concrete structures—part 1.1: general rules and rules for buildings, BS EN 1992-1-1. London (UK): British Standards Institution, 2004.

[14] R. Feasey and A.H. Buchanan, "Post-flashover fires for structural design," Fire Safety Journal, vol. 37(1), pp. 83–105, 2002.

[15] M. A. Ibrahim and S. M. Mahmood, "Finite element modeling of reinforced concrete beams strengthened with FRP laminates," European Journal of Scientific Research, vol. 30(4), pp. 526-541, 2009.

สรุปผลการวิจัย

เพื่อเปรียบเทียบผลการออกแบบความสามารถในการต้านทานโมเมนต์ระหว่างวิธีที่นำเสนอกับแบบจำลองไฟไนเอลิเมนต์ 3 มิติ (ดังแสดงในรูปที่ 7 ของบทความที่ 5) โดยใช้เกณฑ์การตัดสินด้านความสามารถในการต้านทานโมเมนต์และกรณีการศึกษาเช่นเดียวกับบทที่ 5

โดยหน้าตัดคาน 4 รูปแบบ (ดังแสดงในรูปที่ 4 ของบทความที่ 5) และอุณหภูมิไฟทดสอบจำนวน 4 รูปแบบ (ดังแสดงในรูปที่ 5 ของบทความที่ 5) กรณีการวิเคราะห์ความสามารถในการต้านทานโมเมนต์ภายใต้ระยะเวลาการโดนเพลิงไหม้ต่างๆ (แสดงในตารางที่ 1 ของบทความที่ 5) โดยใช้คุณสมบัติเชิงกลของวัสดุต่างๆ ดังแสดงในบทที่ 5 ทั้งนี้มีกรณีการวิเคราะห์ทั้งสิน 48 กรณี

ผลการเปรียบเทียบความสามารถในการต้านทานโมเมนต์ระหว่างวิธีที่นำเสนอกับแบบจำลองไฟไนเอลิเมนต์แสดงในรูปที่ 1 ซึ่งแสดงให้เห็นถึงประสิทธิภาพในการทำนายความสามารถในการต้านทานโมเมนต์ โดยมีค่าสัมประสิทธิ์การตัดสินใจ R^2 =0.9135

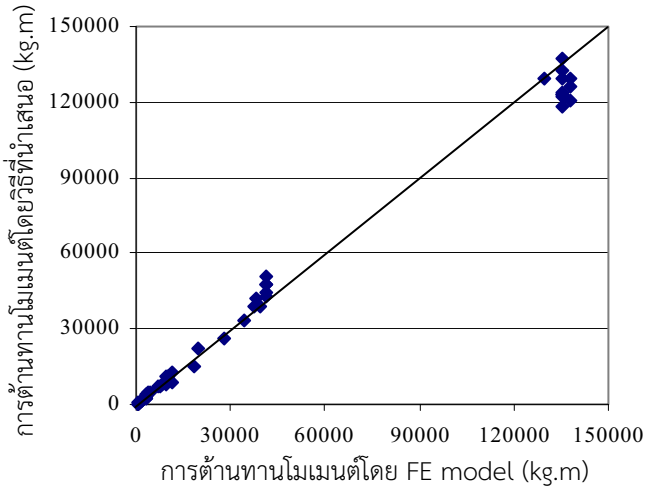

รูปที่ 1 ผลการเปรียบเทียบความสามารถในการต้านทานโมเมนต์ระหว่างวิธีที่นำเสนอกับแบบจำลองไฟไนเอลิเมนต์

วิธีการการออกแบบอย่างง่ายที่นำเสนอในโครงงานวิจัยนี้ มีความแม่นยำในการทำนายความสามารถในการต้านทานโมเมนต์ โดยสามารถใช้งานทดแทนการวิเคราะห์โดยแบบจำลองไฟไนเอลิเมนต์ ที่สามารถใช้งานหน้าทุกกรณีหน้าตัด อุณหภูมิไฟมาตรฐาน และ ช่วงเวลาการสัมผัสความร้อน ซึ่งการประยุกต์ใช้ดังกล่าวช่วยให้วิศวกรโครงสร้างสามารถออกแบบองค์อาคารได้โดยสะดวก โดยใช้เพียง Spreadsheet program พื้นฐานในการสร้างตารางการคำนวน